MECHANISM OF A NATURAL PRENYLFLAVONOID, ICARITIN, AS AN ANTI-OSTEOCLAST AGENT FOR POSTMENOPAUSAL OSTEOPOROSIS: CELLULAR AND ANIMAL STUDIES

TAN EE MIN

B.SC. (HONS.), QUEEN MARY UNIVERSITY OF LONDON

A THESIS SUBMITTED FOR THE DEGREE OF DOCTOR OF PHILOSOPHY

DEPARTMENT OF MEDICINE
NATIONAL UNIVERSITY OF SINGAPORE

2017

SUPERVISORS:
PROF YONG EU LEONG
DR NICHOLAS CHEW
EXAMINED BY:
ASSOCIATE PROFESSOR CHRISTOPH WINKLER
ASSISTANT PROFESSOR TOH WEI SEONG
ASSISTANT PROFESSOR CHOONG SWEE NEO CLEO, NTU

DECLARATION

I hereby declare that this thesis is my original work and it has been written by me in its entirety. I have duly acknowledged all the sources of information which have been used in the thesis.

This thesis has also not been submitted for any degree in any university previously.

Tan Ee Min

1 January 2017

ACKNOWLEDGEMENTS

I thank my lucky stars for the people who have made this journey possible:

To my supervisor Prof Yong Eu Leong, and my co-supervisor Dr. Nicholas Chew, who have been guiding my research and without whom there would have been nothing much to write in this thesis. Thank you for giving me this tremendous learning opportunity, for your advice and guidance.

To Dr Li Lei and Dr inthrani Raja Indran, who selflessly took on the role as my mentors. Thank you for generously sharing your knowledge with me, for your guidance in developing ideas and when experiments go wrong. I thoroughly enjoy the mini- seminar sessions we hold in the corridors of the lab, in the office pantry and am grateful for the critique you've given me on my work. Thank you for your encouragements when I needed them most. And not forgetting Dr. Inthrani's subtly pushing me to work harder by implementing lab meetings; you were right, we just had to set presentation dates and I'd have to figure the rest out in time.

To my lab mates Ryan, Audrey, Bao Hui, Helen and Zhi Wei, thank you for helping me out when my experimental schedule was too packed, when I needed extra pairs of hands in the animal facility, and for sharing your "contacts" with me when I sourced for reagents or equipment. Thank you for the emotional support you've given me, for stocking up pantry snacks, for making me laugh. I couldn't have asked for better companionship these years. And a special mention to Helen and Shankar, who have ungrudgingly helped me with my experiments

even though it's beyond their job scope. Not forgetting the endless supply of coffee Helen has provided me with.

And of course, to my parents who have been nothing but patient and tolerant with me, thank you for this Workaholic gene that I've inherited from you both; I could not have completed this PhD candidature without it. I know that jumping into this PhD is perhaps a decision you may never fully comprehend, but thank you for asking me repeatedly over the years what it is I'm working on; even if you don't understand or remember, at least you keep asking. Thank you for the space you've given me; I know I haven't given you much choice but to grow accustomed to my returning to the lab in the middle of the night for the odd time points, and on weekends. And of course, thank you for all the love and support you have showered me.

TABLE OF CONTENTS

Summary

As women approach menopause, ovarian function declines and the drastic decrease in estrogen levels lead to osteoporosis. Postmenopausal osteoporosis is characterized by a decrease in bone mineral density and strength, leading to a significant increase in the risk of fractures. However, current anti-osteoporotic drugs are associated with clinical adverse events, thus there is a need to identify alternative treatment options with improved risk-benefit profiles.

The findings of this thesis uncover the potential clinical utility of icaritin, a natural prenylflavonoid, as a therapeutic agent for postmenopausal osteoporosis. We show that icaritin treatment inhibited osteoclastogenesis in both mouse and human monocytes, and suppressed osteoclast resorption in these cellular models. We further delineated the mechanism(s) by which icaritin inhibits osteoclast differentiation, summarized in the following diagram: by mediating proteasomal degradation of the critical adaptor protein, TRAF6, icaritin inhibited downstream NFκB, MAPK/AP-1, and ROS signaling pathways, to suppress both NFATc1 expression and transcriptional activity, ultimately downregulating the expression of osteoclast-specific genes. These findings were corroborated in the ovariectomized (OVX) rat model. In the OVX rat model, a well-established model of estrogen deficiency-mediated osteoporosis, icaritin treatment inhibited osteoclast formation and resorption thereby preventing ovariectomy-induced deterioration in bone architecture and strength. Consistent with our cellular studies, the inhibition in

osteoclastogenesis by icaritin treatment was associated with decreased TRAF6 and NFATc1 protein expression in the circulating osteoclast precursors as well as in tibial lysates. We conclude that icaritin inhibits osteoclast differentiation from its precursors by repressing the expression of the TRAF6 adaptor protein, an effect that was consistently observed both *in vitro* and *in vivo.*

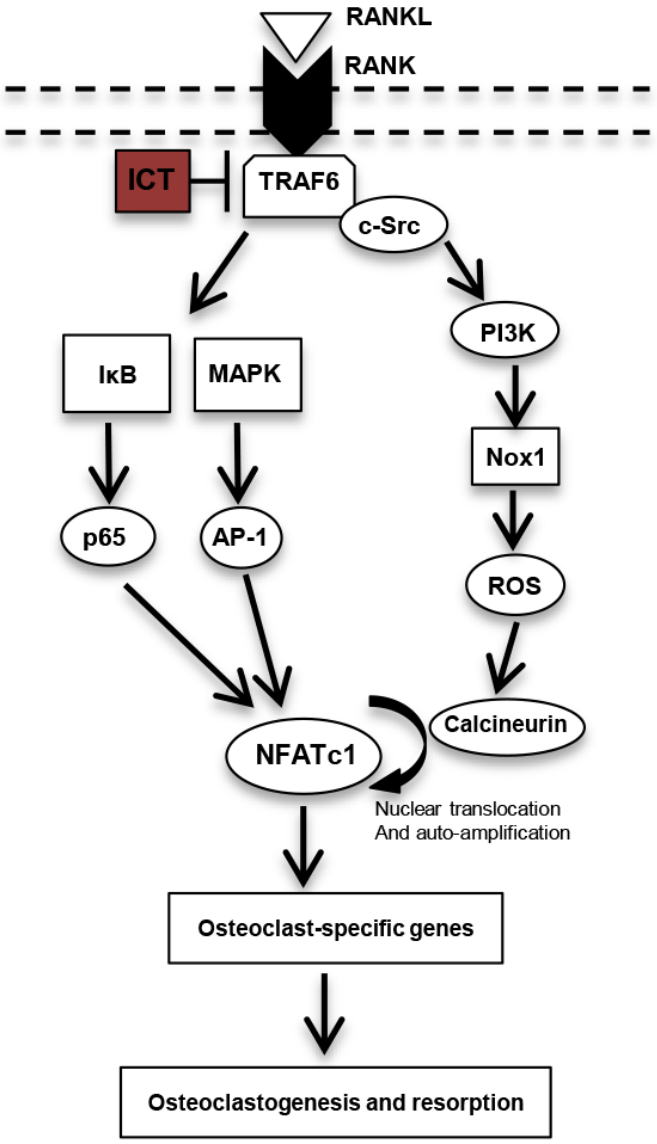

Figure i: Schematic illustration of mechanism(s) by which ICT inhibits osteoclast differentiation

List of tables

List of figures

List of abbreviations

AP-1	Activator protein-1
ATP	Adenosin triphosphate
BMD	Bone mineral density
BMSCs	Bone marrow stromal cells
BMU	Basic multicellular unit
cDNA	Complementary DNA
CEE	Conjugated equine estrogens
CTSK	Cathepsin K
CTx-I	Collagen Type-1 C-telopeptide
DPBS	Dulbecco's phosphate buffered saline
DMEM	Dulbecco's modified eagle's medium
DMSO	Dimethyl sulfoxide
DXA	Dual-energy X-ray absorptiometry
E2	β estradiol 17-valerate
HRT	Hormone replacement therapy
ICT	Icaritin
IOF	International Osteoporosis Foundation
IL	Interleukin
IP	Immunoprecipitation
LB	Lysogeny Broth

MAPK	Mitogen-activated protein kinases
MCSF	Macrophage colony stimulating factor
MMP	Matrix metalloproteinase
mRNA	Messenger RNA
MSCs	Mesenchymal stem cells
NAC	N-acetyl cysteine
NFATc1	Nuclear factor of activated T-cell 1
NFκB	Nuclear factor κ B
ONJ	Osteonecrosis of the jaw
OPG	Osteoprotegerin
OSTA	Osteoporosis self-assessment tool for asians
OVX	Ovariectomized
PTH	Parathyroid hormone
PBMC	Peripheral blood mononuclear cells
RANK	Receptor activator of Nuclear factor κ B
RANKL	Receptor activator of Nuclear factor κ B ligand
ROS	Reactive Oxygen Species
RT-PCR	Reverse transcription polymerase chain reaction
SERMs	Selective estrogen receptor modulator
TNF	Tumour necrosis factor
TRAF	TNF receptor associated factor
TRAP	Tartrate- resistant acid phosphatase
WHI	Women's health initiative study
WHO	World Health Organization

List of publications

Part of this thesis was published in the following publications:

1. **Tan, E. M.**, Li, L., Indran, I. R., Chew, N., & Yong, E. L. (2016). TRAF6 mediates suppression of osteoclastogenesis and prevention of ovariectomy-induced bone loss by a novel prenylflavonoid. *J Bone Miner Res*. doi: 10.1002/jbmr.3031

2. Indran, I. R., Liang, R. L., **Tan, E.M.**, & Yong, E. L. (2016). Preclinical studies and clinical evaluation of compounds from the genus Epimedium for osteoporosis and bone health. *Pharmacol Ther*. doi: 10.1016/j.pharmthera.2016.01.015

CHAPTER 1. INTRODUCTION

1.1 Osteoporosis

Osteoporosis or “porous bones” is a highly prevalent condition characterized by decreased bone mass and density that occurs when undue amounts of protein and minerals are lost from skeletal tissue. This loss in bone mass is accompanied by structural changes that lead to increased brittleness and a decrease in the strength of bones thus resulting in a significant increase in fracture risk (Cagnetta & Patella, 2012). As such, the morbidity and mortality associated with osteoporosis is secondary to the fractures that occur. Since bone loss occurs gradually and asymptomatically with aging, coupled with the demographic transitions occurring worldwide, the prevalence of osteoporosis is rising steadily and is projected to increase substantially (Cooper et al., 2011).

Osteoporosis is traditionally classified into primary and secondary osteoporosis. Type 1 primary osteoporosis affects postmenopausal women, while type 2, also known as senile osteoporosis affects both men and women above the age of 75. Several risk factors have been identified for primary osteoporosis as indicated in Table 1.1. Secondary osteoporosis, as its name suggests, is a bone disorder that results from complications of other medical conditions such as endocrine and metabolic disorders (for eg. hyperthyroidism, hypercortisolism, hyperparathyroidism, intestinal

malabsorption conditions), or due to the extended use of drugs, such as glucocorticoids, selective serotonin reuptake inhibitors and anticoagulants.

Table 1.1 Major risk factors for primary osteoporosis

Advancing age
Female sex
White or Asian race
Low body weight/ body mass index
Family history of osteoporotic fractures
Early menopause
Sedentary lifestyle
Excessive alcohol (> 2 drinks per day), caffeine, and tobacco use
Low calcium and/or Vitamin D intake
Inadequate sun exposure
Athletic amenorrhoea

Summarized from (Kanis et al., 2004; Kanis et al. 2008)

1.1.1 Postmenopausal osteoporosis: epidemiology and financial burden

Postmenopausal osteoporosis affects more than 200 million women worldwide (Reginster & Burlet, 2006) and it is estimated that by the age of 80, 70% of women will be osteoporotic at the hip, lumbar spine or forearm (Melton, 1995). Indeed the high prevalence of osteoporosis is accompanied by a high incidence of osteoporotic fractures. It has been reported that approximately 9 million osteoporotic fractures occur annually worldwide (Kanis et al., 2000). Further, 1 in 3 women above 50 will suffer from osteoporotic fractures, particularly in the hip and spine (Johnell & Kanis, 2006). The lifetime risk of suffering an osteoporotic fracture for a 50 year old Caucasian woman, at ~40%, is similar to that of coronary heart disease (Samelson et al., 2006).

Mortality rates of osteoporotic fractures vary with the type of fracture. Mortality rate in the first year following a hip fractures has been reported to be as high as 20 – 24%, while Johnell et al. (2004) also reported similar mortality rates for clinical spine fractures. Pneumonia and chronic obstructive pulmonary disease are the primary causes of mortality associated with severe vertebral deformities (Teng et al., 2008). Although mortality risk decreases after the first year, mortality at 5 years was still higher than that of the general population of the same age (Johnell et al., 2004). In addition to the high mortality rates, survivors experience an overwhelming loss of function and independence (Schnell et al., 2010). Only 25% of hip fracture patients are able to return to their activities of daily living such as walking, getting out of bed, cooking, bathing, using the toilet and getting dressed (Magaziner et al., 1990).

This loss of independence may result from both the physical inability to walk and fear of falling. Unfortunately, this inactivity perpetuates a vicious cycle worsening osteoporosis thereby increasing the risk of falling and suffering of new fractures (Galsworthy & Wilson, 1996). The prevalence of vertebral deformities in postmenopausal women is estimated at 20% while approximately 10% have deformities severe enough to result in chronic back pain, kyphosis, and height loss (Ettinger et al., 1992). Similarly, chronic back pain, deformity, and immobility, as a result of vertebral fractures, have a significant impact not only on the patients' daily activities but also self-esteem, body image and mood (Fechtenbaum et al., 2005; Tosteson et al., 2001). Gold et al. (2009) reported that chronic pain as a result of vertebral fractures leads to a complex psychosocial reaction from the patient including anxiety, depression, and interpersonal relationship problems.

In addition to the debilitating condition that osteoporotic fractures leave patients, osteoporotic fractures also pose a major public health problem worldwide due to the associated morbidity, mortality and costs. In the US, the average direct medical cost of managing a fracture can amount up to $ 12 000 (Gabriel et al., 2002), however, close to three-quarters of these fractures occur in patients above 65 years old, thus these expenses are typically borne by society. Burge et al. (2007) reported that more than 2 million fractures occurred in the US in 2005, amounting to a direct cost of $17 billion dollars for fracture treatment and care. Similar trends have been reported in Europe, with an estimated cost of 36 billion euros for osteoporotic fractures (Borgstrom et al., 2007). Notably, the annual expenditure for direct medical

care of osteoporotic fractures in the US exceeds that of breast and gynecologic malignancies combined (Hoerger et al., 2009). Furthermore, the cost of osteoporotic fractures has been predicted to double by 2050 (Borgstrom et al., 2007; Burge et al., 2007) due to worldwide ageing demographics.

1.1.2 Postmenopausal osteoporosis in Singapore

The IOF Asian audit (2009) found that 55 000 women in Singapore above the age of 50 suffer from osteoporosis. The prevalence of osteoporosis is projected to increase rapidly as the population of Singapore is ageing, coupled with the increasing life expectancy from 84 years to 92 years by 2050 (World Population Prospects, 2008). As such, the population aged over 50 is projected to be 3.9 million in 2050, making up 46% of the population (World Population Prospects, 2008). The age-adjusted incidence of osteoporotic fractures among women over the age of 50 in Singapore is currently the highest in Asia and is approaching that observed in American Caucasians (Cooper et al., 1992). Indeed, hip fracture incidence rates in women have risen at least 5 fold since the 1960s (Koh et al., 2001). It has been reported that the mortality rate at one year post-fragility hip fracture is approximately 20 – 27%, with 20% of the survivors partially or fully dependent on a care giver and 42% experienced reduced mobility (Mithal & Kaur, 2012).

Osteoporotic fractures also pose a significant public health cost in Singapore. The median hospital stay for surgical treatment of a hip fracture is 16 days, costing approximately 8400 USD for the immediate hospital care, while direct costs in the first year of fracture treatment is estimated at 6000 USD (Zhen et

al., 2012). Given Singapore's ageing population, the total cost of osteoporotic fractures, including both immediate hospital cost and indirect costs, is projected to rise to 145 million USD by 2050. Osteoporotic fractures therefore amount to a tremendous financial burden and social dependence in Singapore.

1.1.3 Screening and diagnosis of postmenopausal osteoporosis

Osteoporosis is an asymptomatic disease and bone loss often goes undetected until it manifests clinically as fragility fractures or symptoms associated with a collapsed vertebrae, such as loss of height over time, stooped posture and back pain.

Cooper et al. (2011) recommended that all women above the age of 65 be screened for osteoporosis, while women below the age of 65 be screened for the presence of risk factors such as early menopause, anorexia, bulimia, smoking habit or alcohol abuse, and the chronic use of drugs associated with an increased risk for osteoporosis. Additionally, possible causes of secondary osteoporosis such as hyperthyroidism, hypercortisolism, hyperparathyroidism, or glucocorticoid- and immobilization-induced osteoporosis should also be excluded in order to establish a diagnosis of postmenopausal osteoporosis. There is increasing evidence to suggest that patients with elevated levels of bone turnover markers can be expected to have greater rates of bone loss if untreated (Garnero et al., 1999). However, due to a lack of standardization of assays that is further complicated by large intra- and inter-subject variability, bone turnover markers have not been recognized as a diagnostic tool.

Although a variety of techniques, such as quantitative ultrasound or quantitative computed tomography, are available to assess bone mineral content, dual-energy X-ray absorptiometry (DXA) is presently considered the gold standard imaging technique for the diagnosis of osteoporosis (Engelke & Gluer, 2006). Due to its sensitivity to the calcium content of bone, DXA has been shown to offer the best predictive value for fracture risk (Bernabei et al., 2014). An estimate of fracture risk may be obtained with DXA of radium, ulna, spinal column or proximal femur. The widespread clinical use of DXA at the proximal femur and lumbar spine is attributed to the prospective studies (Marshall et al., 1996) that have documented a strong gradient of risk for fracture prediction, furthermore, the gradients of risk are higher than those derived using other techniques.

In 1994, the World Health Organization proposed the following descriptive categories for the diagnosis of osteoporosis:

1. Normal: a value for BMD that is higher than 1 standard deviation below the young adult female reference mean (T-score ≥ -1 SD)
2. Osteopenia: a value for BMD more than 1 standard deviation below the young female adult mean, but less than 2.5 SD below this value (-1 SD > T-score > -2.5 SD)
3. Osteoporosis: a value for BMD 2.5 SD or more below the young female adult mean (T score ≤ -2.5 SD)

However, the 1994 WHO criteria did not specify a site of measurement and the

same T-score derived from different sites and techniques yield different information on fracture risk. As such, the International Osteoporosis Foundation recommended the adoption of a reference site and for DXA measurements to be taken at the femoral neck (Kanis & Gluer, 2000).

1.1.4 Fracture risk assessment

To improve patient assessment, WHO developed an algorithm to calculate the 10- year absolute fracture risk of individual patients. This FRAX tool calculates a patient's risk for hip fracture and major osteoporotic fracture (in the hip, spine, wrist and humerus). The algorithm includes the following risk factors: age, prior fracture, parental history of hip fracture, low body weight or BMI, use of glucocorticoids, history of rheumatoid arthritis, cigarette smoking status, excessive alcohol intake of 3 units or more daily and secondary osteoporosis (Silverman & Calderon, 2010). FRAX was developed using baseline and follow-up data from 9 prospective population-based cohorts and validated in 11 (Watts et al., 2009). The FRAX tool has since been developed for 27 country-specific models, including Singapore.

It is noteworthy that there are several assumptions inherent in the country-specific FRAX model: 1) The relationship between BMI and mortality is constant across different racial and ethnic groups. 2) Many countries do not have adequate data on the incidence of nonvertebral fracture and vertebral fractures. Data on these fractures are estimated based on the incidence of hip fracture in US Caucasians as the reference from the NHANES, and this ratio may therefore not be appropriate. Although FRAX was validated in 11 cohorts,

there is at present no randomized controlled trial data on fracture prevention in patients who were selected based on FRAX.

In Singapore, screening for women below the age of 65, has been advocated for those with a high-risk of developing osteoporosis. To identify women below the age of 65, who are at high risk of developing osteoporosis, Koh, Sedrine, et al. (2001) have developed the Osteoporosis Self-Assessment Tool for Asians (OSTA): where the difference between age and weight (in kilograms) of patients is greater than 20, or where patients have a fracture risk of ≥9.3% by FRAX, BMD of these women should be measured. Although the setting of interventional thresholds based on FRAX has to be compared to a validated local population standard, such data is not yet available and interventional thresholds adopted are as recommended by the National Osteoporosis Foundation (Cosman et al., 2014): besides osteoporotic patients, pharmacologic treatment should be initiated for osteopenic patients with a 10- year hip fracture probability of ≥3% or a 10-year major osteoporosis-related fracture probability ≥20% based on FRAX.

1.1.5 Treatment modalities of postmenopausal osteoporosis

General management

Exercise –The skeleton, via bone remodeling, adapts to meet the mechanical demands placed on the skeleton. As such, it is well established that prolonged bed rest or immobilization, due to paralysis or casting of a limb, may lead to disuse osteoporosis (Minaire, 1989; Takata & Yasui, 2001). Although the

amount of weight-bearing exercise optimal for skeletal health in patients has not been established, studies have shown that aerobics, weight bearing and resistance exercises have been shown to lead to BMD improvements in the spine and hip (Bonaiuti et al., 2002). Prince et al. (1991) also demonstrated in a comparative study that exercise plus calcium supplementation or estrogen-progesterone replacement could slow bone loss. Although it was found in this study that exercise alone was less effective than exercise and calcium supplementation in increasing bone mass, it also resulted in less side effects. Nonetheless, the exercise prescription must be appropriate for the needs of the patient otherwise it may lead to negative consequences. The exercise program, whether therapeutic and recreational, should account for the flexibility, muscle strength, cardiovascular fitness, and gait steadiness of the individual. The exercise program should also include balance and lower extremity strength training to prevent falls and fractures. Thus exercise remains an integral component of both prevention and treatment of postmenopausal osteoporosis.

Nutrition – It has been estimated that 38-54% of BMD variance can be modified by environmental factors such as nutrition (Krall & Dawson-Hughes, 1993). Nutrition has a direct and indirect role in preventing osteoporosis – Firstly, by supporting the mineralization of bone during growth, thereby enhancing peak bone mass and maximizing bone strength. Secondly, by decreasing the rate of bone loss with ageing and thirdly, by maintaining the muscle strength and preventing sarcopenia in elderly, thereby precluding the

effect of disuse on the skeleton. However, there is a high prevalence of calcium, protein and vitamin D insufficiency in the elderly (Gennari, 2001; Janssen et al., 2002). Vitamin D supplements, at a daily dose of greater than 700 IU, have been shown to reduce the risk of falling (Bischoff-Ferrari et al., 2004). Additionally, calcium and vitamin D supplements decrease secondary hyperparathyroidism and reduce the risk of proximal femur fractures (Meunier, 1996). As such, intakes of at least 1000 mg/day of calcium, 800 IU of vitamin D and of 1 g/kg body weight protein is recommended for the general management of osteoporosis (Tang et al., 2007).

The consumption of other nutrients has also been shown to affect skeletal health via indirect effects on calcium balance. In spite of interindividual differences in salt sensitivity, excessive sodium intake has been shown to increase urinary calcium excretion thereby negatively affecting calcium balance. It has been shown that for every 100 mmol of sodium excreted, approximately 1 mmol loss of urinary calcium is observed (Massey and Whiting, 1996). Nonetheless, sufficient calcium intake would counteract the detrimental effects of urinary calcium excretion given that there could be up to 2-fold differences in sodium-induced calciuria with low and high calcium intakes (Teucher et al., 2008).

In a 12-year follow-up study, the risk of hip fracture over each 2-year period was significantly increased by the consumption of ≥2.5 units of caffeine per day, where one cup of coffee = one unit of caffeine, and one cup of tea equals 0.5 unit of caffeine (Kiel et al., 1990). While the association between increased caffeine consumption and the elevated fracture risk is not fully understood, it

is hypothesized that caffeine increases urinary and faecal calcium losses and may provoke a negative calcium balance in presence of a low calcium diet (Barger-Lux & Heaney, 1995). However, it has been reported that the detrimental effect of caffeine can be offset by increasing calcium intake by 40 mg calcium for every 177.5 ml serving of caffeine-containing coffee (Barrett-Connor et al., 1994). Interestingly, despite the associations observed between caffeine consumption and bone mineral density or fracture risk, no controlled study has been done with decaffeinated coffee.

There has been controversy regarding the role of protein intake and the development of osteoporosis. While sufficient protein intake is essential for the maintenance of bone homeostasis in the elderly (Rizzoli et al., 1998), excessive protein intake leads to metabolic increase of acid production and acid renal excretion, therefore increasing calcium excretion. Nevertheless, it is agreed that the consumption of dairy products, which are rich in calcium, proteins, phosphorus and potassium, is the best way to preserve the body calcium economy.

Pharmacological interventions

There are several types of anti-osteoporotic agents available that have all been shown to reduce the risk of vertebral fractures. The anti-fracture efficacy of frequently used treatments for postmenopausal osteoporosis is summarized in Table 1.2.

Table 1.2 Anti-fracture efficacy of frequently used anti-osteoporotic treatments

	Effect on vertebral fracture risk		*Effect on non-vertebral fracture risk*		*Side effects*
	Osteoporosis	**Women with a prior fracture**	**Osteoporosis**	**Women with a prior fracture**	
Alendronate	+	+	NA	+ (including hip)	GI discomfort, atypical fractures, osteonecrosis of the jaw, atrial fibrillation
Risedronate	+	+	NA	+ (including hip)	
Zoledronic acid	+	+	NA	+	
HRT	+	+	+	+	↑ risk of breast cancer, thromboembolic diseases, ischaemic heart disease
Raloxifene	+	+	NA	NA	↑ risk of thromboembolic diseases, hot flushes
Teriparatide and PTH	NA	+	NA	+	Nausea, pain in limbs, headaches
Strontium ranelate	+	+	+ (including hip)	+ (including hip)	Nausea, diarrhea, cardiac events, DRESS syndrome
Denosumab	+	+	+	+	Increased risk of infections, cardiovascular adverse events, osteonecrosis of the jaw

+ : effective drug

NA: no evidence available
Summarized from (Boonen et al., 2005; Delmas, 2002; Kanis et al., 2008)

Hormone replacement therapy (HRT) – Current menopausal HRT comprises of 17β-oestradiol or conjugated equine estrogen (CEE) supplemented with medroxyprogesterone acetate for women with intact uterus, or unopposed CEE for women who have undergone hysterectomy. HRT was initially prescribed to manage vasomotor symptoms in women and was suggested by observational studies to have beneficial effects on the cardiovascular system and cognitive function. Although HRT was effective in increasing BMD in the hip and spine thereby preventing osteoporotic fractures (Lindsay et al., 2002; Writing Group for the PEPI, 1996), the findings by the Women's Health Initiative (WHI), a randomised, placebo-controlled trial involving more than 16,000 postmenopausal women revealed that women undergoing HRT had significantly increased risks in the following diseases – breast cancer, ischemic heart disease, thromboembolic disease, dementia and cerebral strokes. The study, initially planned for duration of 8.5 years, was terminated at 5.2 years as the risks exceeded benefits of intervention (Writing Group for the Women's Health Initiative, 2002).

The WHI study fuelled research to identify selective estrogen receptor modulators (SERMs) that elicit different effects on estrogen receptors at different tissues. Tamoxifen, a SERM, antagonizes estrogen receptors in breast tissue and was initially found to inhibit breast cancer growth. However, tamoxifen stabilizes ERα and prolonged use may result in tamoxifen-resistant breast cancer (Early breast cancer trialists' collaborative group, 2005). It has also been suggested that tamoxifen contributes to endometrial cancer (Bernstein et al., 1999). Raloxifene is currently the only SERM available for the

prevention and treatment of postmenopausal osteoporosis. While raloxifene therapy has been shown to lead to increases in bone mineral density in the lumbar spine, total hip and femoral neck (Delmas et al., 1997), thereby mitigating fracture risk by 30 – 50%, raloxifene therapy is associated with a significant increase in the risk of venous thromboembolism and pulmonary embolism (Adomaityte et al., 2008). Additionally, the effects of raloxifene therapy on coronary events in women with established coronary heart disease remains controversial (Barrett-Connor et al., 2006; Collins et al., 2009).

Bisphosphonates – Bisphosphonates, the anti-resorptive therapy, are analogues of pyrophosphate and have strong affinities for bone apatite. Bisphosphonates are potent inhibitors of bone resorption and elicit effects by reducing the recruitment and activity of osteoclasts as well as inducing osteoclast apoptosis. Due to the structural similarity to inorganic pyrophosphate, non-nitrogen containing bisphosphonates are incorporated into molecules of newly formed adenosine triphosphate (ATP) after osteoclast-mediated uptake from the bone mineral surface (Russell, 2006). Intracellular accumulation of these nonhydrolyzable ATP analogues results in cytotoxicity and subsequent osteoclast apoptosis. Nitrogen-containing bisphosphonates have a distinct mechanism of action. By inhibiting the mevalonate pathway, these compounds interfere with the isoprenylation of guanosine triphosphate binding proteins and thereby inhibit cytoskeletal reorganization, membrane ruffling and lead to osteoclast apoptosis (Kavanagh et al., 2006).

Nitrogen-containing bisphosphonates such as alendronate, ibandronate and zolendronate, are currently the most widely prescribed group of bisphosphonates (Drake et al., 2008). Although effective at suppressing osteoclast activity, bisphosphonates are associated with adverse side effects. The incidence of osteonecrosis of the jaw (ONJ) has been reported to occur at 1 in 10 000 patients for intravenous administration of bisphosphonates (Khosla et al., 2007) and this risk increases with the use of the more potent bisphosphonates. ONJ may remain asymptomatic for up to years, and may result in pain or exposed maxillary or mandibular bone following inflammation or infection. Signs and symptoms that may occur before the development of clinically detectable osteonecrosis include pain, tooth mobility, mucosal swelling, redness and ulceration. Although these signs and symptoms may occur spontaneously, they commonly develop at the site of earlier dentoalveolar surgery. Although the mechanism by which bisphosphonates lead to ONJ is not fully understood, the pathogenesis of this process is consistent with defective jawbone physiologic remodeling and wound healing (Rodan & Fleisch, 1996). It has been suggested that bisphosphonates, as a result of osteoclast inhibition and apoptosis, interferes with bone remodeling. Furthermore, bisphosphonates have also been shown to inhibit endothelial cell proliferation (Fournier et al., 2002) and have antiangiogenic properties (Wood et al., 2002), thereby impeding wound healing.

Bisphosphonates, by disrupting osteoclast function, suppresses bone remodeling, resulting in increased bone brittleness and an increased risk of

atypical fractures (Odvina et al., 2005). Bisphosphonate-associated atypical fractures are low trauma-induced stress fractures in the compact bone at the subtrochanteric femur and femoral shaft. A cohort study by Schilcher, Michaëlsson, and Aspenberg (2011) involving 13 000 women treated with bisphosphonates showed that the age-adjusted risk of atypical fractures increased by 47.3% when treated with bisphosphonates and this risk increased with a longer duration of use. It has also been reported that intravenous zoledronic acid therapy is associated with a significantly increased risk of atrial fibrillation (Black et al., 2007). Additionally, short-term adverse effects such as upper gastrointestinal side effects and musculoskeletal pain are common among patients, typically affecting adherence rates.

Parathyroid hormone (PTH) – Under physiological conditions, PTH stimulates both bone formation and resorption. However, intermittent administration of PTH or teriparatide (1-34 N terminal fragment of PTH) results in an increase in the number and activity of osteoblasts, thereby leading to an increase in bone mass and an improvement in skeletal architecture (Aslan et al., 2012). Treatment with both agents has been shown to significantly reduce the risk of vertebral fractures in postmenopausal women (Neer et al., 2001). Additionally, the beneficial effects of teriparatide on non-vertebral fractures have been demonstrated to persist for up to 30 months after discontinuation of treatment (Prince et al., 2005).

Common adverse events in patients treated with PTH or teriparatide are nausea, pain in limbs, headache and dizziness. The use of peptides of the PTH

family is contra-indicated in patients with renal impairment, and osteosaracomas. A major drawback of PTH hormone therapy is the need for daily subcutaneous administration, Furthermore the safety of PTH therapy has only been demonstrated for a maximum of 24 months (Prince et al., 2005).

Strontium ranelate – Strontium ranelate has been shown to exert dual actions on bone, enhancing bone formation (Fernandez et al., 2014), while inhibiting resorption (Caudrillier et al., 2010), thereby leading to increases in bone mineral density and reducing fracture risk by ~30% in the hip and vertebrae (Meunier et al., 2004; Stepan, 2013). Common side effects of strontium ranelate treatment include nausea and diarrhea. However, strontium ranelate has also been shown to lead to significant increases in serum levels of calcium leading to serious cardiac side effects and venous thrombo-embolism (Audran et al., 2013). Though rare, strontium ranelate administration has been reported to be associated with severe, potentially lethal skin reactions such as the drug reaction with eosinophilia and systemic symptoms (DRESS) (Jonville-Bera & Autret-Leca, 2011). Due to the severity and number of possible adverse side effects, strontium ranelate is not recommended as the first choice treatment option for older patients (Bernabei et al., 2014)

Denosumab – Denosumab is a human monoclonal antibody that binds to RANKL and prevents its interaction with the RANK receptor, thereby inhibiting osteoclast differentiation and bone resorption. Denosumab, given twice yearly for 36 months, has been shown to increase BMD by up to 7% in postmenopausal osteoporotic patients (McClung et al., 2006), and lead to a

reduction in vertebral and non-vertebral fracture risk by 70% and 20% respectively (Cummings et al., 2009). Similar to bisphosphonates, denosumab treatment has also been reported to be associated with osteonecrosis of the jaw and atypical femoral/ subtrochanteric fractures (Bone et al., 2013; Shane et al., 2010).

1.1.5 Estrogen deficiency-mediated osteoporosis

It is well established that estrogen is a major hormonal regulator of bone metabolism in both men and women. Falahati-Nini et al. (2000) showed that estrogen accounts for up to 70% of the effects of sex steroids on bone metabolism in men. As previously explained, the protective effects of estrogen on bone has been demonstrated in several clinical studies, in which HRT led to significant improvements in BMD and accordingly, a reduction in fracture risk of postmenopausal women (Cauley et al., 2003; Ettinger et al., 1999). As such, it is widely accepted that estrogen deficiency in women, caused by menopause or ovariectomy, results in osteoporosis, and much efforts have been focused on uncovering the mechanisms by which estrogen modulates bone turnover.

At the cellular level, estrogen has been shown to reduce osteoclast resorption by inducing osteoclast apoptosis (Nakamura et al., 2007) and to inhibit RANKL-induced osteoclast differentiation (Kharkwal et al., 2012; Srivastava et al., 2001). Studies have also demonstrated that estrogen can regulate osteoclast formation and activity indirectly by reducing RANKL production by the T cells and osteoblast, while increasing their production of the soluble decoy osteoprotegerin. It has been demonstrated that osteoclast

differentiation and activity are regulated by a variety of cytokines, including interleukin (IL)-1, -6, and -7, tumour necrosis factor (TNF) and RANKL (Horowitz, 1993; Manolagas & Jilka, 1995). Studies have revealed that estrogen moderates expression and production of these pro-inflammatory cytokines to regulate osteoclast differentiation and activity (Cenci et al., 2000; D'Amelio et al., 2008; Roggia et al., 2001). *Ex-vivo* studies have shown greater production of IL-1 from the human peripheral blood monocytes obtained from untreated osteoporotic women compared with estrogen-treated postmenopausal women or untreated premenopausal women (Pacifici et al., 1991). Although it has largely been established that the protective effect of estrogen is mediated in part by suppressing cytokine production, there remain controversies over the precise target cells of estrogen.

Estrogen deficiency leads to an imbalance in bone remodeling, in particular a net increase in bone resorption, thereby leading to osteoporosis (Khosla et al., 2012). It has been shown that estrogen improves the balance in bone remodeling by inhibiting apoptosis of both osteoblast and bone marrow-derived mesenchymal stem cells *in vitro* (Shao et al., 2015*;* Yang et al., 2013). Both estrogen-deficiency and ageing has been associated with an increased production of reactive oxygen species in bone (Almeida et al., 2007), which has been shown to inhibit the differentiation of osteoblasts from their progenitors and decrease the life-span of the bone-forming cells (Almeida et al., 2010). The anti-oxidative properties of estrogen could therefore be an indirect mechanism by which it increases bone formation.

1.1.6 Flavonoids and osteoporosis

Flavonoids are bioactive polyphenols found in a wide diversity of fruits and vegetables. Flavonoids share the same polyphenolic backbone but differ in their arrangement of hydroxyl, methoxy and glycosidic side groups. Based on their biologic activity, these compounds can be divided into two broad categories: (1) flavonoids or bioflavonoids, including the flavones, flavonols anthocyanidins, and catechins, or (2) isoflavones, also known as phytoestrogens. The structure, sources and representative compounds of these flavonoid subclasses are summarized in Table 1.3.

Epidemiologic associations have been demonstrated between flavonoid intake and markers of bone health. In a retrospective study of 3000 peri-menopausal women, a positive association between total dietary flavonoid intake and bone mineral density of the spine and femoral neck was shown, along with a reduction in markers of bone resorption (Hardcastle, Aucott, Reid, & Macdonald, 2011). Additionally, negative associations between both catechins and flavanones with bone resorption markers were detected in this study. Welch et al. (2012) demonstrated in an observational study of 3000 women a positive association between anthocyanins intake and BMD at both the hip and spine, while flavanone intake was positively associated with hip BMD. Interestingly, consumption of tea, a rich source of catechins, has been reported to reduce the risk of hip fractures (Johnell et al., 1995).

Isoflavones, the major phytoestrogen contained in soybeans, are structurally similar to estrogen and bind to and activate estrogen-receptors (Kuiper et al.,

1998). Observational studies suggest that soy consumption contributes to low rates of hip fractures in Asians (Ross et al., 1991; Ye et al., 2006). In the Shanghai Women's Study involving 75,000 women, hip fracture prevalence was inversely related to soy consumption (Zhang et al., 2005). Furthermore, a stronger relationship was detected in early (< 10 years) rather than late menopausal women. This discrepancy could be due to a greater responsiveness to soy isoflavones during the early phase of estrogen deficiency. Interestingly, soy isoflavones have been shown to lead to a decrease in urine deoxypyridinoline, a bone resorption marker, but did not lead to significant changes in serum bone formation markers alkaline phosphatase and osteocalcin, which could account for the greater responsiveness to soy isoflavones during the early phase of estrogen-deficiency when there is increased bone resorption (Eghbali-Fatourechi et al.; Taku et al., 2011). Meta-analysis of randomized controlled trials involving the dominant soy isoflavone revealed that 120 mg of genistein aglycone was modestly protective for femoral neck BMD compared with placebo (Shedd-Wise et al., 2011). Morabito et al. (2002) showed in a double-blind randomized controlled trial of postmenopausal women that genistein treatment was as effective as HRT in inhibiting bone turnover, leading to increased BMD in the femur and lumbar spine.

Table 1.3 Occurrence of flavonoids in foods

Group	*Structure*	*Source*	*Representative flavonoids*
Flavonol	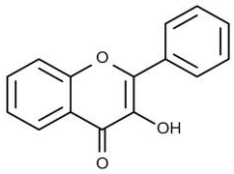	Onion, kale, broccoli, apples, cherries, berries, tea, red wine	Quercetin, rutin, kaempherol
Flavones	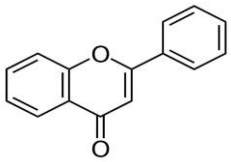	Parsley, thyme	Apigenin, luteolin
Prenylflavonoids	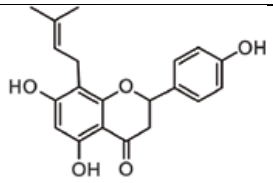	Hops, beer, Epimedium	8-prenylnaringenin, Xanthohumol, Icaritin
Catechins	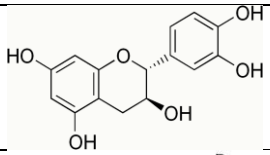	Apple, tea, red wine	Catechin, epicatechin
Anthocyanidins	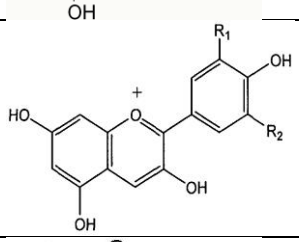	Cherries, grapes, berries, red wine, strawberries, fruit peels with dark pigments	Cyanidin
Isoflavones	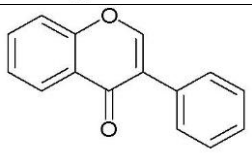	Soy beans, legumes	Dadzein, genistein

Summarized from (Nijveldt et al., 2001; Weaver, Alekel, Ward, & Ronis, 2012)

1.2 Bone metabolism

Bone is a composite material made up of approximately 70% mineral (hydroxyapatite), 22% proteins such as Type I collagen and 8% water by weight. As a vital component of the skeletal system, bone plays a role in several physiological functions: first, it has a structural function in providing support and protection of vital internal organs and bone marrow, as well as muscle attachment sites to enable locomotion. Second, the skeleton, as a reservoir of calcium and phosphate, has an essential metabolic function in maintaining serum homeostasis of these ions. Third, the red bone marrow housed within the skeleton contains haematopoietic stem cells essential for the production of blood cells.

1.2.1 Macroscopic organization of bone

Bone tissue is classified as either compact/ cortical bone or spongy bone depending on the organization of the bone matrix and cells. Bones in the body can be made up of both the compact and spongy bone. The physical structure of a typical long bone is shown in Fig. 1.1.

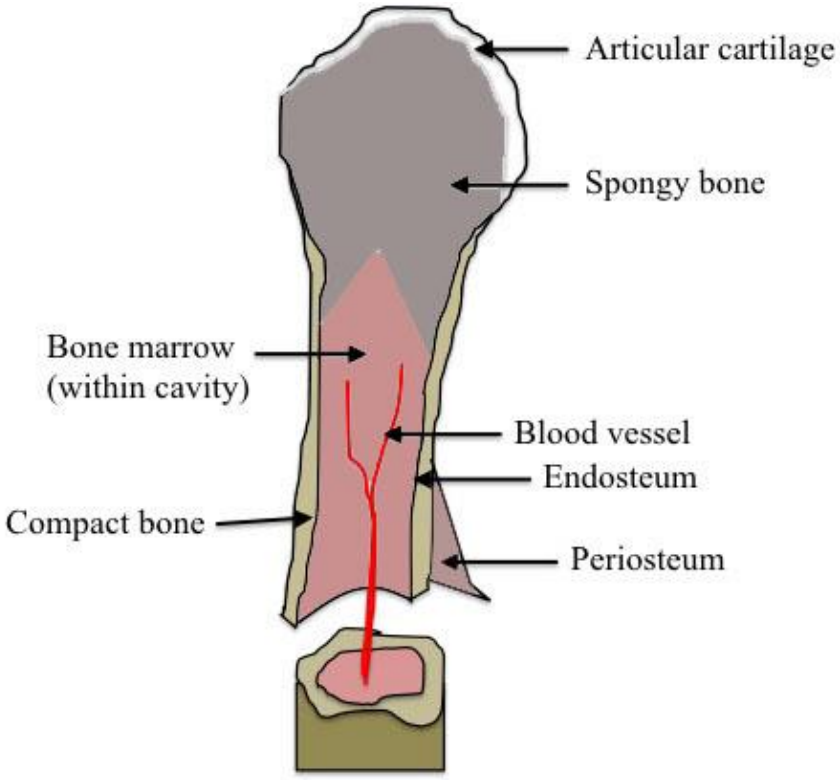

Figure 1.1 Structure of a long bone. The articular cartilage reduces friction at the articulating joints and acts as a shock absorber. The endosteum is a membrane that lines the cavity of bones. The periosteum is the tough fibrous membrane that covers the outside of bones not covered by the articular cartilage. *Adapted from Thompson (2002).*

Compact bone

Compact bone forms the outer layer of all bones. It provides protection and support to the bone and enables long bones to bear the stresses placed on them. Compact bone is loaded mostly by bending moments, resulting in a high percentage of tensile stresses (Augat & Schorlemmer, 2006). The hardness of cortical bone is associated with its mineral content and bone density, whereas its strength is associated with the quality and orientation of the collagen matrix.

The osteon, otherwise known as the Harversian system, makes up the basic three-dimensional unit of compact bone (Fig. 1.2). Each Harversian system comprises of the following parts:

(a) A central Harversian canal that contains blood vessels and nerves. The harversian canal is surrounded by layers of

(b) Lamellae, which are concentric rings of matrix formed from calcium and phosphate salts that crystalize around the collagen fibres.

(c) Lacunae are small spaces between the lamellae in which osteocytes are located.

(d) Canaliculi are minute channels that link the lacunae and provide routes by which nutrients can reach the osteocytes.

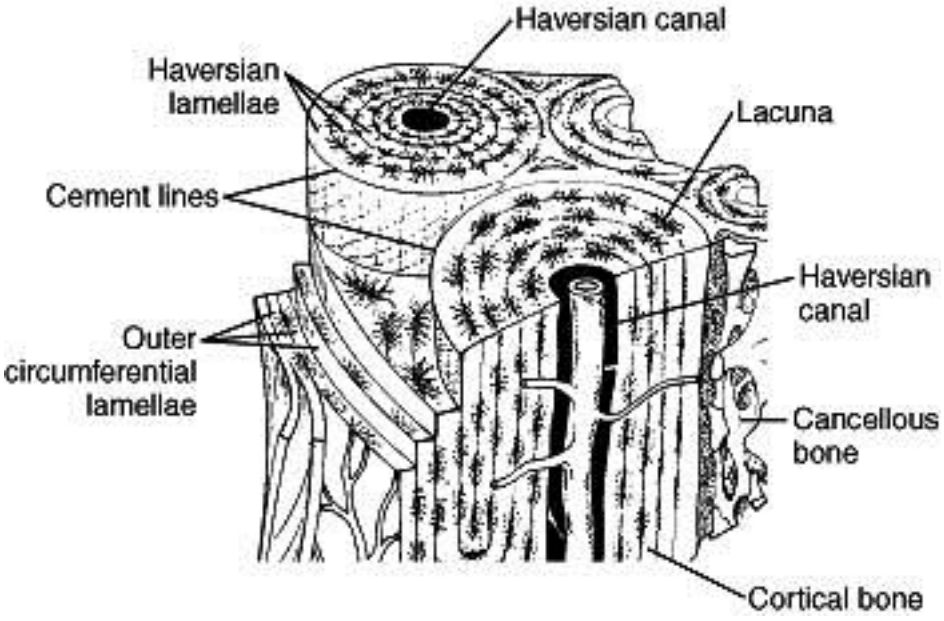

Figure 1.2 Organization of Harversian system. *Adapted from Thompson (2002).*

Spongy bone

The spongy bone is made up of an irregular lattice of trabecular bone, which contains lamellae, osteocytes, lacunae and canaliculi. Blood vessels from the periosteum penetrate into the trabecular lattice to provide nutrients to the osteocytes. Red bone marrow present within the spongy bone is responsible for production of red blood cells, platelets and white blood cells.

1.2.2 Bone remodeling

Bone is a dynamic tissue that undergoes constant remodeling in response to mechanical loads. The remodeling process is the manner in which bone tissue is renewed, with about 10% of bone material renewed each year (Lerner, 2006). This remodeling process (described in Fig. 1.3) is organized in the basic multicellular unit (BMU) and is crucial for the maintenance of the quality and size of the skeleton. The BMU is a temporary anatomic structure that comprises of the osteoblasts, osteocytes and osteoclasts, covered by a canopy of bone lining cells. Bone remodeling requires the coordinated action of these cell types. It has been demonstrated that the rate of advancement of the BMU in the direction parallel to the long axis of bone proceeds at approximately 25 μm/day (Jaworski, 1992). This advancement of the BMU persists for 6 – 9 months (Jilka, 2003).

The remodeling process involves four major but overlapping phases (Feng & McDonald, 2011):

Phase 1 – initiation/ activation of bone remodeling at a specific site

Phase 2 – bone resorption along with the simultaneous recruitment of mesenchymal stem cells (MSCs)

Phase 3 – osteoblast differentiation and its function in osteoid synthesis

Phase 4 – mineralization of the osteoid

It has been proposed that osteocytes are the cells responsible for initiating bone remodeling by transmitting an as yet unidentified signal to recruit osteoclast precursors to specific bone sites. Bone remodeling is initiated in response to bone deformation as a result of mechanical loading or microdamage in old bone (Parfitt, 2002). The bone-remodeling compartment is a closed system that is highly vascular and is characterized by a canopy of bone-lining cells. Osteoclast precursors may be recruited from the bone marrow or from capillaries that penetrate into the remodeling compartment. The osteoclast precursors then attach to the surface of bone and differentiate into osteoclasts (greater detail in following section), resorbing trenches that are 40 – 60 μm deep (Hadjidakis & Androulakis, 2006). The remodeling process proceeds to Phase 2 in which bone resorption is the predominant event. In phase 2, MSCs are also recruited from the bone marrow or capillaries and differentiate into preosteoblasts and osteoblasts. In phase 3, osteoid synthesis supersedes bone resorption as the predominant event. Of the four phases, phase 3 continues for the longest amount of time to allow more bone to be replaced with osteoids produced by the osteoblasts. The osteoids are mineralized in phase 4 to conclude the remodeling cycle (Proff & Römer, 2009). Postmenopausal osteoporosis results from the increase in frequency of

activation of BMUs, with the balance in bone remodeling tipped towards net resorption.

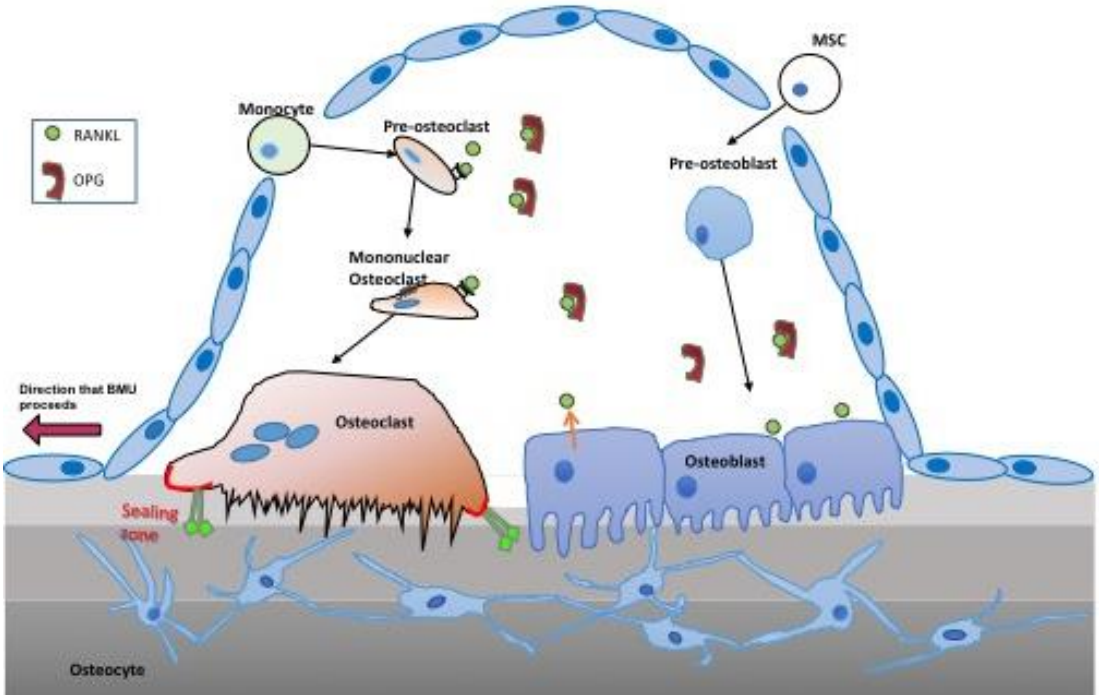

Figure 1.3 Bone remodeling in the basic multicellular unit. During bone turnover, bone-lining cells shift away from the bone surface to allow the osteoclasts, that proceed in front, and osteoblasts, that follow behind, to perform their respective functions. Monocytes enter the remodeling site and undergo differentiation in the presence of the Receptor Activator of NFκB Ligand (RANKL) to become a mature osteoclast, which then initiates bone resorption. The osteoblast precursors, mesenchymal stem cells (MSC), also enter the remodeling site and undergo osteogenic differentiation into mature osteoblasts. Functional osteoblasts then mineralize the areas it is adhered to. In addition, osteoblasts express RANKL, necessary for osteoclast differentiation, as well as OPG, which are decoy recptors that bind RANKL. The osteoblasts therefore modulate osteoclast differentiation via its relative expression of RANKL: OPG. *Adapted from Indran et al. (2016).*

1.2.3 Bone cells

Osteoblasts

Osteoblasts are derived from the multipotent mesenchymal stem cells found in the bone marrow. These mesenchymal stem cells possess the ability to differentiate into osteoblasts, adipocytes, mycoytes, neurons, and chondrocytes. The release of growth factors from the bone matrix during bone resorption activates osteoblast differentiation (Udagawa, 2012). The osteoblasts line the surfaces of bone and are responsible for synthesizing and secreting organic bone material. These cells produce a combination of extracellular proteins, including osteocalcin, alkaline phosphatase and collagen fibrils. The extracellular matrix, made up of type I collagen, is known as the osteoid prior to its mineralization with calcium phosphate. Osteoblasts express RANKL, crucial for the osteoclast differentiation process (as will be further described below). By secreting osteoprotegerin (OPG), the soluble decoy peptide that binds to RANKL and prevents the ligand from binding to its receptor, osteoblasts are able to modulate osteoclast differentiation. Replacement of resorbed bone by a group of osteoblasts is a process that takes approximately 3 months (Jilka, 2003). After which, the remaining osteoblasts that have not undergone apoptosis or become embedded in the bone matrix will become the bone-lining cells over the quiescent bone surface (Boyce et al., 2002; Parfitt, 1990). As such, the lifespan of the osteoblast is approximately 100 days.

The differentiation of osteoblasts is divided into stages of mesenchymal progenitors, preosteoblasts and mature osteoblasts. Preosteoblasts include all cells transitioning from mesenchymal progenitors into mature osteoblasts. While osteoblasts are characterized by the expression of osteocalcin, molecular markers for mesenchymal progenitors and preosteoblasts include transcription factors SOX9, RUNX2 and osterix (Long, 2012).

Osteocytes

Osteoblasts that are trapped within the collagenous matrix are calcified to form osteocytes. These cells are regularly dispersed throughout the mineralized matrix and are the most abundant cell type in bone. Osteocytes extend dendritic processes through the bone in "tunnels" known as cannaliculi to facilitate communication with each other and the bone lining cells and osteoclasts. Given that osteocytes make up 90-95% of all bone cells, coupled with their wide distribution through the bone matrix and high degree of interconnectivity, it has been suggested that the osteocytes function as mechanosensors that transduce mechanical strain into biochemical signals to affect bone remodeling (Bonewald, 2006; Verborgt et al., 2000).

Osteoclasts

Osteoclasts are the cells responsible for bone resorption. These multinucleated cells originate from the hematopoietic lineage and are formed from fusion of mononuclear progenitors such as monocytes or bone marrow macrophages. Receptor activator of NFκB (RANK) is expressed on the membranes of osteoclast precursors and osteoclasts in response to another

critical osteoclastogenic cytokine, macrophage colony stimulating factor (MCSF). Additionally, MCSF induces the proliferation of the osteoclast precursors and enhances the survival of osteoclasts (Teitelbaum, 2000). The binding of RANKL to its receptor leads to the differentiation and fusion of mononuclear precursors into multinucleated osteoclasts (Fig. 1.4). The mature multinucleated osteoclasts, expressing tartrate-resistant acid phosphatase (TRAP), undergo cytoskeletal reorganization to attach to the surface of bone through the formation of the actin-bound sealing zone (Boyce et al., 2003). The sealing zone, as its name suggests, seals the resorbing lacuna and segregates this microenvironment from the extracellular environment. The ruffled border is a specialized membrane that is formed within the circumferential sealing zone and is the site of active secretion. Within the sealing zone, the osteoclasts secrete proteolytic enzymes such as Cathepsin K and matrix metalloproteinase to break down the collagenous matrix. Osteoclasts also maintain an acidic pH within the sealing zone to dissolve the inorganic bone matrix, leading to the formation of resorption pits (Rousselle & Heymann, 2002). The osteoclast is a prominently polarized cell with the functional secreting domain, involved in transcytosis of degraded matrix products, located opposite to the ruffled border (Coxon & Taylor, 2008; Takahashi et al., 2007).

It has also been demonstrated that osteoclast differentiation is regulated by various cytokines such as Interleukin (IL)- 1, -7, and tumour necrosis factor (TNF). IL-1 and TNFα are potent cytokines that have been shown to induce bone erosion in inflammatory sites such as in rheumatoid joints. Both IL-1 and

TNFα have synergistic effects with RANKL on inducing osteoclast formation to upregulate expression of osteoclast-specific genes. Further, RANKL also enhances the expression of IL-1 receptor type I to perpetuate osteoclast differentiation (Kim et al., 2009). IL-1 and TNFα enhance osteoclast differentiation both directly and indirectly. At the molecular level, both cytokines activate pathways that overlap significantly with RANKL-induced signaling cascades (Zhang et al., 2001). IL-1 and TNFα also increase stromal cell production of IL-7. IL-7 indirectly induces differentiation of osteoclast precursors into mature activated osteoclasts by stimulating T-cells production of osteoclastogenic cytokines (Weitzmann et al., 2000). Indeed, it has been suggested that estrogen withdrawal increases the production of pro-inflammatory cytokines that drive osteoclast formation and resorption, contributing to the development of postmenopausal osteoporosis (Mundy, 2007).

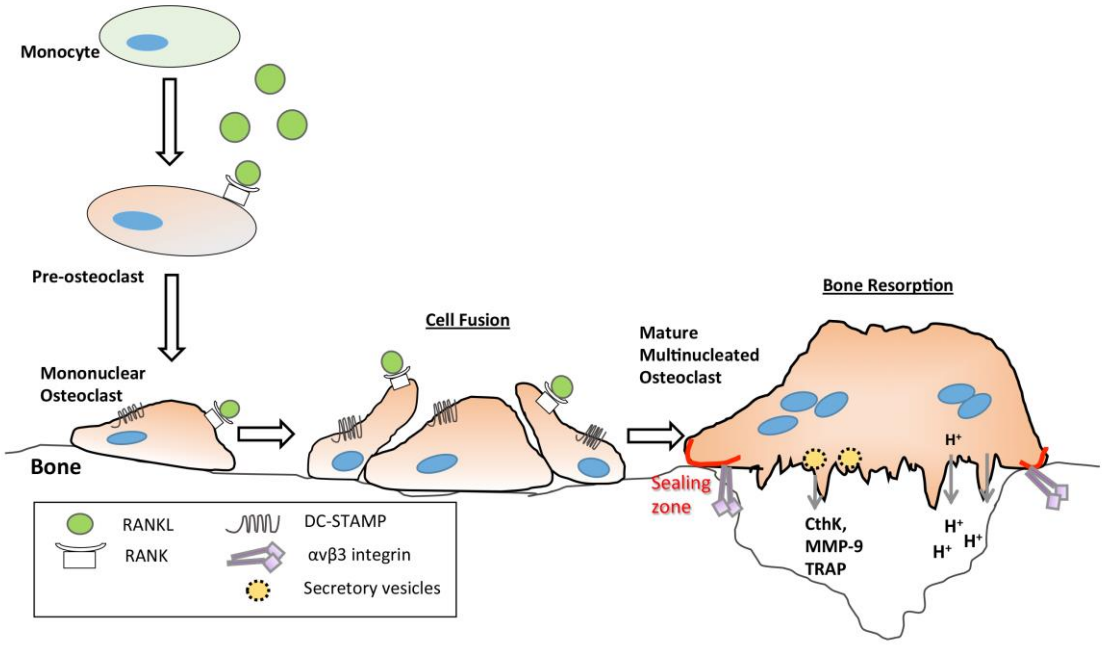

Figure 1.4 Osteoclast differentiation process and bone resorption. RANKL, upon binding to its receptor, RANK, commits a monocyte to osteoclast differentiation. This leads to the expression of osteoclast-specific genes such as the fusion receptor dendritic cell-specific transmembrane protein (DC-STAMP) and secretory enzymes Cathepsin K (CthK), matrix metalloproteinase-9 (MMP-9), and tartrate-resistant acid phosphatase (TRAP). DC-STAMP enhances cell-to-cell fusion of the mononuclear osteoclasts to form a giant multinucleated osteoclast, which attach to the surface of bone by forming the sealing zone. The $\alpha_v\beta_3$ integrin binds to RGD-containing peptides present in abundance in bone and has been shown to play a role in osteoclast movement (Holt & Marshall, 1998). Active secretion by osteoclasts occurs at the ruffled border of the plasma membrane. The osteoclasts maintain an acidic pH in the resorption zone and release enzymes such as CthK, MMP-9, and TRAP via secretory vesicles. *Adapted from Indran et al. (2016).*

1.3 Osteoclastogenesis and the RANKL/RANK signaling pathway

The binding of RANKL to its receptor, RANK, triggers signaling cascades that regulate osteoclast differentiation and activation (Fig. 1.5). The RANK receptor protein, a member of the tumour necrosis factor (TNF) receptor super family, lacks intrinsic kinase activity and relies on the recruitment of intermediate adaptor proteins to activate downstream signaling pathways (Darnay et al., 2006; Walsh, 2014). Activation of RANK is followed by the receptor's trimerization and recruitment of TNF receptor associated factors (TRAFs) that facilitate activation of downstream signaling cascades such as the NFκB, MAPK/AP-1, phosphatidylinositide 3-kinase (PI3K)/AKT signaling pathways (Darnay et al., 2006; Kim & Kim, 2016). Activation of these signaling cascades mediate the expression and activity of nuclear factor of activated T cell-1 (NFATc1), the master transcription factor regulating osteoclastogenesis.

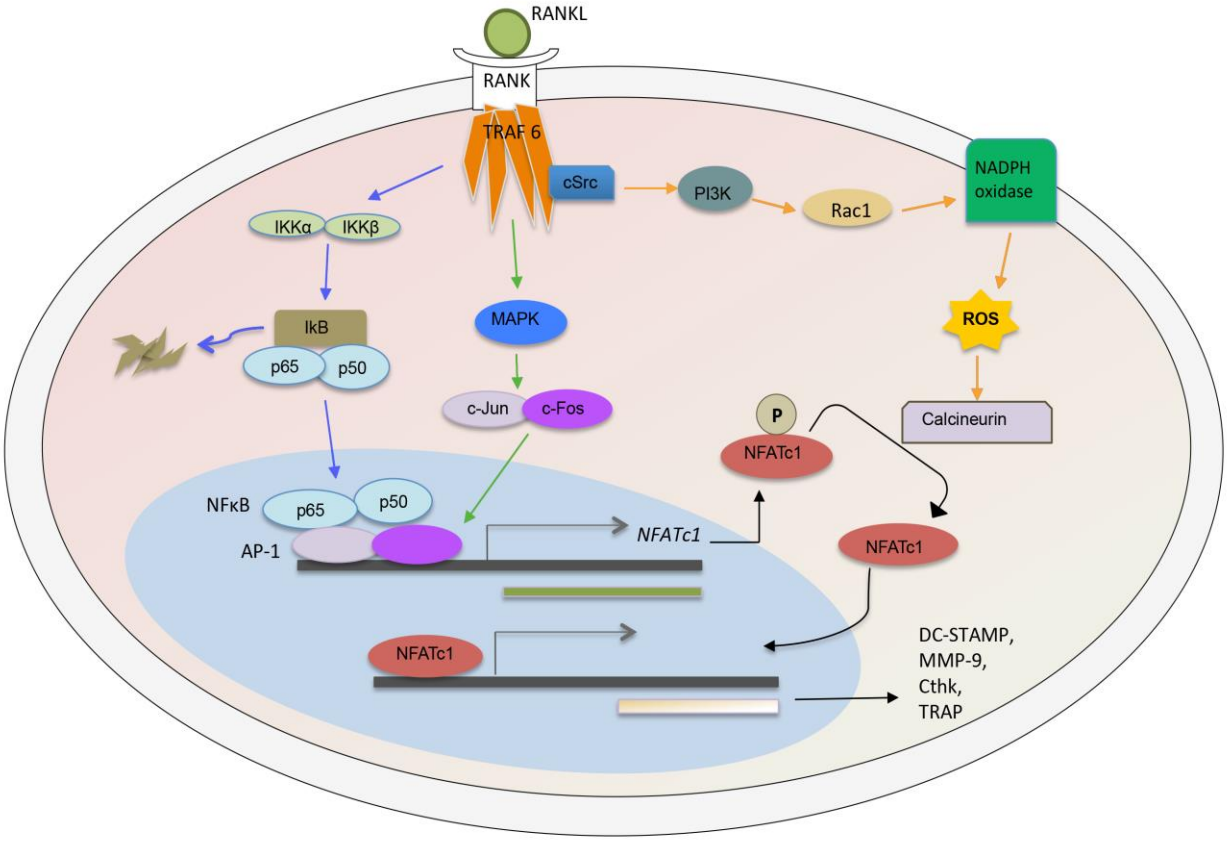

Figure 1.5 RANKL/RANK signaling pathway. The binding of RANKL to its receptor, RANK, triggers the RANKL signaling cascade *in vitro*. The RANKL signaling cascades include the NFκB (blue arrows), MAPK (green arrows) and cSrc/PI3K/Nox1 (orange arrows) pathways, which are modulated via recruitment of the TNF receptor associated factor 6 (TRAF6) adaptor protein. This leads to increased nuclear translocation of transcription factors NFκB and AP-1, thereby increasing gene expression of the NFATc1 transcription factor. RANKL, by activating the Nox1 enzyme, also induces an increased production of intracellular ROS, which then activates the phosphatase calcineurin, thus increasing nuclear translocation of NFATc1. NFATc1 leads to increased expression of osteoclast-specific genes as previously explained, thereby regulating osteoclast differentiation. (Not shown in this diagram) The binding of M-CSF to its surface receptor c-Fms results in dimerization of the receptor and activation of receptor tyrosine kinase (RTK) ultimately leading to increased differentiation into, proliferation of osteoclast precursors, and fusion of these precursors (Hodge et al., 2007; Ross, 2006).

1.3.1 Importance of TRAF6 in RANK signaling

The TRAF family consists of seven known proteins that function as adaptors for the TNF-receptor super family. Although Pullen *et al.* (1999) demonstrated that TRAF1, TRAF2, TRAF3, TRAF5 and TRAF6 interact with the cytoplasmic domain of RANK, only TRAF2, TRAF5 and TRAF6 have been demonstrated to be functionally competent in activating downstream signaling pathways, given that specific deletion of these TRAF-binding regions on the cytoplasmic domain of RANK resulted in failure to activate NFκB *in vitro* (Darnay et al., 1998). The significance of TRAF6 in bone metabolism was made apparent with TRAF6 deficient mice exhibiting defective osteoclastogenesis and severe osteopetrosis (Lomaga et al., 1999), however, the functional significance of TRAF2 and TRAF5 in osteoclastogenesis remains to be elucidated, given that TRAF2 and TRAF5 deletion in mice did not lead to osteopetrosis (Galibert et al., 1998) .

The N-terminal of TRAF6 comprises of a RING finger domain and consequently, TRAF6 has also been shown to function as a ubiquitin E3 ligase (Wang et al., 2001; Wu & Arron, 2003). However, the primary function of TRAF6 is not to target proteins for proteasomal degradation but to activate downstream signaling cascades. Indeed, it has been suggested that auto-ubiquitination of TRAF6 via lysine63-linked polyubiquitin chains is crucial for the formation of complexes that activate downstream cascades (Kanayama et al., 2004). Additionally, TRAF6 catalyzes lysine63-linked polyubiquitin chains to mediate activation of TGFβ-activated kinase 1 (TAK1) that further activates the MAPK kinase 6 and inhibitor of NFκB alpha (IκBα) kinase (IKK) complexes

(Deng et al., 2000; Mizukami et al., 2002).

1.3.2 NFκB signaling cascade in osteoclast differentiation

As suggested by its name, stimulation of RANK leads to strong activation of the Nuclear Factor of κB (NFκB) transcription factors. RANKL, via TRAF6, rapidly stimulates the activation of the classical and alternative NFκB pathways in osteoclast precursor cells. The NFκB family is a group of dimeric transcription factors that consists of five members: cRel, RelA (p65), RelB, NFκB1 (p105/p50) and NFκB2 (p100/p52). TRAF6 facilitates ubiquitination of TAK1 and two adaptor molecules, TAB1/2, leading to activation of the classical NFκB pathway, by activation of the inhibitor of κB (IκB) kinase (IKK) complex. cRel, p65 and p50 are sequestered in the cytoplasm by IκB proteins. The IKK complex phosphorylates IκB, leading to its proteasomal degradation, thereby releasing the bound NFκB dimers to translocate to the nucleus (Fig 1.5, blue arrows). In the alternative pathway, NFκB-inducing kinase (NIK) and IKKα induces the phosphorylation-dependent proteolytic cleavage of NFκB2, allowing RelB-p52 dimers to translocate to the nucleus.

The importance of the NFκB family of dimeric transcription factors to osteoclastogenesis was revealed when deletion of the NFκB1/p50 and NFκB2/p52 subunits led to severe osteopetrosis in mice as a result of osteoclast deficiency (Iotsova et al., 1997; Monje et al., 2005). While RANKL has also been shown to activate the alternative NFκB pathway by triggering the NFκB-inducing kinase leading to the eventual generation of the p52-RelB

dimer (Novack et al., 2003), it remains unclear which of the two NFκB pathways are dominant in osteoclast differentiation. Nevertheless, Asagiri et al. (2005) have shown using ChIP experiments that the p50-p65 subunits are recruited to the NFATc1 promoter following RANKL stimulation, indicating that these NFκB components are crucial in regulating the expression of NFATc1.

1.3.3 MAPK/AP-1 signaling cascade in osteoclast differentiation

C-Fos, a member of the AP-1 family of transcription factors, has been shown to be indispensable for osteoclast differentiation given the osteopetrotic phenotype of c-Fos knockout mice (Grigoriadis et al., 1994; Wang et al., 1992). It was further delineated that c-Fos is crucial to the induction of NFATc1 since recruitment of c-Fos to the NFATc1 promoter has also been demonstrated. Additionally, induction of NFATc1 mRNA by RANKL is abrogated in c-Fos deficient cells (Asagiri et al., 2005; Iotsova et al., 1997). Given that c-Fos can only heterodimerize with members of the Jun family to form the AP-1 heterodimer, Soysa and Alles (2009) demonstration that expression of NFATc1 is Fos/Jun dependent is in keeping with the presence of AP-1 response elements in the NFATc1 promoter (Asagiri et al., 2005).

Expression and activity of the AP-1 transcription factor is regulated by the mitogen-activated protein kinases JNK, ERK and p38 (Fig 1.5, green arrows). The c-Jun N-terminal Kinase (JNK) regulates transcriptional activity of c-Jun by phosphorylation of two serine sites within the transcriptional activation domain (Hilberg et al., 1993). Activation of the extracellular-signal regulated

kinase (ERK) has been shown to increase expression of c-Fos, while phosphorylation of the transactivation domain of c-Fos by p38 increases the transcriptional activity of AP-1 (Monje et al., 2005; Novack et al., 2003). Additionally, there is a wealth of studies demonstrating that RANKL induces activation of the JNK, ERK and p38 kinases, that when disrupted interferes with osteoclast differentiation *in vitro* (Kashiwada et al., 1998; Matsumoto et al., 2000). Hence, MAPK regulated AP-1 expression and activity is crucial for the expression of NFATc1 and osteoclast differentiation.

1.3.4 Intracellular ROS in osteoclast differentiation

There has been a recent accumulation of evidence supporting the importance of intracellular reactive oxygen species (ROS) as a secondary messenger in RANKL-mediated osteoclastogenesis (Kim et al., 2010; Lee et al., 2005; Lee & Jang, 2015; Moon et al., 2011). It was demonstrated that RANKL, by recruitment of TRAF6, activates a signaling cascade involving cSrc, PI3K and the Rac1 GTP-ase in order to activate the Nox1 enzyme responsible for the intracellular ROS production (Fig 1.5, orange arrows). While N. K. Lee et al. (2005) demonstrated that this increase in intracellular ROS occurs in the acute time frame (within 30 min) following RANKL stimulation and lies upstream of MAPK activation, M. S. Kim et al. (2010) showed that the chronic (> 24 hours) and not acute transient ROS production following RANKL stimulation mediates calcineurin activation via calcium oscillations. RANKL induces phosphorylation and activation of phospholipase-Cγ (PLC_Y) which then increases intracellular Ca^{2+} levels ($[Ca^{2+}]_i$) via several sequential steps: PLC_Y hydrolyses phosphatidylionositol-biphosphate into inositol-

triphosphate (IP3). IP3 binds to IP3-receptors in the endoplasmic reticulum triggering the release of Ca^{2+} from ER stores. The increase in $[Ca^{2+}]_i$ leads to activation of calcineurin, which dephosphorylates several phosphoserines on NFATc1 to allow its nuclear translocation and activation (Hogan, 2003). Indeed, Kim et al. (2010) showed that application of the ROS scavenger, N-acetyl cysteine (NAC), or a Nox1 inhibitor, abrogated RANKL-induced $[Ca^{2+}]_I$ oscillations, indicating that RANKL-induced ROS production is crucial for mediating calcineurin activation. Furthermore, both studies demonstrated the importance of intracellular ROS production to osteoclast differentiation, where application of NAC, or silencing the expression of Nox1 completely abolished osteoclast formation.

The anti-osteoclastogenic effects of compounds such as genistein (Lee et al., 2014), resveratrol (He et al., 2010), scoparone (Lee & Jang, 2015) and rutin (Kyung et al., 2008) have also been attributed to their anti-oxidative properties.

1.3.5 Role of NFATc1 in osteoclast differentiation

As previously described, NFATc1 activation is initiated by dephosphorylation of the NFAT regulatory domain. This domain, heavily phosphorylated in resting cells, is dephosphorylated by calcineurin to trigger NFATc1 nuclear accumulation and enhance its transcriptional activity (Beals et atl., 1997; Okamura et al., 2000). The importance of NFATc1 to osteoclast differentiation was demonstrated with NFATc1-deficient stem cells' inability to differentiate into osteoclasts upon RANKL stimulation, while ectopic expression of NFATc1

causes embryonic stem cells to undergo efficient differentiation in the absence of RANKL signaling (Takayanagi et al., 2002). It has been suggested that the exclusive function of NFATc1 in osteoclastogenesis is a result of an NFATc1-specific gene regulatory mechanism. In support of this hypothesis, RANKL induces NFATc1 selectively and potently, while NFATc2 mRNA is expressed constitutively in precursor cells at a low basal level. Furthermore, ChIP experiments revealed that NFATc1 but not NFATc2 is recruited to the NFATc1 promoter after RANKL stimulation, indicating that autoamplification mechanism by NFATc1 is specifically operative in its promoter. Based on promoter analysis, it was found that NFATc1 directly regulates multiple osteoclast-specific genes. These include TRAP, Ctsk, calcitonin receptor, and $\alpha_v\beta_3$ integrin (Matsumoto et al., 2000; Takayanagi et al., 2002). AP-1 is a known transcriptional partner of NFAT in lymphocytes and the NFATc1:AP-1 complex is important for the induction of TRAP, calcitonin receptor genes as well as amplification of NFATc1. NFATc1 also forms an osteoclast-specific transcriptional complex containing AP-1 (Fos/Jun) and microphthalmia-induced transcription factor (MITF) for efficient induction of osteoclast-specific genes (Takayanagi, 2007). The components of the NFATc1 transcriptional complex are not always the same suggesting that differential composition of the transcriptional complex contributes to spatiotemporal expression of each gene during osteoclast differentiation.

1.4 Epimedium (Berberidaceae) for bone health

The dried aerial parts of *Epimedium* (Berberidaceae), colloquially known as Yin Yang Huo, have been used by traditional chinese medicine practitioners to treat a number of conditions. The use of this herb was first prescribed in the Copendium of Materia Medica (Bencao Gangmu), written in 1578. The Epimedium genus comprises of 52 species of herbaceous plants (Stearn, 2002). This herb is used popularly either singularly or in combination with other herbs to treat a plethora of conditions such as osteoporosis, cardiovascular diseases, sexual dysfunction and menstrual irregularity (Meng et al, 2005; Zhang et al, 2006).

1.4.1 Chemical constituents of the genus *Epimedium*

More than 260 compounds have been identified in the plants of the *Epimedium* genus (Ma et al., 2011), of which prenylflavonoids have been found to be the major constituents, forming more than 50% by weight of ethanolic extracts (Shen et al., 2007). Icariin is the most abundant compound, forming up to 6.5% of the dried weight of an ethanolic extract, and is therefore used as the chemical marker for the standardization of the quality of *Epimedium* extracts (Chinese Pharmacopeia, 2010). When consumed orally, the flavonoid glycoside is deglycosylated to form the main active metabolites icaritin and desmethylicaritin (Fig. 1.6). The osteogenic properties of *Epimedium* compounds demonstrated in both preclinical and clinical studies have been reviewed elsewhere (Indran et al., 2016).

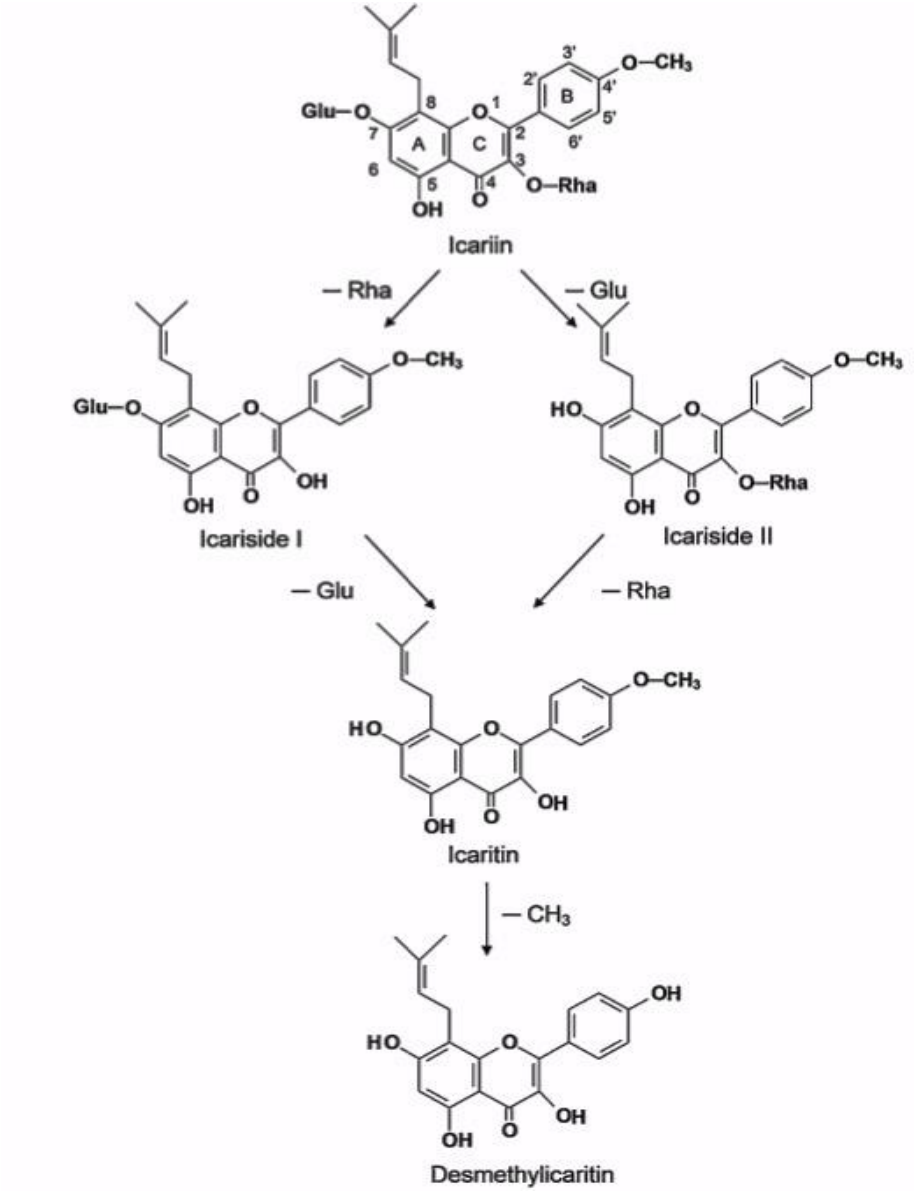

Figure 1.6 Structures of Icariin and its derivatives. Icariin when consumed orally, is deglycosylated with the removal of its rhamnose (Rha) and glucose (Glu) to form the metabolites as indicated. Figure taken from (Wong et al., 2009)

1.4.2 Effects of icaritin on bone

Bone formation

Icaritin enhances rat osteoblast proliferation and differentiation, leading to increased calcium deposition and increased mRNA expression of osteoblast genes (Huang et al., 2007). Icaritin has also been shown to enhance osteogenic differentiation of human MSCs to osteoblasts under osteogenic induction conditions while inhibiting adipogenic differentiation (Yao et al., 2012). Peng et al. (2013) showed that icaritin treatment that began one month but not three months post-ovariectomy led to a significant improvement in the bone architecture and strength of the OVX rats. *Ex-vivo* culture of bone marrow stromal cells (BMSCs) from icaritin-treated OVX rats also showed increased osteogenic differentiation along with suppressed adipogenesis. The osteogenic effects of icaritin have also been demonstrated in bone defect repair models (Chen et al., 2013; Qin et al., 2015; Wang et al., 2013). Icaritin, when incorporated in a poly lactic-co-glycolic and tricalcium phosphohate scaffold to enable its sustained release, significantly reduced the incidence of femoral head collapse and led to improved mechanical properties by enhancing new bone formation (Qin et al., 2015). Mechanistic studies revealed that icaritin led to increased BMSCs recruitment into the icaritin-incorporated scaffolds and led to the increased expression of osteogenesis-related genes in the BMSCs.

Bone resorption

Huang et al. (2007) demonstrated that icaritin treatment inhibits osteoclast formation *in vitro* and suppressed RANKL-induced ROS production in RAW 264.7 mouse macrophage cells. Interestingly, icaritin was found to exhibit a significantly greater inhibition on osteoclast actin ring formation than icariside, icariin, and the soybean isoflavone, genistein. Peng et al. (2013) showed that early icaritin treatment inhibited bone resorption in the OVX rats and led to decreased osteoclast-related gene expression in bone homogenates. However, the molecular mechanisms by which icaritin inhibits osteoclast formation and resorption have not been identified.

1.4.3 Dietary source of icaritin

As previously outlined, icaritin is the main prenylflavonoid derived from the *Epimedium* species of herbs when consumed orally. Zhang et al. (2007) demonstrated in the randomized double-blind placebo-controlled trial that 24 months' treatment with 60 mg icariin, 15 mg dadzein and 3 mg genistein daily lead to significant improvements in lumbar spine BMD. Zhu et al. (2012) studied the effects of the capsular form of the Fufang Xian Ling Gu Bao decoction in postmenopausal women, and although effective in improving BMD, subjects needed to consume a daily minimum of 3g of the decoction. Thus, the primary disadvantage of using Epimedium-derived flavonoids or its herbal formulas is the daily requirement of a high drug volume/ dosage, which has been reported to lead to low adherence levels due to side effects in the digestive tracts. Nevertheless, this drawback can be resolved by identifiying the active molecular compound(s) of the epimedium-derived flavonoids, or by

developing an extraction method that enriches the concentrations of the active compound(s).

1.5 Cellular models of osteoclastogenesis

Since osteoclasts are derived from haematopoietic precursors, *in vitro* models of osteoclastogenesis involve the differentiation of monocytes/ macrophages or splenocyte precursors. Prior to the discovery that osteoblasts or marrow-derived stromal cells release an osteoclast differentiation factor (Quinn et al., 1998), that has since been identified as RANKL (Yasuda et al., 1998), haematopoietic cells or monocytes used to be co-cultured with osteoblasts/ stromal cells. However, the presence of recombinant MCSF and RANKL have allowed *in vitro* differentiation of the precursor cells and cell lines that are commonly used.

1.5.1 Osteoclast-generating cocultures

In this co-culture system, the osteoblast cultures must first be prepared. These osteoblast cultures can be obtained either by sequential collagenase digestion (Bakker & Klein-Nulend, 2012) or the use of osteoblast-like cell lines such as UMR 106, and allowed to reach confluence. Osteoclast precursor cells such as bone marrow macrophages are typically isolated from the long bones of mice, or from peripheral blood as will be explained in later sections and cultured with the osteoblasts in the presence of Vitamin D_3. At the end of the culture, the osteoblast/ stromal cell layer can be detached mechanically by pipetting PBS onto the wall of the well, or by treating co-cultures with collagenase to release the osteoblast/stromal cells, allowing the isolation of osteoclast-like

cells (Abu-Amer et al., 1997; Inoue et al., 2000). Although various techniques have been employed to isolate the target cells in these co-cultures, these procedures are unable to produce pure populations of *in vitro* generated osteoclasts that are required for biochemical and molecular analyses. Ensuring a consistent amount of osteoclast-differentiation stimuli released from the osteoblast/ stromal layer is another challenge to studying molecular signaling pathways in these co-culture systems. These systems, however, remain useful for studying interactions between osteoclasts and osteoblasts, and to determine cell types that are affected in the knock-out or transgenic mice models (Itzstein & van 't Hof, 2012).

1.5.2 Osteoclast precursors

The identification that MCSF and RANKL are indispensable for inducing the differentiation of haematopoietic precursors into mature multinucleated osteoclasts was a paradigm shift for the *in vitro* models of osteoclastogenesis. Using recombinant MCSF and RANKL, a large number of osteoclasts can be generated from primary osteoclast precursor cells (bone marrow macrophages or peripheral blood monocytes), allowing the study of their formation and activity in the absence of other cell types.

Peripheral blood monocytes

Peripheral blood monocytes are frequently used to generate human osteoclasts. In order to isolate these monocytes, the density gradient centrifugation method is employed to obtain the buffy coat layer containing peripheral blood mononuclear cells (PBMCs) from fresh

peripheral/venous blood. Since PBMCs are a heterogenous population of cells consisting of the lymphocytes and monocytes, the monocyte population can then be enriched by several methods. The most common procedure used is monocyte isolation by adherence, in which PBMCs are incubated in a tissue-culture treated polystyrene surface, followed by vigorous washing to remove the lymphocytes that have not adhered (Bennett & Breit, 1994). This adherence method although simple and convenient, has its main disadvantage in the high degree of lymphocyte contamination (Bennett et al., 1992). To further complicate matters, the degree of lymphocyte contamination varies depending on the percentage of lymphocytes in the PBMC, amount of PBMC laid for adherence, strength and number of washes (de Almeida et al., 2000). As such a high degree of variability is inherent in this monocyte enrichment by adherence method.

Other methods for monocyte enrichment from PBMCs include immune selection and density gradients. Selection for the putative monocyte markers such as CD14 (Nicholson et al., 2000) and CD11b (Fujikawa et al., 1996) has been shown to yield a population of cells with the ability to differentiate into osteoclasts. However, immune selection for monocytes is limited by the high costs and need for large volumes of blood in order to obtain a reasonable yield. Density gradient centrifugation although cost effective requires a high degree of manipulation of the PBMCs and has been shown to lead to monocyte transient activation (Bennett & Breit, 1994)

Bone marrow macrophages

Another commonly used source of primary osteoclast precursors are the bone marrow macrophages. This method involves isolating the long bones from the hind limbs of mice (typically), surrounding soft tissues are removed, the ends of the bones are cut and the bone marrow is flushed out. After several washes, the macrophages are separated from the stromal cells by a negative adherence method. The stromal cells are allowed to attach to plastic petri dishes, following which the non-adherent cells are collected, cultured in the presence of M-CSF and allowed to adhere to tissue-culture treated plates. Limitations of using bone marrow macrophages as a source of primary osteoclast precursors include having to cull a live animal, limited yield, technically challenging to ensure sterility of the derived cell population.

Limitations of using primary osteoclast precursors

The use of primary osteoclast precursors, although more reflective of the native osteoclast differentiation process than immortalized cell lines, are models with limited applications. These cells are notoriously untransfectable (Cuetara et al., 2006; Marino et al., 2014) and as a result, are not suitable for genetic manipulation. Coupled with the fact that these primary cells are derived from a mixed population and fail to produce pure populations of *in* vitro generated osteoclasts, these cells have limited usages for the study of cellular and molecular signaling mechanisms. Additionally, the primary osteoclast precursors are non-expandable

indicating constraints on cell number and need for a constant source of these precursors.

RAW 264.7 cell line

The RAW 264.7 murine macrophage cell line is well accepted as a cellular model of osteoclast formation and function (Collin-Osdoby & Osdoby, 2012; Vincent et al., 2009). Further, this immortalized cell line has been identified to express the RANK receptor (Hsu et al., 1999) and the M-CSF receptor, c-FMS (Galal et al., 2007). RANKL has also been shown to activate the NFκB signaling pathway to mediate osteoclast differentiation and bone resorption in the RAW 264.7 cells. The use of this cell line overcomes several limitations of primary cells including ease of transfection, overcoming the need to cull a live animal, and its wide availability translates to a higher yield in cell number. However, since it is an immortalized cell line, RAW 264.7 cells may not react in a similar fashion to primary cells and should therefore be used in parallel with studies in primary cells.

1.6 The ovariectomized rat model

FDA guidelines have necessitated the use of the ovariectomized (OVX) rat model for preclinical development of anti-osteoporotic agents (Thompson et al., 1995). Indeed, the OVX rat is an excellent preclinical animal model as it emulates important clinical features of estrogen deficiency-induced osteoporosis in the human skeleton. The site-specific loss in cancellous

bone following ovariectomy makes the OVX rat one of the most reproducible models in skeletal research (Kimmel, 1996).

Following ovariectomy, a rapid loss in cancellous bone mass and strength occurs, which then proceeds at a less rapid rate in a site-specific fashion. This pattern of bone loss closely mimics that of postmenopausal bone loss in humans. However, cancellous bone loss does not occur at all sites in the rat: the distal tibial metaphysis and caudal vertebral body are known to be resistant to ovariectomy-induced bone loss (Li et al., 1996; Ma et al., 1994). Cancellous bone loss also does not proceed at the same rate at all sites (Table 1.4).

Table 1.4 Cancellous bone changes following ovariectomy

Site	*Earliest time of bone loss (days)*	*Time to 50% bone loss (days)*	*Earliest to achieve steady state (days)*	*Earliest decrease in bone strength (days)*
Proximal tibial metaphysis	~ 14	~ 30 – 60	90	-
Lumbar vertebral body	~ 60	~ 180- 270	270	90
Femoral neck	~ 30	~ 180- 270	270	90

Adapted from (Jee & Yao, 2001)

Since fragility fractures do not occur naturally in the OVX rat model, bone strength is assessed by mechanical testing of bones, such as the vertebral body, femoral shaft and femoral head.

1.6.1 Shortcomings of the OVX rat model

The major drawback of the rat skeleton is that some bones do not have fused epiphyses and have the capacity for continued bone elongation (Erben, 1996). As such, it is crucial to design experiments to include pre-treatment/ -intervention controls to distinguish between cancellous bone loss, depression of bone growth, or a combination of both.

The lack of intracortical remodeling in the rodent is the primary motivation behind FDA guidelines stipulating the need for preclinical evaluation of anti-osteoporotic agents in larger animals (Thompson et al., 1995). However, there is growing evidence to show that the pattern and location of cortical bone loss in the OVX rat is almost identical to that in larger animals and humans (Kaneps et al., 1997; Ke et al., 1993), thus suggesting that rodent studies may be sufficient for evaluation of cortical bone behaviour.

CHAPTER 2. AIMS

2.1.1 Knowledge gaps

As outlined in the introduction, postmenopausal osteoporosis is a highly prevalent disease. Further, osteoporotic fractures are not only deleterious to the quality of life of patients; it is also a tremendous public health problem. Despite the treatment options available for postmenopausal osteoporosis, these anti-osteoporotic drugs are associated with significant clinical adverse events. Thus, there is a need to identify alternative treatment modalities for osteoporosis with improved risk-benefit profiles.

Since estrogen-deficiency leads to an imbalance in bone remodeling, in particular, a net increase in bone resorption as a result of increased osteoclast numbers and activity, compounds that inhibit osteoclast formation and activity may be a viable treatment option. Although *Epimedium* flavonoids (as total flavonoid extracts or in herbal decoctions) have been shown to improve bone mineral density of postmenopausal women, the daily requirement of a high drug volume/ dosage, has been reported to lead to low adherence levels due to side effects in the digestive tracts (Zhang et al., 2006; 2007; Zhu et al., 2012). Nevertheless, this drawback can be mitigated by identifiying the active molecular compound of the *Epimedium*-derived flavonoids.

Although studies have demonstrated the osteogenic effects of icaritin in both MSCs and osteoblasts, along with its anabolic effects *in vivo*, the effect of

icaritin on inhibiting osteoclast formation and resorption is not well examined. Furthermore, given the anti-oxidative properties of icaritin demonstrated in an animal model of myocardial ischaemia and reperfusion injury (Zhang et al., 2015), coupled with the important functions of intracellular ROS during osteoclast differentiation, perhaps icaritin inhibits osteoclastogenesis as a result of its anti-oxidative properties.

2.1.2 Hypothesis and specific aims

We therefore hypothesized that apart from its anabolic effects, icaritin improves bone health by inhibiting osteoclastogenesis and osteoclast resorptive function.

The overall objective of this thesis was to understand the cellular mechanism(s) of icaritin in regulating osteoclastogenesis, and to investigate the therapeutic potential of icaritin in estrogen deficiency-mediated osteoporosis. The specific aims of this thesis are as follows:

Aim 1. To examine the functional effects of icaritin on osteoclastogenesis, and osteoclast bone resorptive capacity.

(a) Using established cellular models of osteoclastogenesis, the effects of icaritin on osteoclast formation will be assessed by osteoclast numbers, expression of the osteoclast marker TRAP and expression of osteoclast-specific genes.

(b) Osteoclast function will be assessed by resorption assays.

Aim 2. To elucidate the molecular mechanism(s) by which icaritin modulates osteoclast differentiation and resorptive function by

(a) Examining the effects of icaritin on RANKL-induced signaling cascades: NFκB, MAPK/AP-1, and intracellular ROS-mediated signaling pathways.

Aim 3. To investigate the therapeutic effects of icaritin in an animal model of estrogen deficiency-mediated osteoporosis.

(a) Using the OVX-rat model, the effects of icaritin treatment on bone will be assessed by bone density, architecture and strength. Bone turnover status will be assessed using serum markers of bone turnover.

(b) OVX-induced osteoclast formation will be assessed by histological analyses of the bone.

(c) Effect of icaritin treatment on osteoclast-specific gene expression will be examined in circulating osteoclast precursors and bone homogenates.

CHAPTER 3. MATERIALS & METHODS

3.1 Cellular experiments

3.1.1 Chemicals

Icaritin (ICT; > 97% purity) was purchased from C-tech Global (Singapore); β-estradiol 17-valerate (E2), N-Acetyle-L- Cysteine (NAC) and MG 132 were purchased from Sigma (St. Louis, MO, USA). Estrogen receptor antagonist ICI 182,780 was purchased from Tocris Bioscience (Bristol, UK). All compounds were dissolved in dimethyl sulfoxide, except NAC in double-distilled deionized water. The final concentration of solvents in culture media was 0.1%. Bacteria-derived recombinant mouse and human RANKL and M-CSF were purchased from R&D Systems (Minneapolis, MN, USA). Lipofectamine 3000 transfection reagent (ThermoFisher Scientific, Carlsbad, CA, USA) was used to transfect RAW 264.7 cells.

3.1.2 Cell Culture

RAW 264.7 mouse monocyte cell line

RAW 264.7 cells were purchased from ATCC (TIB 71; Rockville, MD, USA) and were cultured in DMEM medium without phenol red containing 4.5 g/L glucose, 4 mM L-glutamine, 1 mM sodium-pyruvate, supplemented 10% fetal-bovine serum and 1% streptomycin-penicillin. Cells were grown and passaged in a humidified incubator at 37 $^{\circ}$C with 5% CO_2.

Preparation and culture of human peripheral blood mononuclear cells (PBMC)

Whole blood was obtained from healthy donors after approval from National University of Singapore research ethics committee. Human PBMC were isolated by density gradient centrifugation. Whole blood was diluted 1:1 in Dulbecco's Phosphate Buffered Saline (DPBS), layered over ficoll-paque Plus (GE Healthcare, Amersham, UK) then centrifuged at 400 g, 18°C for 30 minutes with no deceleration. The buffy coat layer was collected, washed twice with DPBS and resuspended in the DMEM culture media described above.

3.1.3 Osteoclastogenesis Assay

RAW 264.7 cells and human PBMC were seeded in 96-well plates at a density of 25,000/cm^2 and 1.5 x 10^6/cm^2 respectively. After an overnight culture, differentiation into multinucleated osteoclasts was induced in the presence of 50 ng/ ml RANKL and 25 ng/ ml M-CSF, supplemented with various doses of ICT or 10 nM E_2. RAW 264.7 cells and human PBMC were cultured for 6 days and 21 days respectively. Differentiating media was refreshed every 2 days.

Tartrate Resistant Acid Phosphatase (TRAP) staining

After 6 or 21 days' culture, spent media was removed, cells were fixed in pre-warmed 4% paraformaldehyde for 10 min at room temperature and stained for TRAP activity (Sigma, USA). To quantify number of osteoclasts, wells were examined using a bright-field microscope with the 10x objective (Nikon Instruments). TRAP-positive multinucleated cells with >3 nuclei and a purple cytoplasm were counted as osteoclasts.

TRAP enzyme activity

After 6 or 21 days' differentiation, cells were lysed with radio-immunoprecipitation assay (RIPA) buffer (ThermoFisher Scientific, Carlsbad, CA, USA) containing a mini EDTA protease inhibitor cocktail (Roche Life Science, Madison, WI, USA). Using the acid phosphatase kit (Sigma, USA), TRAP activity was quantified by incubating cell lysates in the presence of a 4-nitrophenyl phosphate substrate solution and measuring absorbance at 405 nm. Phosphatase activity was normalized against total protein as determined by Bradford assay (described in Section 3.1.8).

3.1.4 Osteoclast Function

Sealing zone formation

RAW 264.7 cells and human PBMC were differentiated in the presence of respective treatments on glass bottom chamber slides (Nunc LabTek, ThermoFisher Scientific, USA). After 6 or 21 days' culture, cells were fixed in pre-warmed 4% paraformaldehyde for 10 min at room temperature. Wells were washed with DPBS, incubated in 0.1% Triton-X-100-PBS (Bio-Rad Laboratories, Hercules, CA, USA) for 10 min then stained with Alexa Fluor® 594- phalloidin and hoechst 33342 (Molecular Probes, Carlsbad, CA, USA) in DPBS for 1 hour. Z-stack images were acquired with a confocal laser scanning microscope (Olympus FV1000, Melville, NY, USA) and analyzed using ImageJ (NIH, Bethesda, MD, USA).

Resorption assay

RAW 264.7 cells and human PBMC were differentiated in the presence of respective treatments on calcium hydroxyapatite-coated 24-well plates (Corning osteoassay surface, Corning Incorporated, NY, USA). After 6 or 21 days, adherent cells were removed by incubating wells in 5% sodium hypochlorite solution and vigorous pipetting. For 2D visualization of erosion area, wells were imaged with a laser microscope (Olympus LEXT OLS4100, Melville, NY, USA). Area covered by resorption pits and erosion tracts was analyzed by thresholding against a blank sample in ImageJ (NIH, Bethesda, MD, USA) (Fig. 3.1). Three random fields were imaged for pit area measurements. To measure pit volume, z-stack images of the wells were taken with a confocal laser scanning microscope (LSM 5 meta, Carl Zeiss, UK) set in reflection mode. Pits were identified by contrast against a blank sample and negative controls. Pit volume measurements were calculated using TopoJ and topographical projections of z-stacks generated using SurfaceJ (ImageJ, NIH, US). Six random pits were imaged per sample.

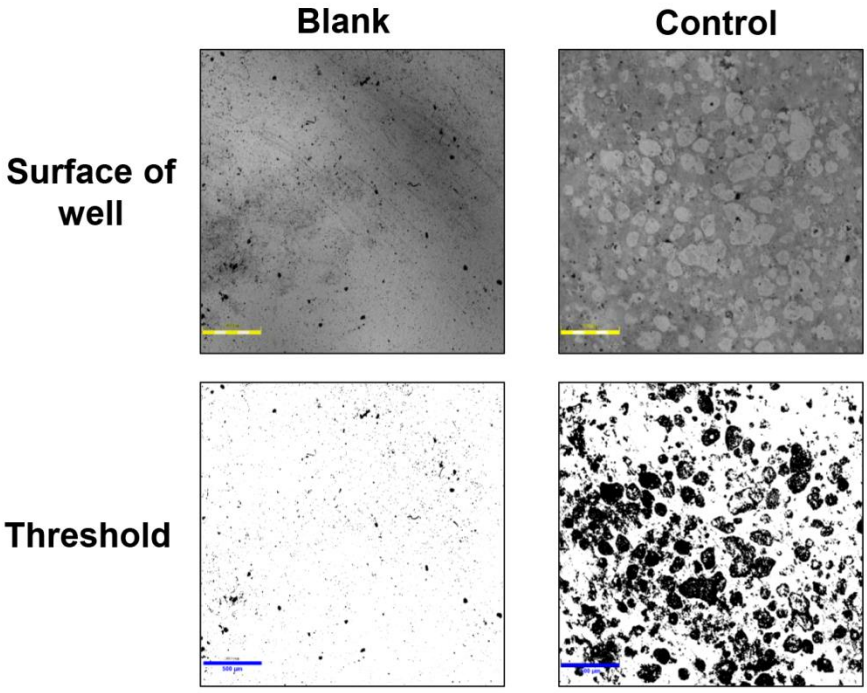

Figure 3.1 Surface of calcium-coated well showing resorption pits and erosions tracts. Scale bar = 500 µm.

3.1.5 Real-time Polymerase Chain Reaction

For gene expression experiments, RAW 264.7 cells were plated at a density of 30 000/cm^2 in six-well plates. After subculturing for 24 h, cells were treated with DMSO (vehicle), ICT at doses indicated, or 10 nM E_2 in DMEM supplemented with 10% charcoal-treated FBS, either alone or in combination with 50 ng/ml RANKL.

Total RNA was extracted using RNeasy Mini Kit (Qiagen, Valencia, CA, USA), according to the manufacturer's instructions. The extracted RNA was then quantified using the ND-1000 Spectrophotometer (Nanodrop Technologies, USA). Only RNA with a quality ratio of A260/A280 between 1.9 and 2.1 was used for downstream analysis. The extracted RNA was reverse transcribed to cDNA using the High Capacity cDNA Reverse Transcription Kit (Invitrogen, Carlsbad, CA, USA) according to the manufacturer's instruction. RT-PCR was performed using StepOnePlus RT-PCR System (Applied Biosystems, Carlsbad, CA, USA) following the manufacturer's protocol using specific primers from Taqman® Gene Expression Assays (Applied Biosystem, USA). Relative gene expression values were determined by the $-2^{\Delta\Delta Ct}$ method with 18S rRNA as the reference gene.

<u>Primers for RT-PCR</u>

Taqman® Gene Expression Assays (Applied Biosystem, USA)

NFATc1: Mm00479445_m1

Cathepsin K (Ctsk): Mm00484039_m1

TRAF6: Mm00493836_m1

DC-STAMP: Mm04209236_m1

18s RNA: Mm03928990_g1

3.1.6 Immunoprecipitation (IP)

For IP assays, RAW 264.7 cells were plated at a density of 30 000/cm^2 in six-well plates. After subculturing for 24h, cells were treated with DMSO (vehicle), 100 nM ICT in DMEM supplemented with 10% charcoal-treated FBS, either alone or in combination with 50 ng/ml RANKL for 24 h. Cell were lysed with RIPA buffer containing a mini EDTA protease inhibitor cocktail.

0.4 ml of lysates was pre-cleared in Protein A/G agarose beads (Santa Cruz Biotechnology, Santa Cruz, CA, USA) to prevent non-specific binding, at 4°C for 60 min with gentle rocking. Supernatant was collected and lysates were then incubated with 2 µg of the TRAF6 antibody and Protein A/G agarose beads (20 µl in 50% slurry) overnight at 4°C. The lysates were washed three times with 0.5 ml of lysis buffer, resuspended in 100 µl 2x SDS loading buffer and heated at 95°C for 5 minutes.

3.1.7 Cell fractionation

RAW 264.7 cells were plated at a density of 30 000/cm^2 in six-well plates. After subculturing for 24h, cells were treated with DMSO (vehicle), ICT at doses indicated, or 10 nM estradiol in DMEM supplemented with 10% charcoal-treated FBS, either alone or in combination with 50 ng/ml RANKL. After the indicated incubation durations, cells were washed with ice cold

DPBS, removed from monolayer and collected. Cellular fractionation was performed according to the protocol supplied with the NE-PER kit (Pierce, Rockford, IL, USA). Briefly, cells pellets were resuspended in a detergent solution and disrupted by mechanical agitation, followed by centrifugation to separate the cytoplasmic and nuclear extracts.

3.1.8 GTP-bound Rac1 Isolation

RAW 264.7 cells were plated at a density of 30 000/cm^2 in six-well plates. After subculturing for 24 h, cells were treated with DMSO (vehicle), ICT at doses indicated, or 10 nM estradiol in DMEM supplemented with 10% charcoal-treated FBS, either alone or in combination with 50 ng/ml RANKL. GTP-bound Rac1 was isolated using the Active Rac1 pull down and detection kit (Pierce, Rockford, IL, USA). After the indicated incubation durations, cell monolayers were washed with ice-cold DPBS, removed from monolayer and lysed. 20 µg GST-bound p21-binding domain (PBD) of the p21-activated kinase (PAK) were added to cell lysates with equal amounts of protein per sample. The mixture was incubated with a glutathione-resin with gentle agitation at 4°C for 60 min. The complexes were washed three times with lysis buffer not containing GST-Pak1-PBD. GTP-bound Rac1 was eluted with SDS-loading buffer. A total of 5% of the original lysate was also electrophoresed to determine total levels of Rac1.

3.1.9 Protein extraction & immunoblot analyses

RAW 264.7 cells were plated at a density of 30 000/cm^2 in six-well plates. After subculturing for 24 h, cells were treated with DMSO (vehicle), ICT at doses indicated, or 10 nM estradiol in DMEM supplemented with 10% charcoal-treated FBS, either alone or in combination with 50 ng/ml RANKL.

After the indicated incubation durations, cells were washed with ice cold DPBS then lysed with RIPA buffer containing a mini EDTA protease inhibitor cocktail. Bio-Rad Bradford protein assay (Bio-Rad Laboratories, USA) was used to determine total protein concentration with serial dilutions of Bovine Serum Albumin as a standard. 20 µg of cellular protein lysates (whole cell lysates or subcellular fractions) in 4x SDS-loading buffer were heated at 95°C for 5 minutes. Protein lysates or immunoprecipitates were resolved on SDS-PAGE gel using the Mini PROTEAN 3 electropheresis cell (Bio-Rad, USA) and transferred onto a PVDF membrane using the semidry transfer method. After transfer, nitrocellulose membranes were blocked in 5% non-fat milk (Sigma, USA) in PBS for 1 hour. The membranes were then incubated with primary antibodies overnight at 4°C. The membranes were washed 3 times (5 minutes each) with 0.1% Tween 20- PBS (PBST), then incubated with either anti-rabbit or anti-mouse secondary antibodies conjugated to horseradish peroxidase (Dako, USA) at room temperature for 2 h (1: 10 000 dilution in 5% non-fat milk). Protein expression signal was detected using Amersham ECL (GE Healthcare, Amersham, UK) and the blots were exposed to CL-XPosure Films

(Thermo scientific, USA). The exposed films were developed using an X-Ray Developer (Carestream Health, USA).

Primary antibodies

The following antibodies were purchased from Santa Cruz Biotechnology (Santa Cruz, CA, USA).

P-NFATc1 (Ser 259): SC-32979

NFATc1: SC-7294

Cathepsin K: SC-48353

TRAF6: SC-7221

c-Src: SC-18

GAPDH: SC-47724

HDAC: SC-8410

The following antibodies were purchased from Cell Signalling Technology (Beverly, MA, USA).

MAPK pathway sampler kit: #9926

NFκB pathway sampler kit: #9936

p-PI3K: #4228

PI3K: #4257

RANK: #4845

Anti-Nox1 antibody was purchased from Abcam (ab55831; Cambridge, UK) and β actin from Sigma (A5316, USA).

3.1.10 Cell viability assay

RAW 264.7 cells and human PBMC were seeded in 96-well plates at a density of 25,000/cm^2 and 1.5 x 10^6/ cm^2 respectively. Cells were cultured until 80% confluence then treated with DMSO (vehicle), ICT at doses indicated, or 10 nM estradiol in DMEM supplemented with 10% charcoal-treated FBS, either alone or in combination with 50 ng/ml RANKL. After 48 h treatment, cell viability was determined using the standard protocol of CellTiter 96® AQueous One Solution Cell Proliferation Assay (MTS; Promega, Madison, WI). The relative luminescence units (RLUs) were measured using a fluorescence microplate reader (TECAN, Maennedorf, Switzerland) at a wavelength of 490 nm.

3.1.11 Immunofluorescence analysis

RAW 264.7 cells were seeded at a density of 20 000 cells/well in 8-well glass bottom chamber slides (Nunc LabTek, ThermoFisher Scientific, USA). After overnight culture, cells were treated with DMSO (vehicle), ICT at doses indicated, or 10 nM estradiol in DMEM supplemented with 10% charcoal-treated FBS, either alone or in combination with 50 ng/ml RANKL. After indicated durations, spent media was removed, wells were washed twice with DPBS and cells were fixed in pre-warmed 4% paraformaldehyde for 10 min at room temperature.

To analyze p65 nuclear translocation, wells were incubated in 0.1% Triton-X-100-PBS (Bio-Rad Laboratories, Hercules, CA, USA) for 10 min. This perforation of cell membranes was omitted where surface RANK expression was analyzed. Wells were washed with DPBS then blocked in 5% BSA-PBS

solution for 1 hour and incubated with p65 (#8242, Cell Signaling Technology) or RANK (#4845, Cell Signaling Technology) primary antibodies overnight at 4°C. Wells were washed thrice in 3% BSA-PBS then incubated with anti-rabbit secondary antibodies conjugated to a fluorescent tag (Goat anti-rabbit Alexa Fluor® 594 or Alexa Fluor® 488, Molecular Probes) at room temperature for 2 h (1: 10 000 dilution in 5% BSA-PBS). Wells were washed thrice in 3% BSA-PBS and counterstained with Hoechst 33342 (Molecular Probes). 3 random fields per well were imaged with a confocal laser scanning microscope (Olympus FV1000, Melville, NY, USA) and analyzed using ImageJ (NIH, Bethesda, MD, USA). Fluorescence intensity was normalized to cell number as identified by the number of nuclei.

3.1.12 Intracellular ROS detection

RAW 264.7 cells were plated at a density of 30 000/cm^2 in 12-well plates. After subculturing for 24h, cells were treated with DMSO (vehicle), ICT at doses indicated, or 10 nM estradiol in DMEM supplemented with 10% charcoal-treated FBS, either alone or in combination with 50 ng/ml RANKL. After indicated durations, media was aspirated, cells washed with pre-warmed DPBS and incubated with 10 μM CM-H2DCFDA (Molecular Probes, USA) for 30 minutes at 37°C. Cells were removed from monolayer, washed and filtered through a 40 μm pore size filter. 10, 000 events were analyzed for fluorescence intensity with flow cytometry (CyAN ADP, Beckman Coulter, USA) with the excitation set at 490 nm and emission set at 510 nm. Data collected was analyzed with the Summit 4.3 software (Beckman Coulter).

3.1.13 Assessment of NFATc1, NFκB and AP-1 transcriptional activities

Plasmid information

A pGL4.30 vector containing an NFAT response element that drives the transcription of the luciferase reporter gene (Luc2P) was purchased from Promega (Madison, WI, USA). The vector backbone contains the ampicillin resistance gene and a hygromycin resistance gene for mammalian selection (Fig. 3.2). The pRL vector that provides constitutive expression of Renilla luciferase was purchased from Promega. For use as an internal control, the pRL vector with a relatively weak HSV-thymidine kinase promoter (pRL-TK) was chosen to provide neutral constitutive expression of Renilla luciferase.

pGL4.30[*luc2P*/NFAT-RE/Hygro] Vector Features List and Map:

NFAT response element	33–122
Minimal promoter	136–166
luc2P reporter gene	228–2003
SV40 late poly(A) signal	2043–2264
SV40 early enhancer/promoter	2312–2730
Synthetic hygromycin (Hyg^r) coding region	2755–3792
Synthetic poly(A) signal	3816–3864
Reporter Vector primer 4 (RVprimer4) binding region	3931–3950
*Col*E1-derived plasmid replication origin	4188
Synthetic β-lactamase (Amp^r) coding region	4979–5839
Synthetic poly(A) signal/transcriptional pause site	5944–6097
Reporter Vector primer 3 (RVprimer3) binding region	6046–6065

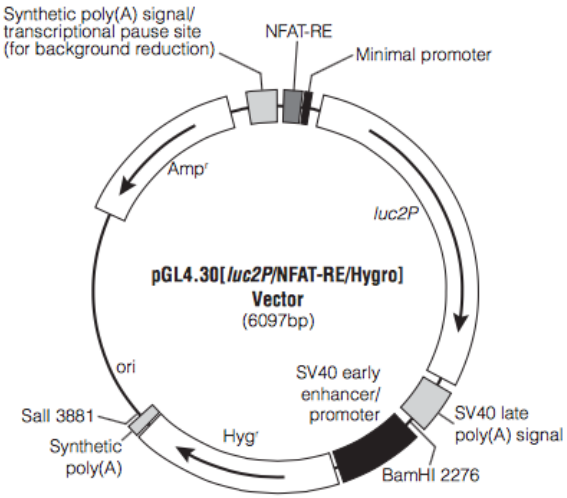

Figure 3.2 Map of pGL4.30 (Luc2P/NFAT-RE/Hygro) vector from Promega

Plasmid amplification

Chemically competent (One Shot® Omni-Max™ 2 T1, Thermo Scientific) cells were transformed with the pGL4.30 (Luc2P/NFAT-RE/Hygro) or pRL-TK plasmids. 50 µl of competent cells were incubated with 100 ng of plasmids at 4°C for 20 minutes, followed by a heat-shock for 45 seconds at 42°C. Cells were recovered at 4°C for 2 minutes and 450 µl of SOC-LB medium (Thermo Scientific) was added to the cells. The mixture was incubated in a shaker (200 rpm) for 1 hour at 37°C with 5% CO_2. After which, 200 µl of the mixture was plated onto LB plates prepared with 50 µg/ml ampicillin, and incubated at 37°C overnight.

After the overnight incubation, a single cell colony was selected from the agar plate and incubated in 3 ml of LB medium containing 50 µg/ml ampicillin for 8 hours at 200 rpm, 37°C with 5% CO_2. After 8 hours, 0.4 ml of the starter culture was added to 200 ml of LB medium with ampicillin and cultured overnight at 200 rpm, 37°C with 5% CO_2.After the overnight culture, cells were harvested by centrifugation at 6000 g for 15 minutes at 4°C. Plasmid DNA was isolated using a plasmid DNA purification kit (Endofree Plasmid Maxi Kit, Qiagen, USA). DNA concentration was determined by using the ND-1000 Spectrophotometer (Nanodrop Technologies, USA).

Luciferase reporter assay

RAW 264.7 cells were plated at a density of 30 000/cm^2 in 12-well plates. After subculturing for 24 h, cells were co-transfected with 0.5 μg of plasmids encoding NFAT-luciferase reporter plasmid and 20 ng of Renilla luciferase reporter as a control for transfection efficiency. Cells were also transfected with 0.5 μg of NFκB- or AP-1 luciferase constructs purchased from SABiosciences (Qiagen, Valencia, CA), that were pre-mixed with constitutively expressed Renilla luciferase construct at a ratio of 40:1. 48 h after transfection, cells were treated with DMSO (vehicle), ICT at doses indicated, or 10 nM estradiol in DMEM supplemented with 10% charcoal-treated FBS, either alone or in combination with 50 ng/ml RANKL. Following indicated incubation durations, wells were washed with DPBS and luciferase activity was measured using dual luciferase assay system (Promega) according to manufacturer's protocol. Constructs contain either the AP-1 (TGAGTCAG) or NFκB (GGGACTTTCC) transcriptional regulatory element sequences that drive the expression of the luciferase reporter gene.

3.1.14 Calcineurin-specific phosphatase assay

RAW 264.7 cells were plated at a density of 30 000/cm^2 in six-well plates. After subculturing for 24h, cells were treated with DMSO (vehicle), ICT at doses indicated, or 10 nM estradiol in DMEM supplemented with 10% charcoal-treated FBS, either alone or in combination with 50 ng/ml RANKL.

After the indicated durations, cells were washed with ice cold DPBS and lysed with RIPA buffer containing a protease inhibitor cocktail. Calcineurin-specific

phosphatase activity in cell lysates was measured using a colorimetric assay kit (BML-AK816-0001, Enzo Life Sciences, NY, USA). To remove excess phosphate as well as nucleotides which are hydrolyzed to release free phosphates, cell lysates were passed through a desalting column resin. To assess total phosphatase activity, cell lysates were incubated with an assay buffer supplemented with Ca^{2+}/calmodulin along with RII phosphopeptide as a substrate. Cell lysates were also incubated with EGTA buffer (Ca^{2+}/calmodulin free) and the RII phosphopeptide substrate. Serial dilutions of phosphate were used as a standard and total amount of phosphate present in each well quantified by measuring absorbance with a microplate reader. Calcineurin phosphatase activity was reflected by subtracting amount of phosphate present when incubated in EGTA buffer from the total. Calcineurin phosphatase activity was normalized against total protein as determined by Bradford assay.

3.1.15 Statistical analyses

All results are expressed as mean ± SEM. Statistical analyses were performed using Graphpad Prism 6 (GraphPad Software, Inc., San Diega, CA, USA). Statistical differences were assessed by independent t-test for comparison between two groups, or one-way ANOVA followed by Tukey's post hoc analysis for multiple comparisons between different groups. Differences were considered statistically significant at $P < 0.05$.

3.2 Animal Experiments

3.2.1 Establishing the OVX-rat model

10-12-week old female Sprague-Dawley rats were housed at the Laboratory Animal Centre, National University of Singapore. Rats were maintained on a minimal isoflavone diet (Teklad Diets, Envigo, NJ, USA) and water *ad libitum.* Following one week's acclimatization, the rats were divided into 6 groups: (1) Pre-treatment sham-operated (Sham-Pre), (2) pre-treatment OVX (OVX-Pre), (3) Vehicle-treated sham-operated (Sham-Veh), (4) vehicle-treated OVX (OVX-Veh), (5) ICT-treated OVX (OVX-ICT) and (6) estradiol valerate-treated OVX (OVX-E2). The rats were then subjected to bilateral ovariectomy (OVX) or sham surgery. 4 weeks after surgery, Sham-Pre and OVX-Pre rats were euthanized while the remaining rats received intraperitoneal injection of 0.9% saline (vehicle-treated groups) or ICT solution (40 mg/kg/day), or subcutaneously administered estradiol valerate (10 μg/kg/day) 5 times a week for 8 weeks. After 8 weeks' treamtent, rats were euthanized by carbon-dioxide asphyxiation. Femora, tibiae and the L5 vertebrae were harvested, wrapped in 0.9% saline-soaked gauze and stored at -20°C for subsequent analyses. The study was reviewed and approved by the Animal Ethics Committee at National University of Singapore (protocol R13-4877).

3.2.2 Preparation of treatments

ICT (> 98% purity) was purchased from Ctech Scientific Pte Ltd (Singapore). ICT was dissolved in a mixture solvent containing Kollipher EL: ethanol: PEG 400: saline (13:7:40:40, v/v). 40 ml of saline was added to 40 ml PEG 400 and

mixed well. Separately, 13 ml Kolliphor EL was added to 7 ml of 100% ethanol, mixed thoroughly and sonicated until resulting solution was clear. ICT was dissolved in the Kolliphor EL-ethanol mixture, followed by dropwise addition of the saline- PEG 400 mixture. The resulting mixture was mixed well and sonicated to ensure complete dissolution of ICT then passed through a 0.2 μm filter. ICT solution was prepared to a final concentration of 4 mg/ml. Sufficient ICT solution was prepared for a week's use, aliquoted and stored at -20°C. Vehicle-treated rats were given the same Kolliphor EL- ethanol- PEG 400 – saline mixture solvent.

β-estradiol 17-valerate was purchased from Sigma (St. Louis, MO, USA) and dissolved in sesame oil (3457; Sigma, USA). The resulting solution was sonicated then passed through a 0.2 μm filter. Fresh E2 solution was prepared every week, to a final concentration of 3 μg/ ml. Sufficient solution was prepared for a week's use, aliquoted and stored at -20°C.

3.2.3 Vaginal smears

Vaginal smears were taken between 10:00 – 11: 00 hours each day, for 7 days before sham surgery or bilateral ovariectomy and for 14 days after. The tip of a moistened cotton bud swab was inserted into the vagina, at a 45° angle to the rat's body. Cells from the vaginal lumen and walls were removed by rotation of the swab then transferred onto a glass slide. Stage of the estrus cycle of each rat was determined by microscopic analysis of the predominant cell type in the vaginal smears. Morphology of predominant cell types in the stages of the estrus cycle is described in Fig 3.3.

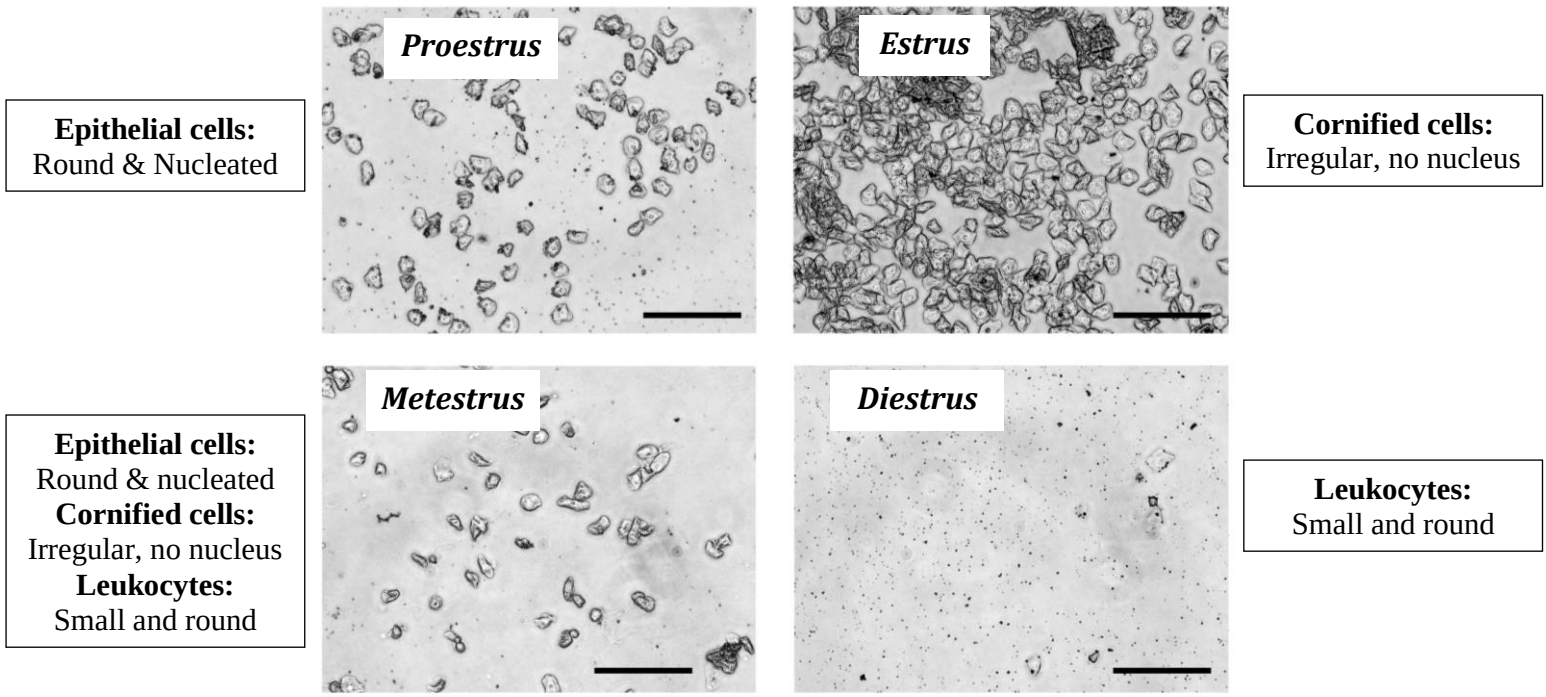

Figure 3.3 Cytological appearance of vaginal smears from cycling rats
Scale bar = 150 µm.

3.2.4 Blood sampling and parameters

Tail blood was obtained to assess estradiol, bone turnover markers (osteocalcin, CTx-I) and RANKL concentrations in the serum. In cycling rats, blood samples were obtained in the diestrous phase. Serum was collected and stored at -80°C. Serum concentrations of estradiol (Enzo Life Sciences, NY, USA), osteocalcin (Takara Bio, Shiga, Japan), CTx-I (Cusabio, Wuhan, China) and RANKL (R&D systems, Minneapolis, MN, USA) were measured using an ELISA kit according to the manufacturer's instructions. The coefficients of variation and sensitivities of the respective ELISA kits are summarized in Table 3.1.

Table 3.1. CV and sensitivity of ELISA kits used

	Intra-CV (%)	Inter-CV (%)	Sensitivity
Estradiol	7.16	9.83	14.0 pg/ml
Osteocalcin	4.48	8.10	0.25 ng/ml
CTx-I	5.57	11.46	31.25 pg/ml
RANKL	3.32	6.28	5 pg/ml

3.2.5 Micro-computed tomography measurements

After the rats were euthanized, the right hind leg and lumbar vertebrae were excised and stripped of adherent muscles. To facilitate identification, lumbar vertebrae were excised together with the lowest rib and pelvis. The right femora, femur neck and L5 were scanned *ex vivo* at a voxel size of 20 µm using a microCT system (PerkinElmer Quantum FX, Waltham, MA). 350 slices (7

mm) were scanned at the region of the distal femur beginning at the growth plate and extending proximally along the femur diaphysis. For analysis of the trabecular bone, 75 slices (1.5 mm) were selected beginning 0.3 mm from the proximal aspect of the growth plate at the distal femora. The entire femur neck was scanned with 350 slices and trabecular bone mineral density at the femur neck was measured within 100 consecutive slices, with the middle slice having the lowest total area in 2D analysis. 350 slices were scanned at the region of the L5 vertebrae, for analysis of trabecular bone 100 slices of the vertebral body were selected beginning 0.4 mm from the cartilaginous endplate. 3D reconstructions and trabecular parameters including trabecular bone volume fraction (BV/TV) and trabecular thickness/number/separation (Tb.Th, Tb.N, and Tb.Sp) were evaluated using the softwares CTAn and CTVol (Bruker SkyScan, Belgium). Bone density was normalized using a phantom containing five rods of varying hydroxyapatite densities (QRM GmbH, Moehrendorf, Germany).

3.2.6 Mechanical tests

The mechanical properties of femur neck, femur shaft and L5 were evaluated using a materials testing machine (Instron 4465, MA, USA). Prior to evaluation, the geometric properties of the specimens were measured using digital vernier calipers. Destructive three-point bend tests were performed at the right femur midshaft, using a span length of 15 mm (Fig. 3.4*A*), with a compression rate of 5 mm/min and stabilized with a static preload of 0.5 N.

Following the three-point bend's test, mechanical properties of the femur neck were assessed by a femur neck-bending test. The femur head was mounted in dental cement, ensuring that the femur diaphysis is parallel to the loading axis (Fig. 3.4*B*). The load was applied to the top of the femoral head, with static preload of 0.3 N and compressed at a rate of 5 mm/ min.

Mechanical properties of the L5 vertebrae were evaluated by a compression test. Posterior elements and endplates were removed from the L5 vertebrae and specimens were compressed to failure with the loading axis vertically aligned to the vertebral body. Vertebrae specimens were stabilized using a static preload of 5 N before being loaded to failure at a speed of 2 mm/min.

Load and deformation data for all specimens were collected at 100 Hz using the Instron Bluehill software (version 3.0, MA, USA), which computed the ultimate load (N), stiffness (N/mm), flexural modulus (N/mm^2) and energy to failure (mJ) of specimens. The following parameters were then derived as:

1) Ultimate strength (N/mm^2) = ultimate load (N) ÷ cross sectional area (mm^2);
2) Elastic modulus (N/mm^2) = Stiffness ÷ cross sectional area (mm^2) x initial length or height of specimen (mm)
3) Toughness modulus (mJ/ mm^3) = energy to failure (mJ) ÷ volume deformed (mm^3)

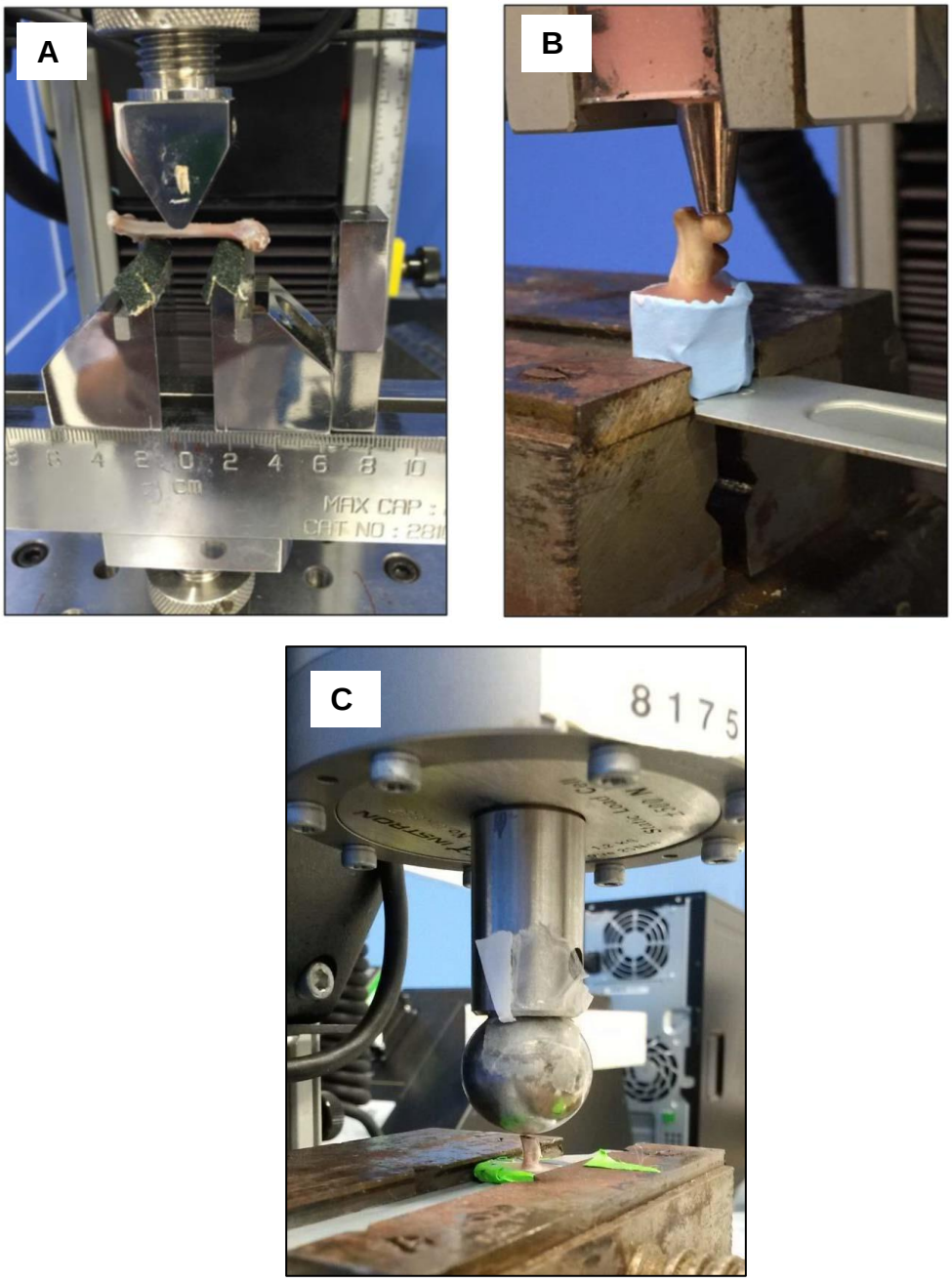

Figure 3.4 Evaluating mechanical properties of rat bone using a materials-testing machine
(*A*) Three-point bend tests at femur midshaft, (*B*) Femur neck bending test and (C) L5 compression test

3.2.7 Identification and analysis of circulating osteoclast precursors

Bone marrow Aspiration

After the rats were euthanized, the left hind leg was excised and cleaned of adherent muscles. Femur and tibiae were separated at the joint and soaked in DPBS for 5 minutes. The two ends of the femur and tibiae were excised. A 23-gauge needle attached to a 5 ml syringe filled with DMEM culture media was inserted into the bone. Marrow was then flushed out slowly with DMEM. The bones were flushed repeatedly until they appeared pale. Bone marrow cells were pelleted by centrifugation at 2000 g for 5 min and resuspended in 10 ml DMEM. 30 ml RBC lysis solution (Qiagen, USA) was added to the cell suspension and mixed by inverting 10 times. The suspension was incubated at room temperature for 5 minutes, then centrifuged at 2000 g for 5 minutes. Bone marrow cells were then fixed in 4% paraformaldehyde for subsequent analyses of osteoclast precursor populations.

Isolation of PBMC from rats

The rats were euthanized by carbon dioxide asphyxiation and after confirming a lack of toe-pinch reflex, 10 ml of blood was collected by cardiac puncture. Blood was diluted in an equal volume of DPBS and layered over Ficoll-paque Plus (GE Healthcare, Amersham, UK), then centrifuged at 400 g, 18°C for 30 minutes with no deceleration. The buffy coat layer was collected, resuspended in 5 ml DMEM culture media. 15 ml RBC lysis solution (Qiagen, USA) was added to the cell suspension and mixed by inverting 10 times. The suspension was incubated at room temperature for 5 minutes, then centrifuged at 2000 g

for 5 minutes. PBMC were then fixed in 4% paraformaldehyde for subsequent analyses of osteoclast precursor populations.

Identification of osteoclast precursors from rats by cell sorting

To identify cells with osteoclastogenic potential, bone marrow cells or PBMC from 3 rats were pooled. Fixed cells were washed with DPBS, blocked in 3% BSA-PBS for 1 hour then stained overnight at 4°C with efluor- conjugated anti-rat CD11b (Ebiosciences, San Diego, CA, USA) and FITC-conjugated anti-rat Gr-1 (ab25024; Abcam, Cambridge, UK) antibodies. Cells were washed twice with 3% BSA-PBS and filtered through a 40 μm pore size filter prior to fluorescence assisted cell sorting (Sony Sy3200 Cell Sorter, San Jose, CA, USA). Cell populations from the bone marrow and PBMC were collected separately and incubated with RANKL and M-CSF (Section 3.1.3) to assess osteoclastogenic potential.

For analysis of osteoclast precursor expressions of TRAF6 and NFATc1

Fixed bone marrow cells or PBMC from rats were washed with DPBS, blocked in 3% BSA-PBS for 1 hour then were stained overnight at 4°C with efluor-conjugated anti-rat CD11b (Ebiosciences, San Diego, CA, USA) and FITC-conjugated anti-rat Gr-1 (Abcam, Cambridge, UK) antibodies. Cells were washed thrice with 3% BSA-PBS and permeabilized by incubation in 0.1% Triton-X-100 solution for 10 min at room temperature. Cells were washed with 3% BSA-PBS and incubated in NFATc1 (sc-13033, Santa Cruz Biotechnology) or TRAF6 (sc-7221, Santa Cruz Biotechnology) antibodies for 2 hours at room temperature, followed by anti-rabbit Alexa Fluor® 594

antibody (Molecular Probes) for 1 hour at room temperature. Cells were washed thrice, filtered through a 40 μm pore size filter and analyzed by BD LSRFortessa flow cytometer (BD LSRFortessa, BD Biosciences). $Cd11b^{+}/Gr\text{-}1^{-/low}$ cells were gated and 10 000 events analysed for fluorescence intensity with excitation set at 590 nm and emission at 610 nm. Data collected was analyzed with the Summit 4.3 software (Beckman Coulter).

3.2.8 Bone histology

The left distal femora were fixed in formalin overnight, decalcified in 10% EDTA (E5134; Sigma, USA) for 2 weeks (solution was refreshed every 4^{th} day), dehydrated and paraffin embedded. Samples were serially sectioned and stained with hematoxylin and eosin. 5 μm sections of distal femora were stained for TRAP (Sigma, USA) to label osteoclasts. Representative sections from 8 rats per group were imaged using a brightfield microscope (Nikon Instruments). Histomorphometric analyses for bone surface covered by osteoclasts (Oc.S/BS), eroded surface as a ratio to bone surface (ES/BS), and number of osteoclasts normalized to bone perimeter (N.OC/B.pm) were calculated using ImageJ.

3.2.9 Protein extraction and immunoblot analysis

After marrow was flushed out, the bones were crushed with a mortar and pestle and transferred to a microcentrifuge tube. RIPA lysis buffer (Thermo scientific, USA) containing a mini EDTA protease inhibitor cocktail (Roche, USA) was added to the bone fragments which were homogenized (Ultra

Turrax T10 basic homogenizer, IKA, Malaysia) for 3 min at 20 000 rpm. Tools were cleaned thoroughly with 70% ethanol to prevent contamination between samples. The homogenized bone in RIPA buffer was then sonicated in a biorupter (Bioruptor® Plus, Diagenode, NJ, USA) for 5 cycles (sonication cycle: 10s on, 10s off) at 4°C. The suspension was centrifuged at maximum speed for 15 min at 4°C and the supernatant collected. Bio-Rad Bradford protein assay (Bio-Rad Laboratories, Hercules, CA, USA) was used to determine total protein concentration with serial dilutions of Bovine Serum Albumin as a standard. 20 µg of protein lysate in 4x SDS-loading buffer from each treatment group were heated at 95°C for 5 minutes. Protein lysates were resolved on SDS-PAGE gel using the Mini PROTEAN 3 electropheresis cell (Bio-Rad, USA) and transferred onto a nitrocellulose membrane using the semidry transfer method. After transfer, nitrocellulose membranes were blocked in 5% non-fat milk (Sigma, USA) in PBS for 1 hour. The membranes were then incubated with NFATc1 (sc-13033, Santa Cruz Biotechnology) or TRAF6 (sc-7221, Santa Cruz Biotechnology) antibodies overnight at 4°C. The membranes were washed 3 times (5 minutes each) with 0.1% Tween 20- PBS (PBST), then incubated with either anti-rabbit secondary antibodies conjugated to horseradish peroxidase (Dako, USA) at room temperature for 2 h (1: 10 000 dilution in 5% non-fat milk). Protein expression signal was detected using Amersham ECL (GE Healthcare, Amersham, UK) and the blots were exposed to CL-XPosure Films (Thermo scientific, USA). The exposed films were developed using an X-Ray Developer (Carestream Health, USA).

3.2.10 Statistical analysis

All results are expressed as mean ± SEM. Statistical analyses were performed using Graphpad Prism 6 (GraphPad Software, Inc., San Diega, CA, USA). Statistical differences were assessed by independent t-test for comparison between two groups, or one-way ANOVA followed by Tukey's post hoc analysis for multiple comparisons between different groups. Differences were considered statistically significant at $P < 0.05$.

CHAPTER 4. RESULTS

4.1 Effect of icaritin on osteoclastogenesis and function *in vitro*

As reviewed in the introduction, the mouse monocyte cell line, RAW 264.7, and human peripheral blood mononuclear cells (PBMC) are well-established cell models for studying osteoclastogenesis (Collin-Osdoby & Osdoby, 2012). As such, RAW 264.7 cells and human PBMC were chosen to investigate the effects of ICT on osteoclastogenesis. Estradiol was used as a positive control as its effects on osteoclastogenesis in these models have been studied extensively (Kharkwal et al., 2012; Srivastava et al., 2001).

4.1.1 Icaritin inhibited osteoclast formation

As previously explained, exposure to two cytokines RANKL and M-CSF, is essential and sufficient to induce differentiation of the RAW 264.7 cells and human PBMC into mature osteoclasts. Compared to undifferentiated monocytes, osteoclasts were identified by their multinucleated structure and expression of the osteoclast marker, TRAP (Fig. 4.1*C*, monocytes vs ctrl). In both cellular models, the presence of ICT led to a dose-dependent reduction in the number of osteoclasts present in the wells. Compared to RANKL-treated controls, ICT treatment at 10 nM and 100 nM reduced osteoclast numbers by 30% and 49% respectively in RAW 264.7 cells, and reduced resultant osteoclast numbers by 24% and 40% in human PBMC ($P < 0.001$) . Accordingly, ICT treatment also reduced TRAP activity of cell lysates in a concentration-dependent manner. Maximal inhibition in osteoclast formation was achieved with 100 nM ICT, which was comparable to the effects of the positive control, 17β- estradiol (Fig. 4.1, striped bars).

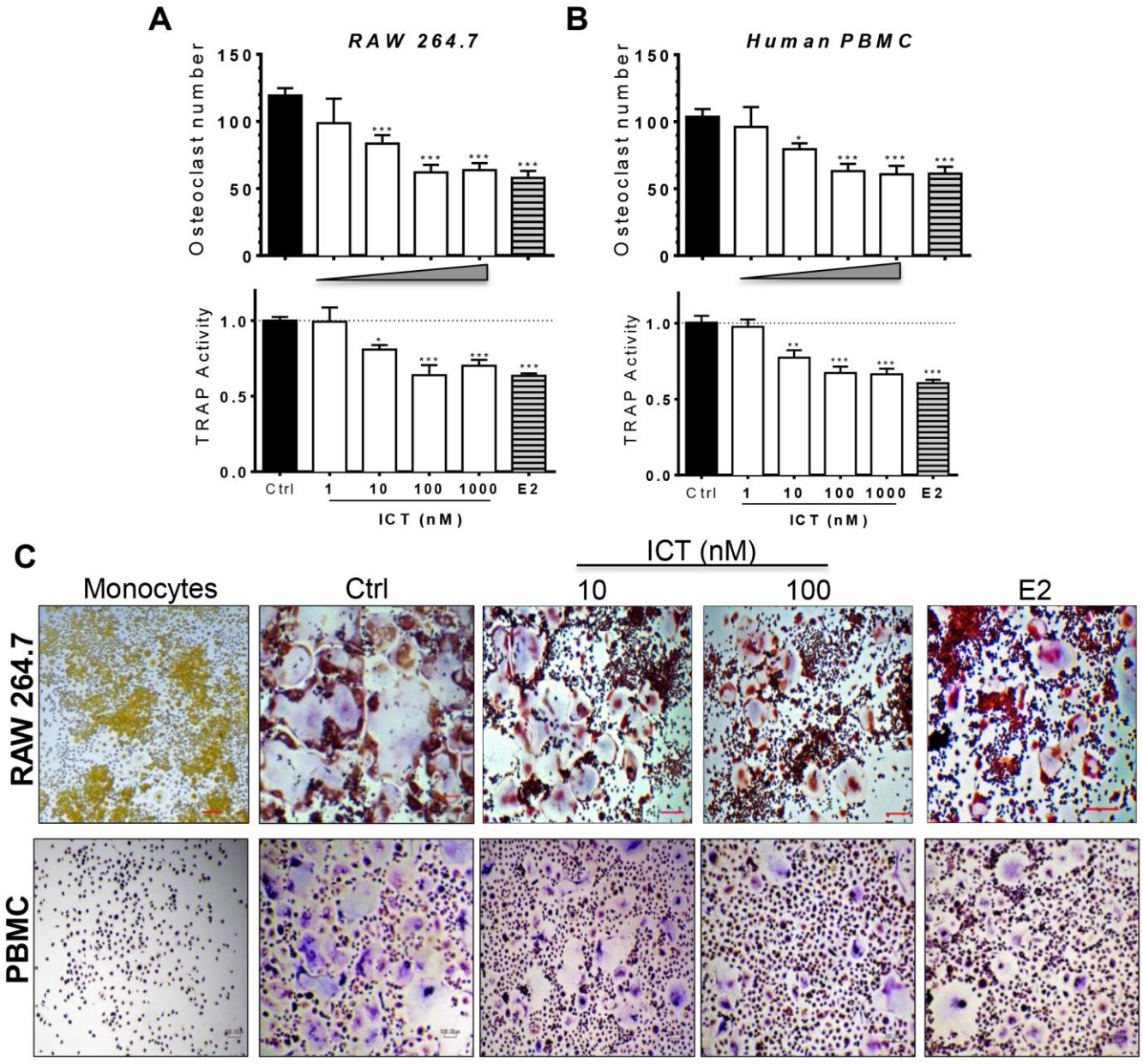

Figure 4.1 Effects of ICT on osteoclast formation in RAW 264.7 cells and human PBMC. (*A*—*C*) Mouse monocytes (RAW 264.7) and human PBMC were incubated with RANKL and M-CSF to induce differentiation into osteoclasts, in the absence or presence of icaritin (ICT) at doses indicated, or estradiol (E2, 10nM). The number of TRAP positive (purple cytoplasm) multinucleated osteoclasts in each well was counted (scale bar = 200 μm in representative images, *C*), and TRAP enzyme activity in cell lysates measured and expressed as fold change compared to control (Ctrl). Data represented as mean ± SEM of 4 independent experiments performed in triplicates. * $P < 0.05$, *** $P < 0.001$ vs Ctrl.

4.1.2 Icaritin inhibited expression of osteoclast-specific genes

To further ascertain ICT's effects on osteoclastogenesis, we analyzed the expression of osteoclast-specific genes: (1) NFATc1, the master transcription factor that mediates osteoclast differentiation, and (2) Cathepsin K, a proteolytic enzyme released by mature osteoclasts for bone resorption. Quantitative RT-PCR revealed that ICT led to a dose-dependent suppression of NFATc1 mRNA expression (Fig. 4.2*A*, open bars). ICT at doses of 10 nM and 100 nM reduced NFATc1 mRNA expression by 17.2% and 30.5% respectively, compared with RANKL-treated control ($P < 0.001$). A similar effect was observed for estradiol that inhibited NFATc1 mRNA expression by 34.5%. Immunoblot analyses also revealed a dose-dependent inhibition of RANKL-induced NFATc1 protein expression by ICT (Fig 4.2*C*). 100 nM ICT inhibited NFATc1 protein expression to a similar extent as estradiol.

Similarly, quantitative RT-PCR revealed that ICT led to a dose-dependent suppression of Cathepsin K (Ctsk) mRNA expression (Fig 4.2*B,* open bars). ICT at doses of 10 nM and 100 nM reduced Ctsk mRNA expression by 16.8% and 27.7% respectively, compared with RANKL-treated control ($P < 0.001$). The positive control estradiol suppressed Ctsk mRNA expression by 33.5%. Immunoblot analyses revealed a dose-dependent inhibition of RANKL-induced Ctsk protein expression by ICT (Fig 4.2*D*). 100 nM ICT inhibited Ctsk protein expression to a similar extent as estradiol.

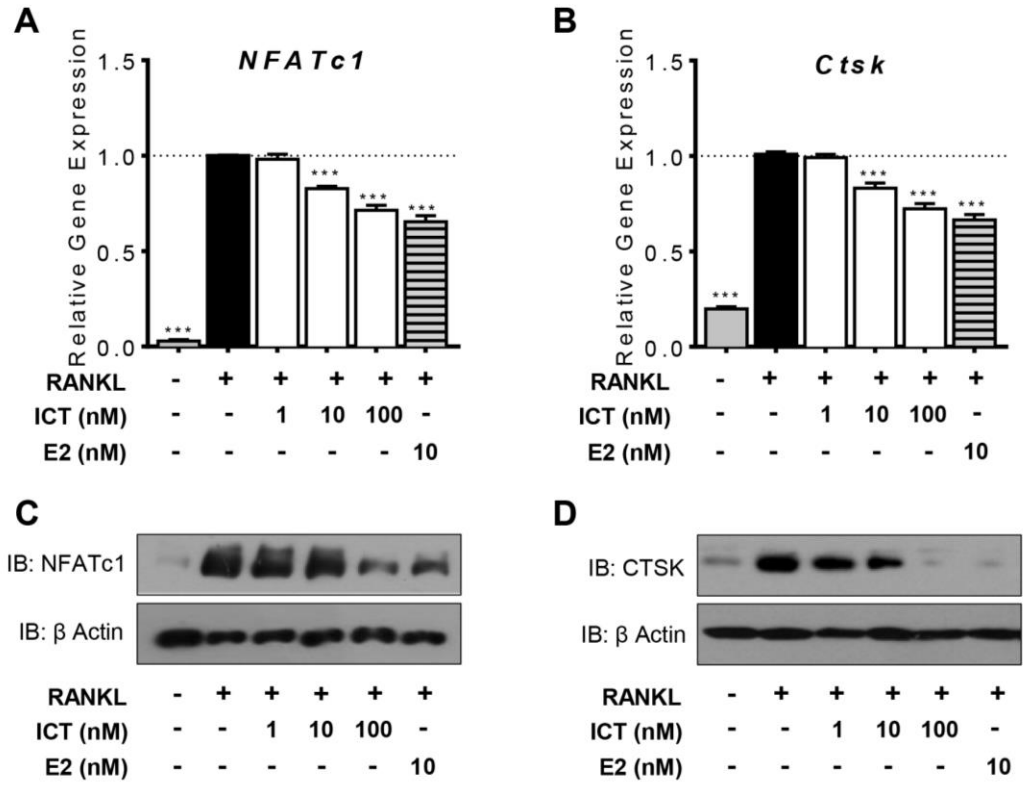

Figure 4.2 Effects of ICT on expression of osteoclast-specific genes. (*A,B*) NFATc1 and Ctsk gene expression: Total RNA was extracted from cells following exposure to indicated treatments for 16h (NFATc1) or 48h (Ctsk), and reverse transcribed to cDNA. Relative gene expression was analysed using RT-PCR and normalised to 18s rRNA. Estradiol effects are in striped bars. Data expressed as mean ± SEM of 3 independent experiments, expressed as fold change relative to RANKL-stimulated controls, *** $P < 0.001$ vs controls (black bars). (*C,D*) NFATc1 and Ctsk protein expression following the indicated treatments were analysed by immunoblotting. β-actin was used as a loading control.

4.1.3 Icaritin inhibited bone resorption in RAW 264.7 cells and human PBMCs

Having shown that ICT inhibits osteoclastogenesis, we then examined the effects of ICT on osteoclast resorption. Since 100 nM ICT led to maximal inhibition in osteoclast formation, we chose this as our working concentration of ICT, and 10 nM estradiol as the positive control. The actin-bound sealing zone is the site of attachment of multinucleated osteoclasts to the bone surface within which the osteoclasts maintain a microenvironment necessary to resorb bone. We assessed the effect of ICT on sealing zone formation by confocal microscopy (Fig. 4.3*A*). In both cellular models, the presence of ICT led to a reduction in the size and number of actin-ring structures, to an extent similar to the positive control estradiol.

To assess resorptive function, RAW 264.7 cells and human PBMC were cultured on calcium hydroxyapatite-coated multiwell plates in the presence of indicated treatments. In both cellular models, ICT led to a dose-dependent reduction in osteoclast resorption, as indicated by the total erosion area covered by the resorption pits (Fig. 4.3*B*). 10 nM and 100 nM ICT treatment led to a reduction in erosion area by 38.3% and 49.9%, respectively, in RAW 264.7 cells, and reduced erosion area by 25.6% and 39.7% in human PBMC ($P < 0.001$). The positive control estradiol also led to reductions in erosion area by 48.6% and 41.5% in RAW 264.7 cells and human PBMC respectively ($P< 0.001$). Notably, 3D measurements (Fig 4.3*C*) indicate that ICT also reduced the volumes of the resorption pits in a concentration-dependent manner compared to controls ($P< 0.001$). Maximal inhibitory effect (42.7%) on volume

of resorption pits was observed with 100 nM of ICT, which was similar to the effects of estradiol (40.1%). Together, our data suggest that ICT suppressed the formation of sealing zones and inhibited resorptive function in both mouse and human osteoclasts.

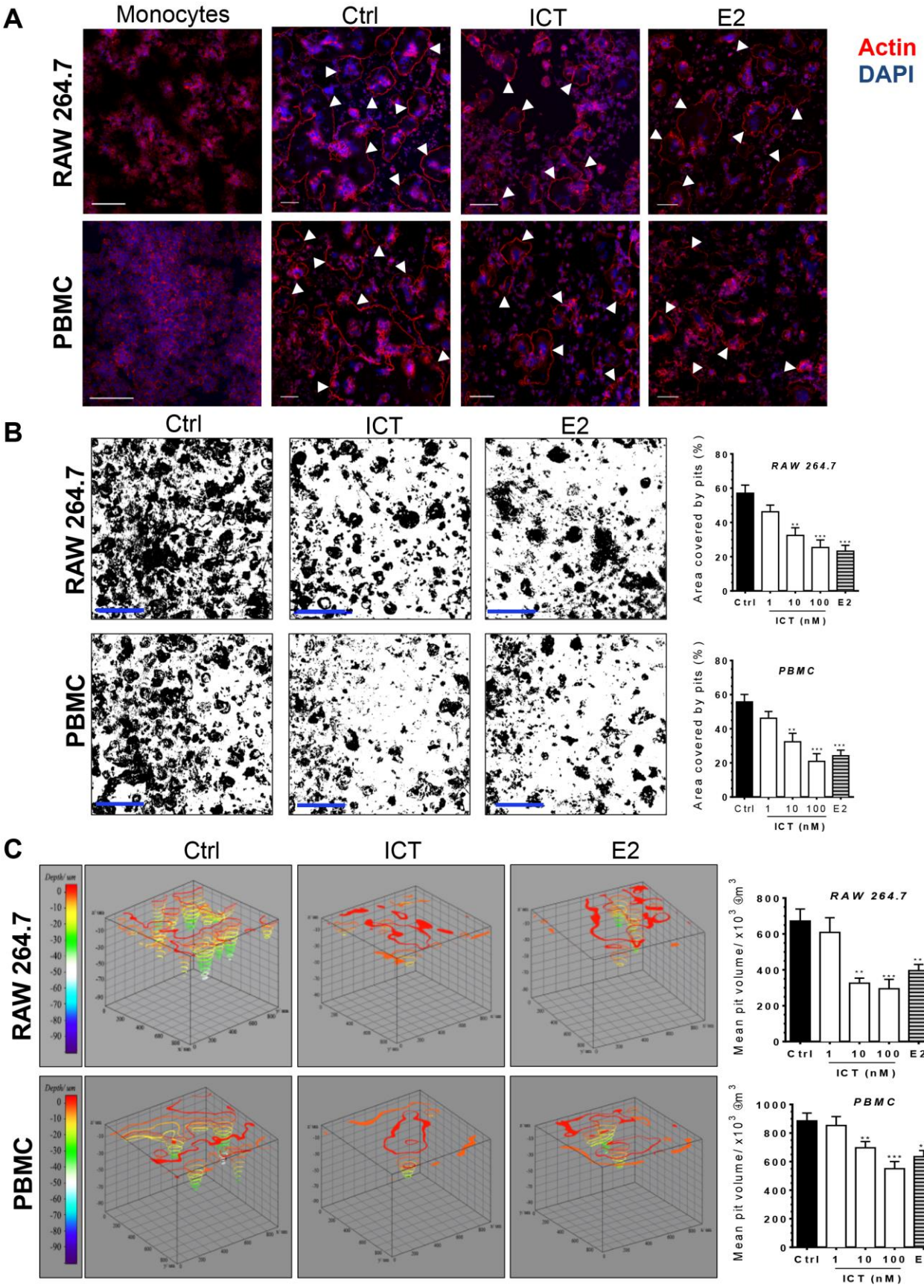
A
Monocytes
Ctrl
ICT
E2
RAW 264.7
PBMC
Actin
DAPI
B
Ctrl
ICT
E2
RAW 264.7
PBMC
Area covered by pits (%)
RAW 264.7
PBMC
Ctrl 1 10 100 E2
ICT (nM)
C
Ctrl
ICT
E2
RAW 264.7
PBMC
Depth/ um
Mean pit volume/ x10^3 @m^3
RAW 264.7
PBMC
Ctrl 1 10 100 E2
ICT (nM)

Figure 4.3 Effects of ICT on osteoclast function. (*A*-*C*) RAW 264.7 cells and PBMC were differentiated in the presence of indicated treatments. (*A*) Representative confocal images show multinucleated osteoclasts (blue nuclei) and their actin-bound (red) sealing zones. Actin-rings are indicated by white arrowheads, scale bar = 100μm. (*B*,*C*) Cells were differentiated on hydroxyapatite-coated wells. Adherent cells were removed and (*B*) images of resorption pits (area in black, scale bar = 500 μm) were acquired by laser microscopy, and area covered by pits measured. Data expressed as mean ± SEM of 9 regions (3 regions each in 3 independent experiments. (*C*) Topography of resorption pits was reconstructed in ImageJ and volume of resorption pits measured. Data expressed as mean ± SEM of 18 pits (6 pits in each of 3 independent experiments). * $P< 0.05$, ** $P< 0.01$, *** $P< 0.001$ vs control.

4.1.4 Inhibitory effects of icaritin not due to non-specific cytotoxicity

To determine if the inhibitory effects of icaritin on osteoclast formation and function was due to cell toxicity, viability of monocytes (Fig. 4.4*A*) and osteoclast precursors (in presence of RANKL, Fig. 4.4*B*) was determined by the MTS assay. There was no change in viability of both RAW 264.7 cells and human PBMC when subjected to ICT at concentrations of 10 and 100 nM (the working concentrations used in other experiments) and up to 1000 nM. However, there was a 35% decrease in viability at 10 000 nM ICT. Similar effects of ICT were observed in the osteoclast precursors (in the presence of RANKL), suggesting that the inhibitory effect of ICT on osteoclastogenesis at the lower working concentrations was not due to cytotoxicity.

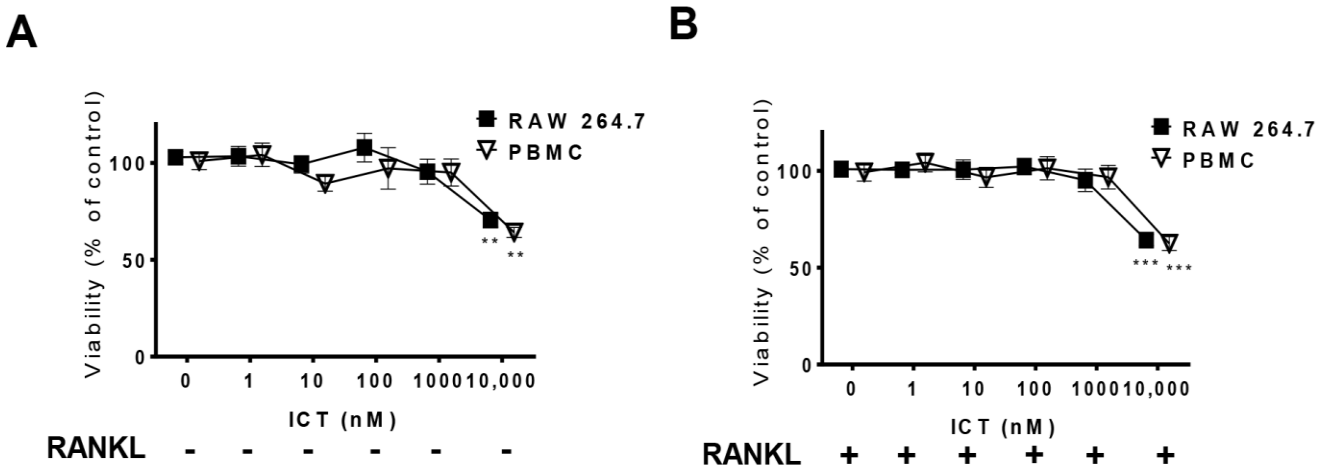

Figure 4.4 Effects of ICT on cell viability. RAW 264.7 cells and PBMC were cultured for 48 h in the (*A*) absence (*B*) or presence of RANKL and indicated doses of ICT. Cell viability was determined by MTS assay and expressed as percentage of untreated controls. Data expressed as mean ± SEM, n=3, ** P< 0.01, *** P< 0.001 vs untreated control.

4.1.5 Icaritin does not have effect on mature osteoclasts

To explore if the reduction in osteoclast numbers with ICT treatment was due to its effect on mature osteoclasts, RAW 264.7 cells and human PBMC were differentiated in the presence of RANKL and M-CSF, with ICT treatment commencing on progressive days: days 0, 1, 2, and 3 in RAW 264.7 cells and days 0, 7, 12, and 15 in human PBMCs (Fig. 4.5*A*). The number of osteoclasts formed was quantified after differentiation for 6 (RAW 264.7 cells) or 21 (human PBMCs) days. Interestingly, ICT inhibited osteoclast formation only when added in the early stages osteoclast differentiation (days 0 and 1 for RAW 264.7 cells, days 0 and 7 for human PBMCs), but had minimal effects when added in the late stages, indicated by resultant osteoclast numbers per well (Fig 4.5*B,C*).

To further ascertain if ICT had effects on mature osteoclasts, RAW 264.7 cells were first differentiated in the presence of RANKL and M-CSF for 3 days, by which time multinucleated osteoclasts have begun to form, ICT was then added to these osteoclast cultures (Fig. 4.5*D*). Indeed, ICT when added to mature osteoclasts did not have effects on sealing zones formed (Fig. 4.5*E*) or resorptive function of the osteoclasts as indicated by area covered by resorption pits (Fig. 4.5*F*). Put together, these results suggest that the reduction in osteoclast numbers by ICT was not due to non-specific cytotoxicity or its effects on mature osteoclasts, instead, suggesting that ICT inhibits osteoclast differentiation from its precursors.

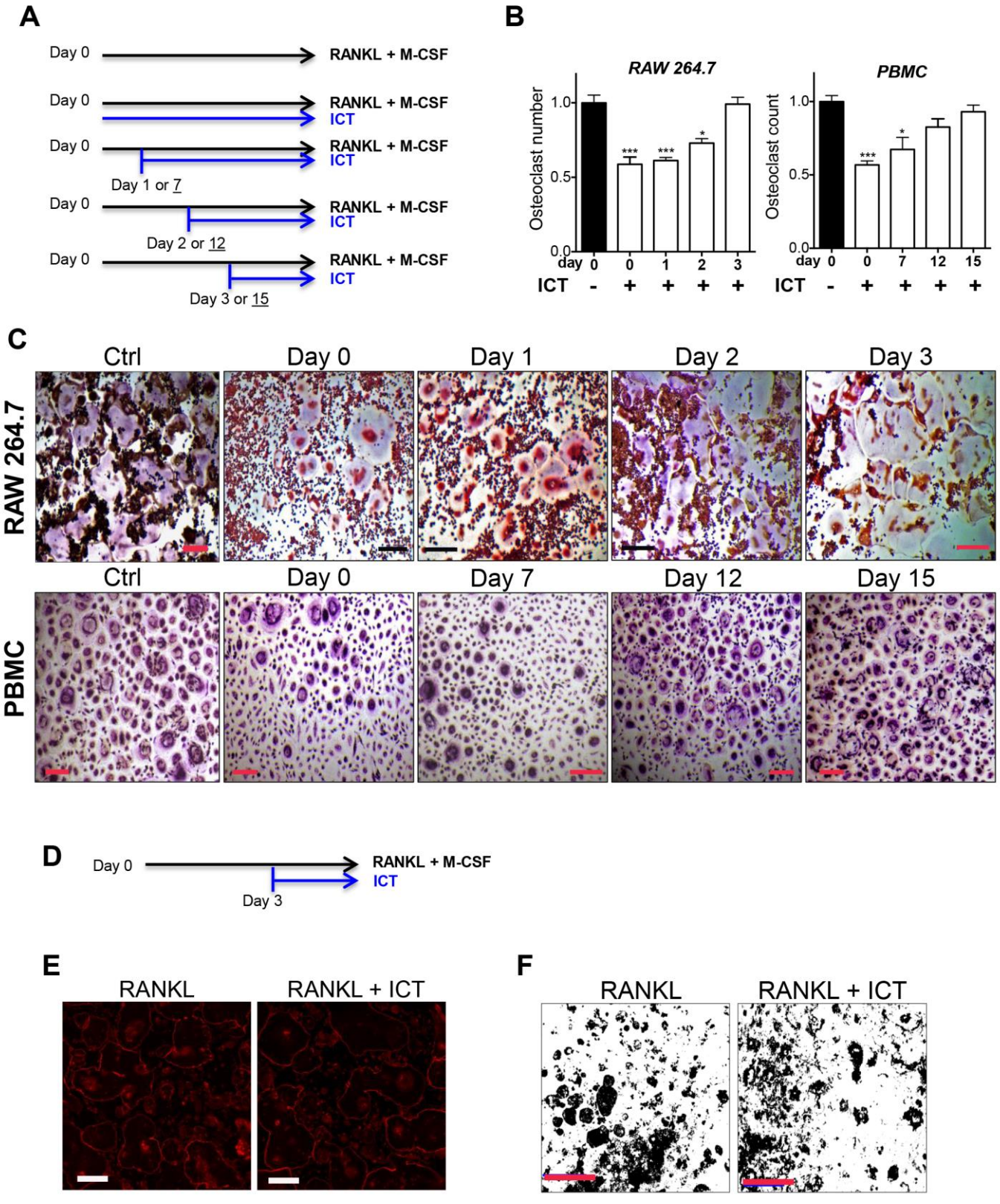
A
Day 0
RANKL + M-CSF
Day 0
RANKL + M-CSF
ICT
Day 0
RANKL + M-CSF
ICT
Day 1 or 7
Day 0
RANKL + M-CSF
ICT
Day 2 or 12
Day 0
RANKL + M-CSF
ICT
Day 3 or 15
B
RAW 264.7
PBMC
Osteoclast number
Osteoclast count
1.0
0.5
0.0
***
*
day 0 0 1 2 3
day 0 0 7 12 15
ICT - + + + +
C
Ctrl
Day 0
Day 1
Day 2
Day 3
RAW 264.7
Ctrl
Day 0
Day 7
Day 12
Day 15
PBMC
D
Day 0
RANKL + M-CSF
ICT
Day 3
E
RANKL
RANKL + ICT
F
RANKL
RANKL + ICT

Figure 4.5 Effects of ICT on mature osteoclasts. (*A-C*) Cells were differentiated in RANKL and MCSF, with ICT (100 nM) treatment commencing on days 0, 1, 2 and 3 for RAW 264.7 cells and days 0, 7, 12 and 15 for human PBMCs. (*B*) TRAP positive multinucleated cells in each well were counted, with ICT treatment initiated on the indicated days, and expressed as fold change compared to untreated controls. Data expressed as mean ± SEM, n=3, * $P < 0.05$, *** $P < 0.001$ vs untreated control. (*C*) Representative light microscope images of osteoclasts present in each well after ICT treatment initiated as indicated, scale bar = 100 μm. (*D-F*) After 3 days' incubation in RANKL and M-CSF, 100 nM ICT was added to osteoclast cultures for another 3 days. (*E*) Actin-bound sealing zones visualized by confocal microscopy, scale bar = 100 μm and (*F*) representative laser microscope image of well showing area covered by resorption pits in black, scale bar = 500 μm. Experiments were repeated thrice.

4.2 Mechanism by which icaritin inhibits osteoclast differentiation

The activation of RANK by its ligand activates several downstream signaling cascades, collectively known as the RANKL signaling pathway (Fig 1.5), to upregulate the expression of osteoclast-specific genes thereby enabling osteoclast differentiation (Boyle et al., 2003). Since ICT has been shown to inhibit osteoclast differentiation, we investigated the effects of ICT on the RANKL signaling pathway in RAW 264.7 cells.

4.2.1 Effects of icaritin not mediated via estrogen-receptor signaling

Given that ICT has been shown to exert estrogenic activity *in vitro* (Tiong et al., 2012; H. Y. Ye & Lou, 2005) and activation of estrogen receptor (ER)-signaling suppresses RANKL-induced AP-1 activity (Shevde, Bendixen, Dienger, & Pike, 2000), we investigated whether the suppressive effects of ICT on osteoclast differentiation were due to activation of ER-signaling. RAW 264.7 cells were differentiated in the presence of RANKL and M-CSF, supplemented with ICT or estradiol, with and without the ER-antagonist ICI 182 780 (1 μM). Compared to vehicle-treated controls, ICT and estradiol treatment inhibited osteoclast formation by 35% ($P < 0.01$) and 45% ($P< 0.05$) respectively. The presence of the ER-antagonist, ICI 182 780, was unable to reverse ICT's inhibition in osteoclast differentiation (Fig 4.6*A,B*), suggesting that the suppressive effects of ICT were not mediated via ER-signaling.

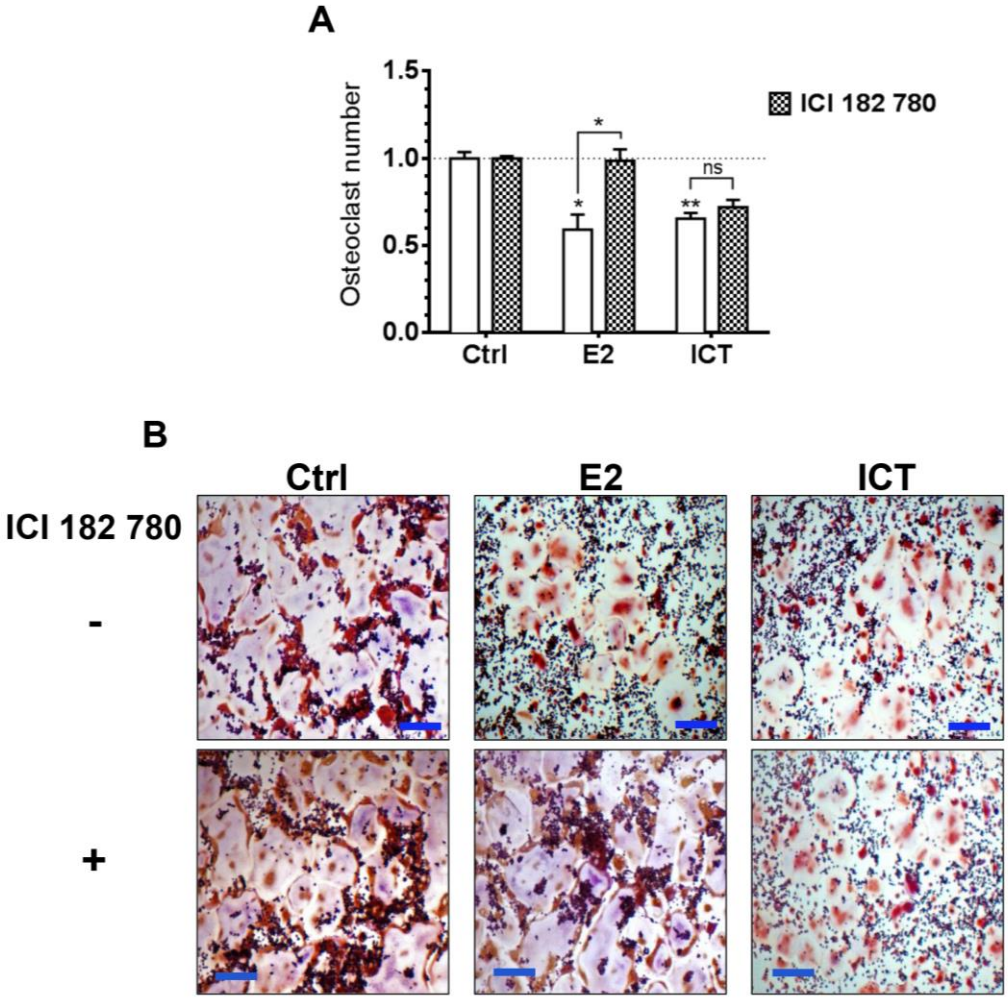

Figure 4.6 Effects of ICT on osteoclast differentiation in presence of ER-antagonist RAW 264.7 cells were differentiated for in RANKL and MCSF in the absence (white bars) and presence (shaded bars) of ICI 182,780 (1 μM,), supplemented with indicated treatments. After 6 days' treatment, (*A*) TRAP positive multinucleated cells in each well were counted and expressed as fold change compared to untreated controls. Data expressed as mean ± SEM, n=3, * $P < 0.05$, ** $P < 0.001$ vs untreated control. (*B*) Representative light microscope images of osteoclasts present in each well after indicated treatments, scale bar = 100 μm.

4.2.2 Icaritin did not reduce RANK expression of osteoclast precursors

To study the effect of ICT on the RANKL signaling pathway, we examined the effect of ICT on expression of the surface receptor RANK. Expression of RANK is regulated by the critical osteoclastogenic cytokine, M-CSF (H. Takayanagi, 2007). Protein levels of RANK were measured by immunoblotting of whole cell lysates (Fig 4.7*A*). The presence of M-CSF led to an increase in RANK protein expression (Fig 4.7*A*, lanes 1 and 4), while ICT had no effect on RANK protein expression in the absence or presence of M-CSF. To further corroborate our findings, cell surface expression of RANK was assessed by immunofluorescence. Consistently, the presence of M-CSF led to a 30% ($P< 0.001$) increase in cell surface expression of RANK (Fig 4.7*B*). ICT had no effect on surface RANK expression in the absence or presence of M-CSF. On the contrary, estradiol reduced surface RANK expression by 10.5% ($P< 0.05$) in the absence of M-CSF, and 14.2% ($P< 0.001$) in the presence of M-CSF, which is consistent with previous reports (Galal et al., 2007). These findings suggest that ICT action is mediated downstream of RANK, thus we examined the effects of ICT on the downstream NFκB and MAPK signaling pathways.

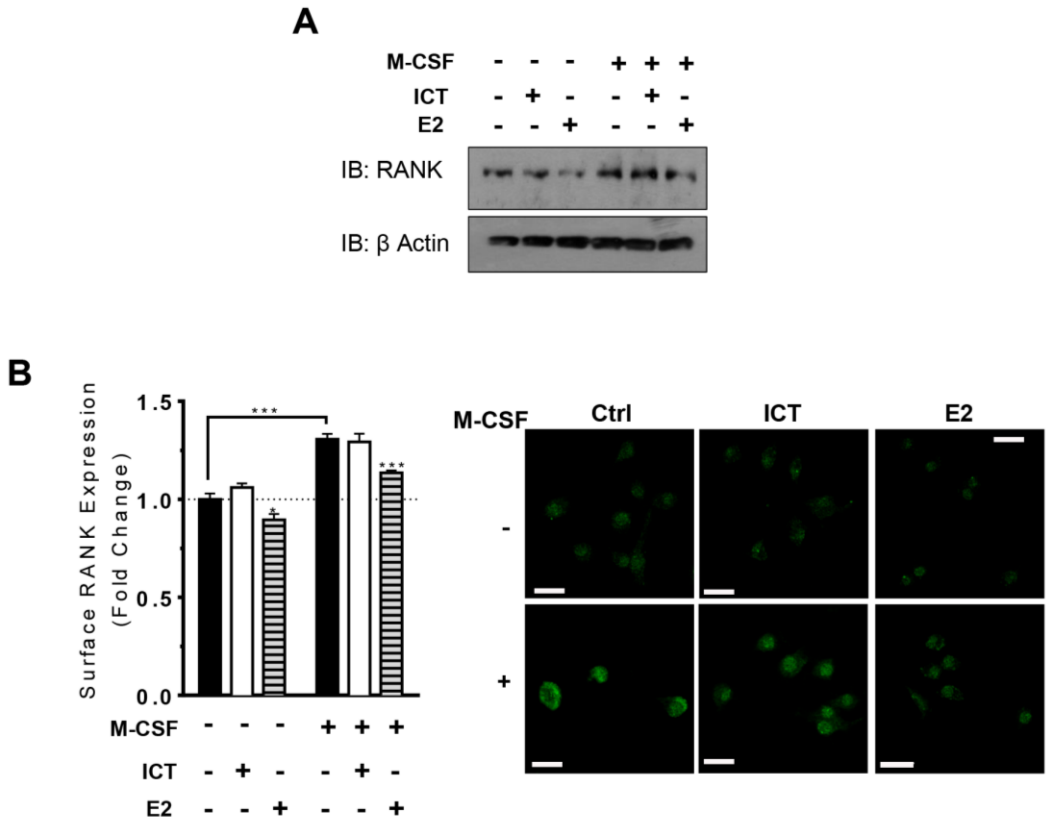

Figure 4.7 Effects of ICT on RANK expression. RAW 264.7 cells were cultured for 48 h in indicated conditions. (*A*) RANK protein expression was analyzed by immunoblotting of whole cell lysates. β actin was used as a loading control. (*B*) Cell were fixed and surface RANK expression analyzed by confocal microscopy. Data in graph represented as mean ± SEM of 3 fields in 3 independent experiments, * $p< 0.05$, *** $p< 0.001$ vs matched control. Representative confocal images showing surface RANK protein expression (green), scale bar = 20 μm.

4.2.3 Icaritin inhibited RANKL-induced NFκB signaling pathway

Having shown that ICT action is mediated downstream of RANK, we investigated the effects of ICT on NFκB-mediated osteoclastogenesis by examining RANKL-induced phosphorylation and degradation of the inhibitory subunit of NFκB (IκB). Time course analysis showed that RANKL led to increased phosphorylation of IκB and a corresponding decrease in total IκB levels 15 – 30 min post-stimulation (Fig. 4.8*A*, upper panels). We therefore assessed the effects of ICT on RANKL-induced NFκB pathway at the 30 min time-point. Indeed, ICT dose-dependently inhibited IκB phosphorylation and prevented its degradation to an extent similar to estradiol (Fig. 4.8*B*, upper panels). The degradation of IκB releases NFκB/p65 thus allowing for its phosphorylation and nuclear translocation. Similarly, ICT dose-dependently inhibited RANKL-induced phosphorylation of p65 (Fig. 4.8*B*). Consistent with its ability to reverse RANKL-induced IκB degradation, immunoblot analyses of cytosolic and nuclear fractions showed that ICT inhibited RANKL-induced nuclear translocation of p65 in a dose-dependent manner (Fig. 4.8*C*). These findings were corroborated by immunofluorescence studies. In the absence of RANKL, p65 (red) was mostly located in the cytosol, while with RANKL stimulation p65 was mostly present in the nucleus (blue). The presence of ICT prevented this nuclear translocation (Fig. 4.8*D*). Estradiol, as a positive control (Kharkwal et al., 2012), also inhibited nuclear translocation of p65 (Fig. 4.8*C,D*).

We examined the effect of ICT on NFκB transcriptional activity using a luciferase reporter gene assay. Indeed, RANKL exposure led to a marked increase in NFκB transcriptional activity, which was inhibited by ICT in a dose-dependent manner (Fig. 4.8*E*). Compared to RANKL-stimulated controls, 100 nM ICT led to a 48.2% reduction in NFκB-dependent luciferase expression, while estradiol suppressed NFκB-dependent luciferase expression by 36.7%. Collectively, these results suggest that ICT inhibited RANKL-induced osteoclast differentiation by inhibiting the NFκB signaling pathway.

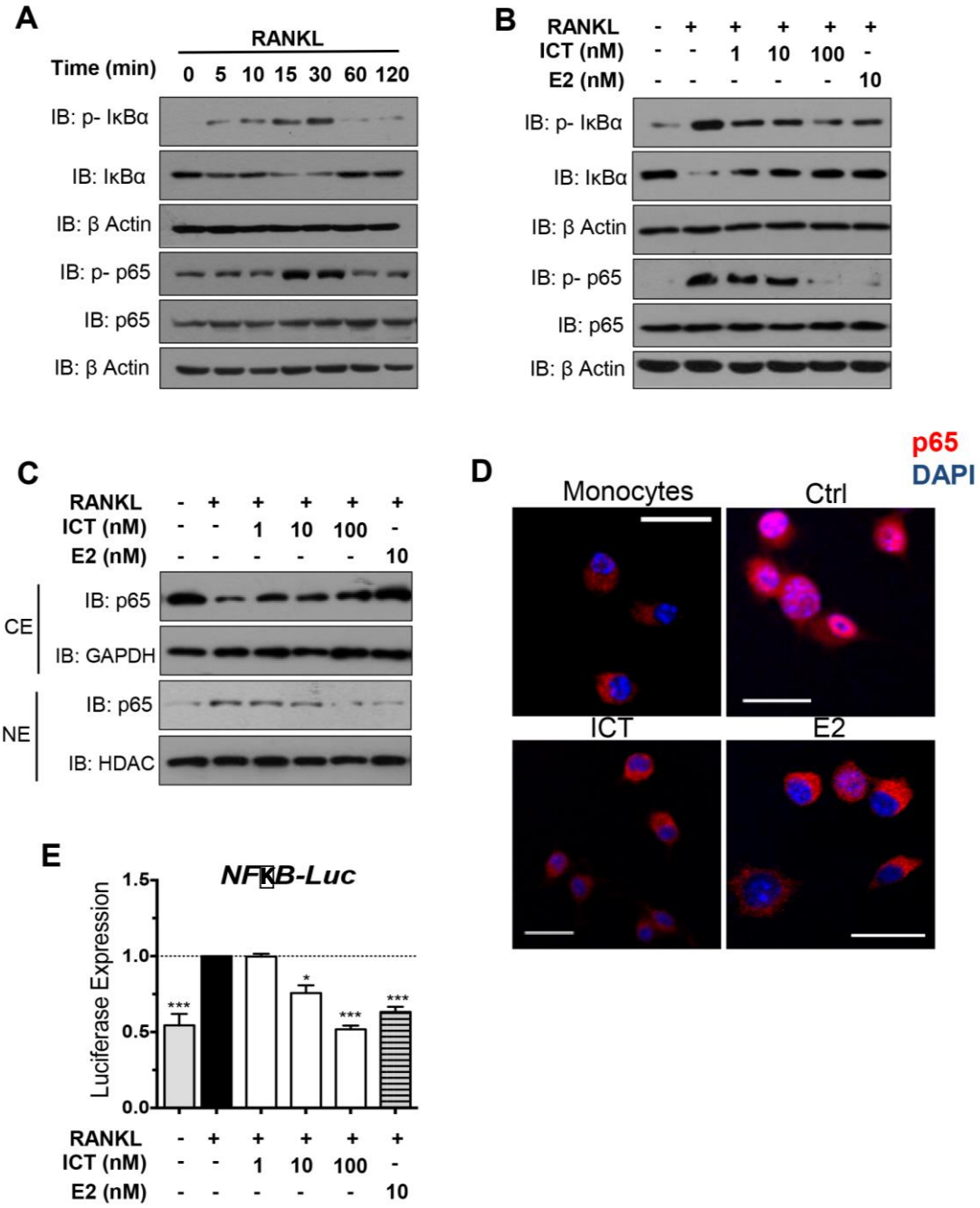

Figure 4.8 Effects of ICT on RANKL-induced NFκB signaling pathway. (*A*) RAW 264.7 cells were incubated with RANKL for indicated durations. Cell lysates were subjected to immunoblot analysis with indicated antibodies. (*B-D*) RAW 264.7 cells were treated with indicated doses of ICT or estradiol (E2) for 2h followed by RANKL for 15 min. Cell lysates were extracted and subjected to immunoblot analysis with specified antibodies. (*B*) Dose-dependent effect of ICT on RANKL-induced activation of NFκB signaling pathway. (*C*) Immunoblot analysis of cytoplasmic (CE) and nuclear (NE) extracts to examine nuclear translocation of p65. (D) Representative confocal microscope images of p65 (red) and nuclei (blue), scale bar = 20 μm.. (*E*) NFκB –dependent luciferase reporter gene expression in RAW 264.7 cells transfected as described in *Materials & Methods*, stimulated with RANKL for 1h. Results normalized to renilla luciferase expression and expressed as fold change compared to control. Data in graph represented as mean ± SEM of 3 independent experiments, * P< 0.05, *** P< 0.001 vs RANKL-treated control.

4.2.4 Icaritin inhibited RANKL-induced MAPK/AP-1 signaling pathway

Activation of MAPK, downstream of RANK, induces the expression of NFATc1 via the AP-1 transcription factor (Boyle et al., 2003; H. Takayanagi, 2007). AP-1 is a heterodimer of the c-Jun and c-Fos transcription factors that are regulated by the c-Jun N-terminal kinase (JNK), p38, and extracellular signal-regulated kinase (ERK) MAPK (M. Matsumoto et al., 2000; Monje et al., 2005). We thus examined the phosphorylation of JNK, p38, and ERK. Consistent with previous reports that activation of MAPK following RANKL induction is an acute event (Boyle et al., 2003; H. Takayanagi, 2007), we show that maximal activation of these MAPK by RANKL was detected at 15 min (Fig. 4.9*A*). We therefore assessed the effect of ICT on MAPK activation following 15 min of RANKL exposure. Treatment with ICT significantly decreased phosphorylation of JNK, p38 and ERK in a dose-dependent manner (Fig. 4.9*B*). We examined the effect of ICT on AP-1 transcriptional activity using a luciferase reporter gene assay. Indeed, RANKL exposure led to a marked increase in AP-1 transcriptional activity, which was inhibited by ICT in a dose-dependent manner (Fig. 4.9*C*). Compared to RANKL-stimulated controls, 100 nM ICT led to a 45.9% reduction in AP-1-dependent luciferase expression, while estradiol suppressed AP-1-dependent luciferase expression by 48.1%. The above data indicate that anti-osteoclast effects of ICT may be mediated, in part, via the MAPK/AP-1 signaling pathway.

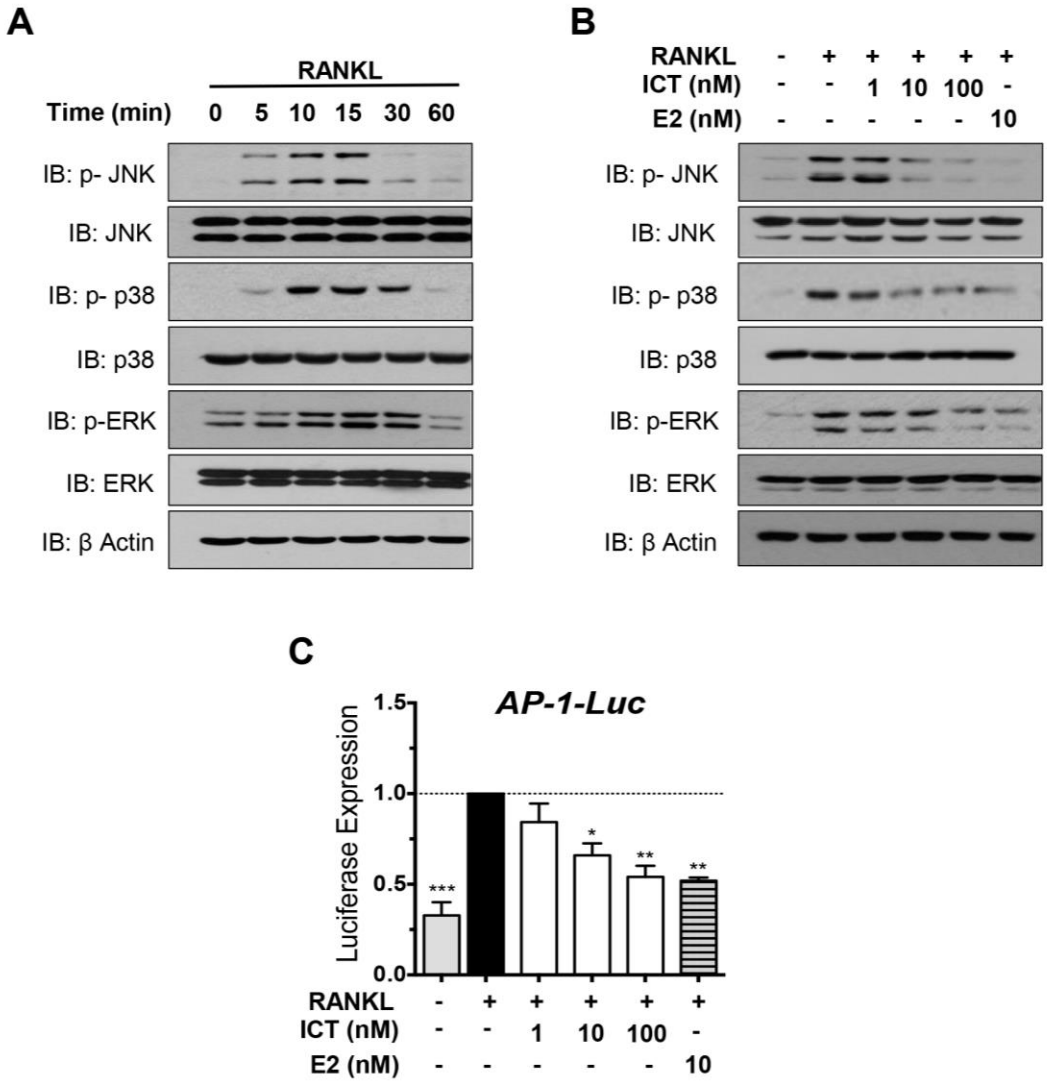

Figure 4.9 Effects of ICT on RANKL-induced MAPK/AP-1 signaling pathway. (*A*) RAW 264.7 cells were incubated with RANKL for indicated durations. Cell lysates were subjected to immunoblot analysis with indicated antibodies. (*B*) Dose-dependent effect of ICT on MAPK activation: RAW 264.7 cells were treated with indicated doses of ICT or estradiol (E2) for 2h followed by RANKL for 15 min. Cell lysates were extracted and subjected to immunoblot analysis with specified antibodies. (*C*) AP-1- dependent luciferase reporter gene expression in RAW 264.7 cells transfected as described in *Materials & Methods*, stimulated with RANKL for 1h. Results normalized to renilla luciferase expression and expressed as fold change compared to control. Data in graph represented as mean ± SEM of 3 independent experiments, * P< 0.05, ** P< 0.01 vs RANKL-treated control.

4.2.5 Icaritin suppresses RANKL-induced intracellular ROS production

Given that the production of intracellular ROS has been shown to play an essential role in osteoclast differentiation (M. S. Kim et al., 2010; N. K. Lee et al., 2005), we examined the effect of ICT on RANKL-induced intracellular ROS production. Intracellular ROS was measured by using the cell permeable dye CM-H2DCFHDA, which is highly fluorescent when oxidized. Fluorescence intensity was quantified by flow cytometry. Time course analysis revealed that RANKL-induced osteoclast differentiation was accompanied by an increase in intracellular ROS (Fig. 4.10*A,B* Control). Intracellular ROS production was significantly attenuated by positive controls, ROS scavenger N- Acetyl Cysteine (Fig 4.10, NAC, checked bars) and estradiol (Fig 4.10*B*, striped bars). The presence of ICT suppressed RANKL-induced intracellular ROS production in a concentration-dependent manner. Compared to RANKL-stimulated controls, addition of 10 nM and 100 nM ICT led to a reduction in intracellular ROS by 16% and 25.7% (Fig. 4.10*B*).

Since the activation of the NADPH Oxidase 1 (Nox1) enzyme has been shown to be responsible for ROS-mediated osteoclast differentiation (M. S. Kim et al., 2010; Sasaki et al., 2009), we then examined if ICT suppressed ROS production by acting on Nox1. Immunoblot analyses showed that ICT attenuated RANKL-stimulated Nox1 protein levels in a dose-dependent manner (Fig. 4.10*C*). Since GTP-bound Rac1 is a cytosolic component of Nox1 and is required for Nox1 activation, we examined ICT's effects on GTP-Rac1 levels as an indicator of Nox1 activation. Immunoblot analyses revealed that RANKL enhanced GTP-bound Rac1 levels, without altering total Rac1 levels, and these stimulatory

effects of RANKL were abrogated by ICT in a dose-dependent manner (Fig. 4*.10C*), suggesting that ICT suppressed Nox1 activation. These results indicate that ICT may modulate osteoclastogenesis, in part, by inhibiting RANKL-induced ROS production, through attenuating Nox1 translation and activation.

4.2.6 Icaritin inhibited RANKL-induced TRAF6/cSrc/PI3K signalling

It has been demonstrated that downstream of TRAF6, the sequential activation of tyrosine kinase c-Src and PI3K (Park et al., 2004) is responsible for Nox1 activation (N. K. Lee et al., 2005; S. H. Lee & Jang, 2015) and ROS production in response to RANKL stimulation, we therefore investigated the effect of ICT treatment on this pathway. Immunoblot experiments revealed that RANKL led to increased protein levels of TRAF6, c-Src and phosphorylated PI3K (Fig 4.10*D,* lanes 1 and 2). Remarkably, addition of ICT dose-dependently decreased RANKL-induced TRAF6 levels, c-Src translation and PI3K phosphorylation (Fig. 4.10*D*). This suggests that the inhibitory effect of ICT on ROS production could be mediated through the TRAF6/tyrosine kinase c-Src/PI3K pathway. A similar inhibitory effect on TRAF6/c-Src/PI3K signaling was also observed for estradiol.

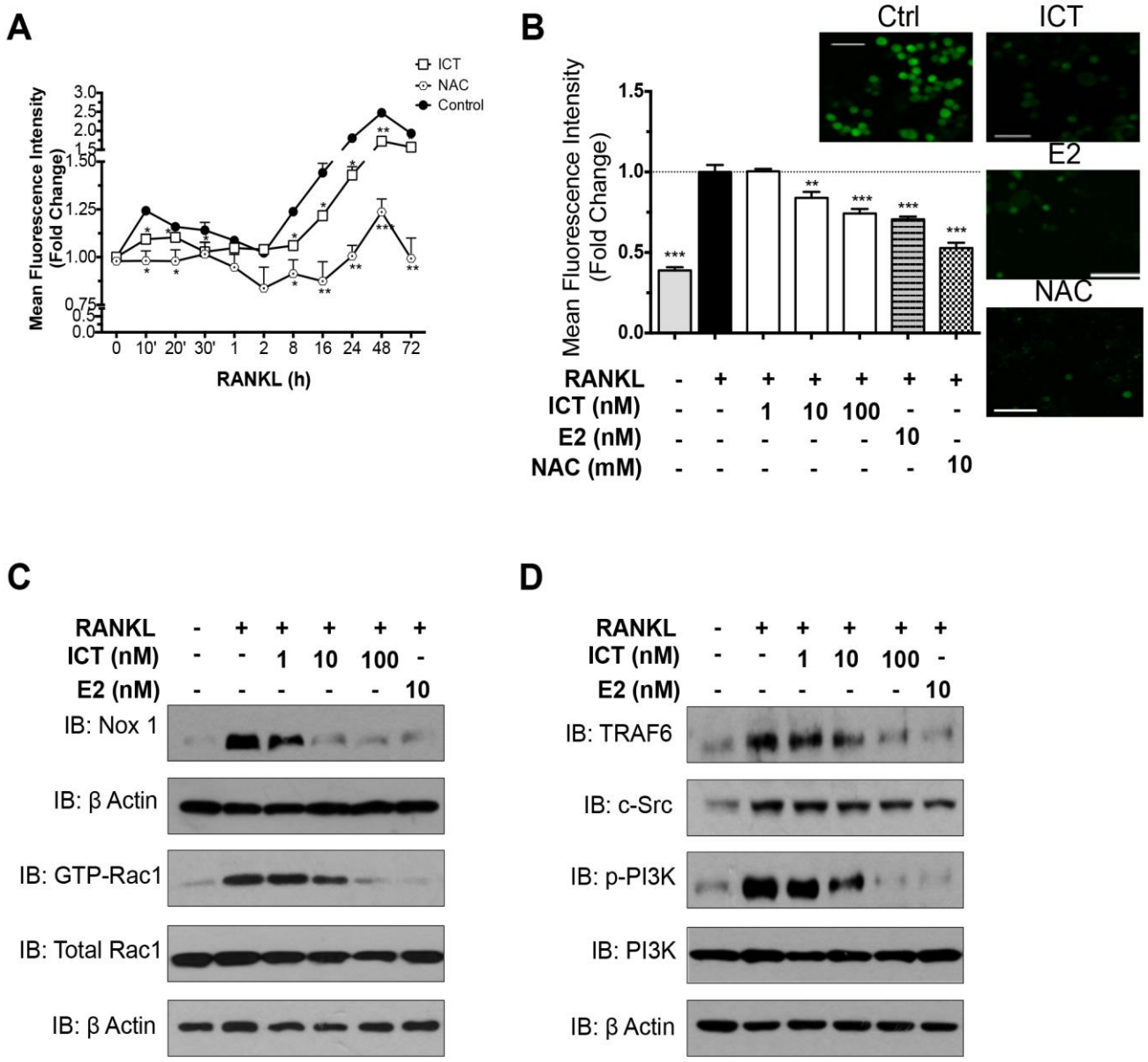

Figure 4.10 Effects of ICT on RANKL-induced TRAF6/Nox1/ROS signaling (*A,B*) RAW 264.7 cells were treated as indicated and intracellular ROS measured by flow cytometry as explained in *Materials & Methods* to determine (*A*) time course of RANKL-induced intracellular ROS production and (*B*) dose-dependent effect of ICT on intracellular ROS (indicated by green fluorescence, insert, scale bar = 100 μm). Data expressed as mean ± SEM of 4 independent experiments, * P< 0.05, ** P< 0.01, *** P< 0.001 vs matched control. (*C,D*) Immunoblot analysis of signaling proteins in the RANKL-induced TRAF6/Nox1/ROS pathway after RAW 264.7 cells were treated as indicated.

4.2.7 Inhibition of ROS-mediated calcineurin phosphatase activity and NFATc1 activity

It has been shown that the RANKL-induced ROS generation leads to the dephosphorylation of cytoplasmic NFATc1 (M. S. Kim et al., 2010), allowing its nuclear translocation to mediate osteoclastogenesis. The dephosphorylation of NFATc1 is also well-known to be dependent on the phosphatase calcineurin (H. Takayanagi, 2007). To examine the effect of ICT treatment on calcineurin phosphatase activity, we used a calcineurin-specific activity assay kit. RANKL stimulation led to a marked increase in calcineurin-phosphatase activity that was dose-dependently attenuated by ICT, in a manner similar to the positive controls, estradiol and NAC, the ROS scavenger (Fig. 4.11*A*). Addition of 10 nM and 100 nM ICT inhibited calcineurin activity by 23.1% and 34.7% compared to RANKL-stimulated controls. Consistently, the inhibition of calcineurin phosphatase activity by ICT was accompanied by increased cytoplasmic levels of phosphorylated NFATc1 and suppression in nuclear translocation of NFATc1 (Fig. 4.11*B*, right vs. left). To further corroborate our findings that ICT reduces NFATc1 nuclear translocation and activity, we performed an NFATc1-luciferase reporter gene assay. ICT inhibited NFATc1-dependent luciferase expression in a concentration dependent manner (Fig. 4.11*C*). Compared to RANKL-stimulated controls, addition of 10 nM and 100 nM ICT suppressed NFATc1-dependent luciferase expression by 25.5% and 39.1%. Put together, our data suggest that ICT inhibited RANKL-induced intracellular ROS production and consequent calcineurin phosphatase activity to result in suppression of NFATc1 activity.

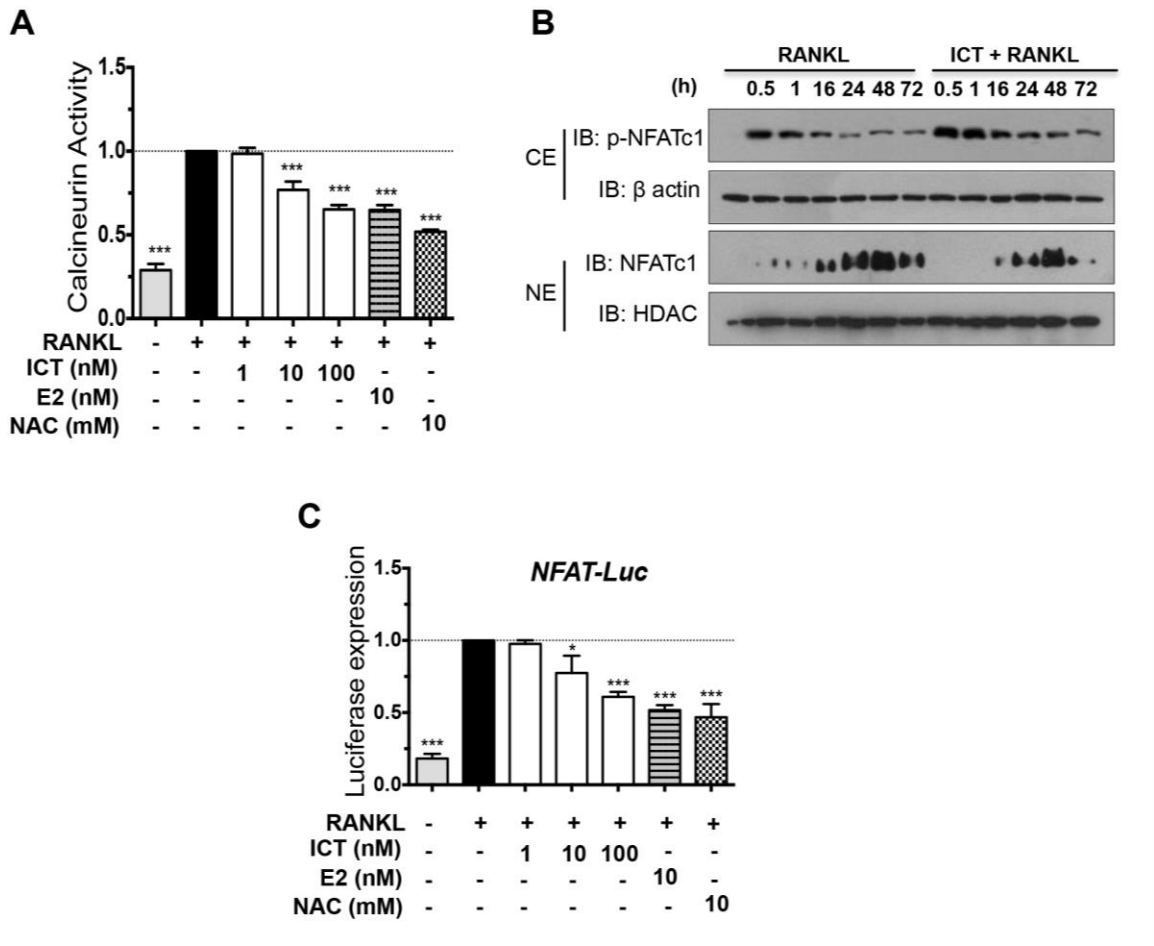

Figure 4.11 Effects of ICT on NFATc1 nuclear translocation and activity (*A*) RAW 264.7 cells were treated as indicated and calcineurin phosphatase activity in cell lysates quantified using a calcineurin-specific phosphatase activity assay kit. Data expressed as mean ± SEM of 3 independent experiments. (*B*) NFATc1 nuclear translocation: Cell cytosolic (CE) and nuclear extracts (NE) were subjected to immunoblot analysis with indicated antibodies. (*C*) NFATc1- dependent luciferase reporter gene expression measured in RAW 264.7 cells transfected as described in *Materials & Methods*, stimulated with RANKL for 24 h. Results normalized to renilla luciferase expression and expressed as fold change compared to control. Data expressed as mean ± SEM of 3 independent experiments. * P< 0.05, ** P< 0.01, *** P< 0.001 vs RANKL-treated control.

4.2.8 Icaritin mediates proteasomal degradation of TRAF6

Our data, thus far, suggest that suppression of RANKL-induced NFκB, MAPK/AP-1 and ROS signaling pathways led to downregulation of NFATc1 expression and its transcriptional activity. However, it remained unclear how these pleiotropic actions of ICT were derived. Since these effects of ICT were not mediated through activation of ER-signaling (Fig. 4.6) and ICT had no effects on RANK expression (Fig. 4.7), we hypothesized that the inhibition of the various signaling pathways by ICT may act through the RANK adaptor protein, TRAF6. As such, we conducted a time course experiment to study the levels of TRAF6 in RAW 264.7 cells following RANKL exposure, in the absence and presence of ICT. RANKL stimulation was associated with increased TRAF6 protein levels (Fig. 4.12*A,* left lanes). Notably, treatment with ICT inhibited this increase in TRAF6 (Fig. 4.12*A,* right vs left). Since the presence of ICT did not alter TRAF6 mRNA expression (Fig. 4.12*B*), we hypothesized that ICT may exert its effects through degradation of this protein. We therefore examined TRAF6 protein levels in the presence of the proteasomal inhibitor MG 132. As expected, presence of ICT led to decreased TRAF6 protein levels (Fig. 4.12*C*, lanes 1 and 2). Strikingly, MG 132 reversed the effects of ICT on TRAF6 levels (Fig. 4.12*C*), indicating that suppression of TRAF6 by ICT was regulated via proteasomal degradation. To further corroborate our findings, we differentiated RAW 264.7 cells in the presence of ICT and MG 132. Indeed, presence of the MG 132 reversed the suppressive effects of ICT on osteoclast differentiation (Fig 4.12*D*). These results suggest that ICT suppressed osteoclastogenesis by mediating proteasomal degradation of TRAF6.

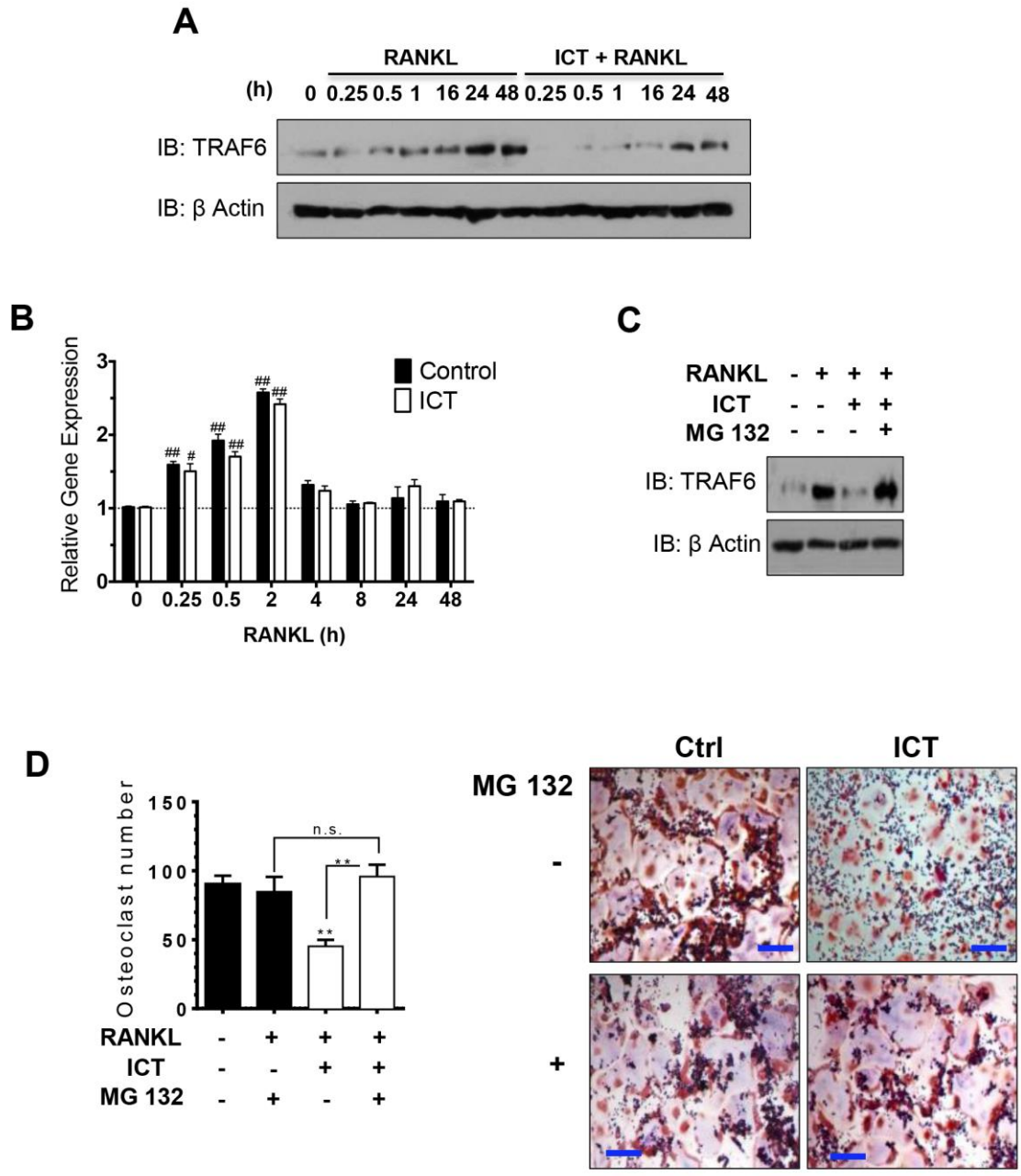

Figure 4.12 ICT mediates proteasomal degradation of TRAF6 (*A,B*) RAW 264.7 cells incubated with RANKL, with or without ICT, for indicated durations. (*A*) Cell lysates subjected to immunoblot analysis with the TRAF6 antibody. (*B*) TRAF6 gene expression: Total RNA was extracted from cells and reverse transcribed to cDNA. Relative gene expression was analysed using RT-PCR and normalised to 18s rRNA. Data expressed as mean ± SEM. # P< 0.05, ## P< 0.01 vs 0 h control. (*C,D*) RAW 264.7 cells incubated with the proteasomal inhibitor MG132 (1 μM) in the presence or absence of RANKL and ICT: (*C*) Cell lysates were harvested after 48 h treatment and subjected to immunoblot analysis performed with TRAF6 antibody, and (*D*) number of TRAP positive (purple cytoplasm) multinucleated osteoclasts in each well was counted after 6 days' treamtent, with corresponding representative images, scale bar = 100 μm. Data in graph represented as mean ± SEM of 3 independent experiments, ** P<0.01 vs RANKL-treated control.

4.2.9 Icaritin and TRAF6 ubiquitination

The degradation of intracellular proteins by the proteasome is a specific and regulated process. This specificity is ensured by attaching a small protein tag (ubiquitin) to mark the proteins for destruction by the 26S proteasome (Glickman & Ciechanover, 2002; Lim & Lim, 2011). Having shown that ICT mediates proteasomal degradation of TRAF6 in the presence of RANKL, we then examined the effect of ICT on ubiquitination of TRAF6. TRAF6 was pulled down by immunoprecipitation and subjected to immunoblot analyses which showed that in the absence of RANKL, ICT did not lead to significant changes in ubiquitination of TRAF6 (Fig 4.13*A*, lanes 1 and 3). However, in the presence of RANKL, ICT treatment led to a significant increase in TRAF6 ubiquitination (Fig 4.13*A*, lanes 2 and 4). Lysine 48-linked polyubiquitin chains is a well-regarded tag to direct proteins for proteasomal degradation (Mallette & Richard, 2012; Thrower, Hoffman, Rechsteiner, & Pickart, 2000), we therefore examined lysine 48-linked polyubiquitination of TRAF6. In the absence of RANKL, ICT did not lead to significant changes in lysine 48-polyubiquitination of TRAF6. However, in the presence of RANKL, ICT treatment led to a significant increase in TRAF6 lysine 48- polyubiquitination. These results suggest that indeed, ICT mediates proteasomal degradation of TRAF6 via the ubiquitin-proteasome pathway. Overall, our cellular data suggest that ICT suppressed osteoclastogenesis by regulating proteasomal degradation of the critical adaptor protein TRAF6; thereby inhibiting RANKL/RANK-mediated NFκB, MAPK and ROS signaling pathways.

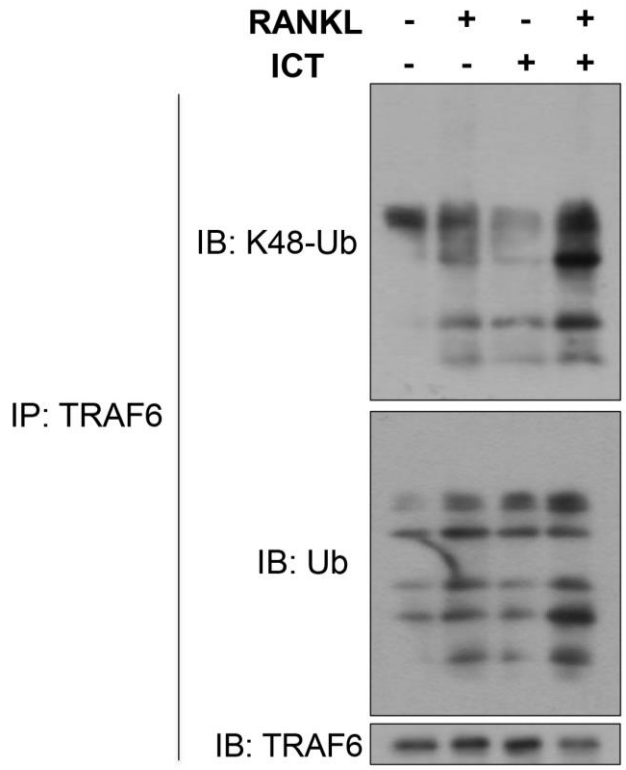

Figure 4.13 Effects of ICT on ubiquitnation of TRAF6. RAW 264.7 cells in the presence or absence of RANKL and ICT for 24 h and immunoprecipitation was carried out with TRAF6 antibody. Immunoprecipitates were subjected to immunoblot analysis with the indicated antibodies.

4.3 Effects of icaritin in the OVX rat model

As outlined in the introduction, the ovariectomized (OVX) rat is an excellent preclinical animal model as it emulates important clinical features of estrogen deficiency-induced osteoporosis in the human skeleton, resulting in rapid loss in cancellous bone mass and strength (Kimmel, 1996; Thompson et al., 1995). Given the promising properties of ICT demonstrated in the cellular models, we employed the OVX rat model to investigate the potential therapeutic effects of ICT on treating estrogen deficiency-mediated osteoporosis and to corroborate our *in vitro* findings in an animal model.

It has been reported that intraperitoneal administration of ICT to adult female Sprague Dawley rats at doses of 20, 40 and 60 mg/kg led to a dose-dependent increase in concentrations of ICT detected in blood plasma (Zhang, 2014). It was demonstrated that at a dose of 40 mg/kg, a maximum concentration of ~ 1.5 μM ICT was detected in the blood plasma and ≥ 700 nM ICT was detected in the plasma for up to 8 h post administration. Similarly, our group previously reported that intraperitoneal administration of 40 mg/kg ICT to SCID mice induced a rapid rise in serum concentrations of ICT, which reached a maximum of ~ 5 μM (Sun et al., 2015). Additionally, we showed that serum concentrations of ICT remained well within levels of ICT shown to inhibit osteoclastogenesis (Fig. 4.1) for up to 9 h post-adminstration As such, intraperitoneal administration of ICT at 40 mg/kg/day was chosen for our subsequent *in vivo* experiments.

4.3.1 To establish and validate the OVX-rat model

To ascertain completeness of bilateral ovariectomy, the oestrus cycles of rats were monitored for 3 weeks, beginning 1 week post-ovariectomy. Sham-operated rats had a normal oestrus cycle of 4-5 days, while OVX rats were acyclic and remained in the diestrus phase (Fig 4.14*A*). Additionally, serum estradiol levels of the OVX rats were significantly lower than that of sham-operated counterparts ($P < 0.05$), indicating that OVX rats were in a state of estrogen-deficiency. Put together, these results suggest that bilateral ovariectomy of rats was complete.

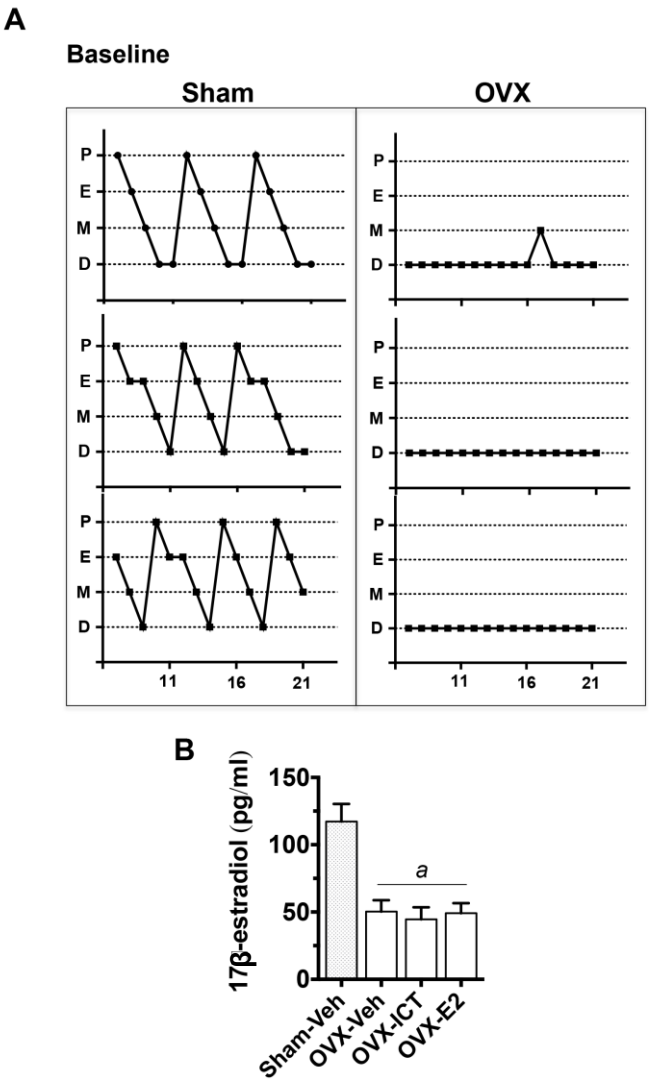

Figure 4.14 Establishing the OVX rat model based on (*A*) Oestrous cycles of rats 3 weeks after sham surgery or bilateral ovariectomy. Three representative rats from each group are presented. P, proestrus; E, oestrus; M, metoestrus; D, dioestrus. (*B*) Serum estradiol (E2) levels measured by ELISA. Data represented as mean ± SEM, n=8. *a* $p < 0.01$ vs baseline Sham-Veh.

4.3.2 Icaritin treatment prevented OVX-induced deterioration in bone architecture

To examine the effects of ICT treatment on bone architecture, the femora (Fig. 4.15) and 5th lumbar vertebrae (Fig. 4.16) of rats were subjected to MicroCT imaging and subsequent histomorphometric analysis. Analysis of baseline controls (Sham-pre and OVX-pre) show that ovariectomy resulted in marked decrease in trabecular bone volume (BV/TV, P< 0.01) and trabecular number (Tb.N, P< 0.001). Accordingly, there was a marked increase in trabecular spacing (Tb.Sp, P< 0.01) of the OVX-pre rats compared with Sham-pre, indicating an increase in trabecular porosity. A drastic decrease in bone mineral density (BMD) of OVX-pre rats compared to Sham-pre was detected at the (Fig 4.15*E*) and L5 vertebral body (Fig. 4.16*E*). The deterioration in bone microarchitecture as well as the decrease in BMD validates our OVX-induced osteoporosis model.

Analysis of the trabecular parameters shows a further deterioration in trabecular architecture of the vehicle-treated OVX rats (OVX-Veh) compared to OVX-pre rats. Treatment with ICT (OVX-ICT) prevented OVX-induced deterioration in bone architecture such that BV/TV, Tb.N and Tb.Sp were non-significantly different from that of OVX-pre. These effects of ICT were consistently demonstrated in both the femora and L5 vertebrae. There was a drastic decrease in BMD measured at the femoral neck (Fig 4.15*E*) and L5 vertebral body (Fig. 4.16*E*) of the vehicle-treated OVX rats compared with Sham-Veh rats. Notably, treatment with ICT prevented this decrease in BMD to levels that were non-significantly different from OVX-pre controls. Similar

bone-protective effects were observed in OVX rats treated with the positive control, estradiol (OVX-E2). Histological analysis of the distal femur also revealed similar findings in trabecular bone architecture, where ovariectomy resulted in decreased trabecular number and density, with increased trabecular spacing compared to sham-operated controls (Fig. 4.15*F,* Sham-Veh vs OVX-Veh). Treatment with ICT and the positive control, E2, prevented this deterioration in trabecular architecture. Additionally, H&E-stained histological sections of the distal femur showed that there was a significant increase in marrow adiposity of OVX-Veh rats compared with Sham-Veh, which was reduced by ICT treatment.

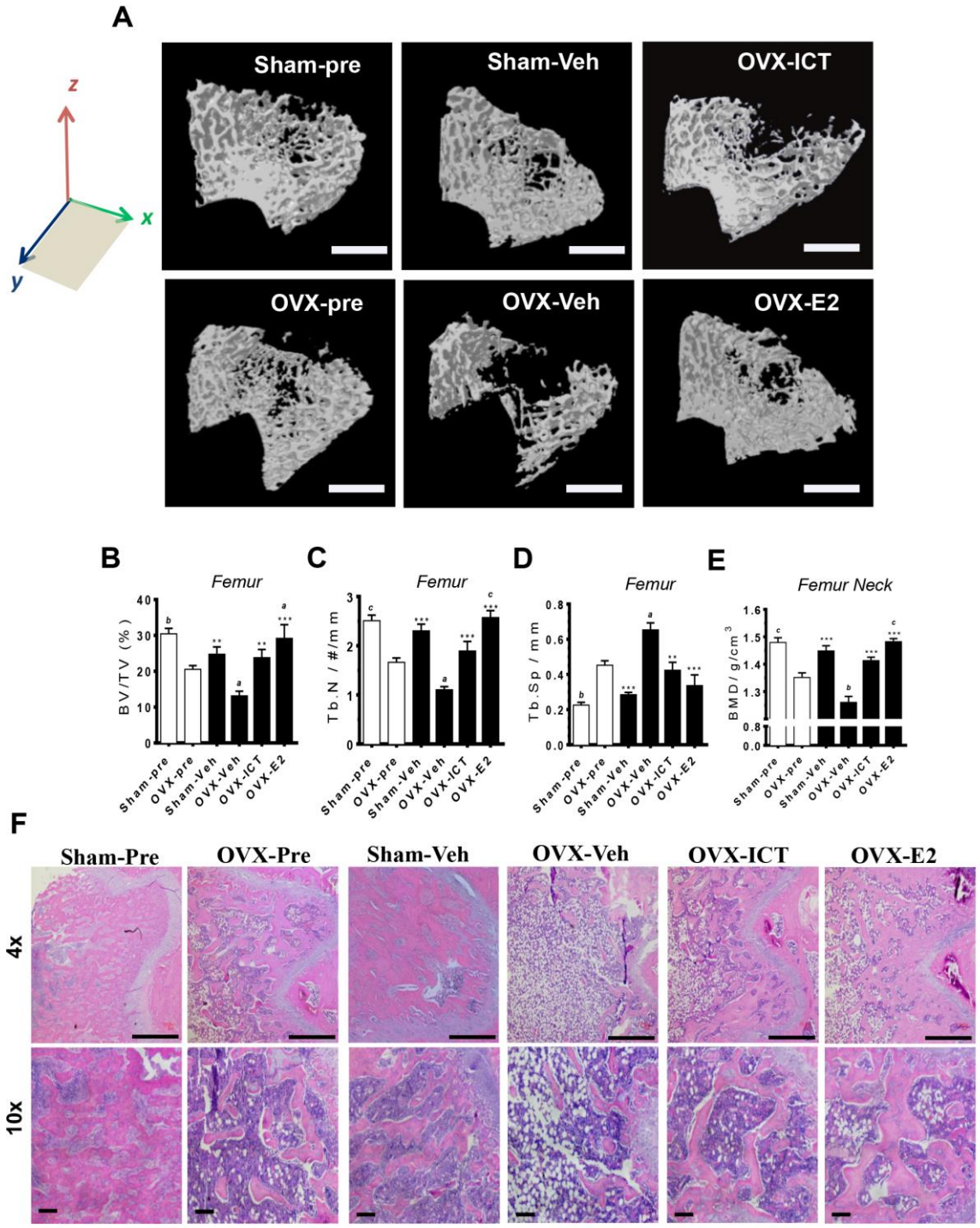

Figure 4.15 Effects of ICT on trabeculae of the distal femur (*A*) Representative microCT reconstructions of trabecular bone in distal femur, scale bar = 1mm. (*B*) Bone volume/ total volume (BV/TV), (*C*) trabecular number (Tb.N) and (*D*) trabecular space (Tb.Sp), and (*E*) Bone mineral density (BMD) of femur were analyzed with the CTan software. Data in graphs represented as mean ± SEM (n=8). *a* P< 0.05, *b* P< 0.01, *c* P< 0.001 vs OVX-pre; * P< 0.05, ** P< 0.01, *** P 0.001 vs OVX-Veh. (*F*) Representative H&E-stained histologic sections of distal femora, scale bar = 100 μm.

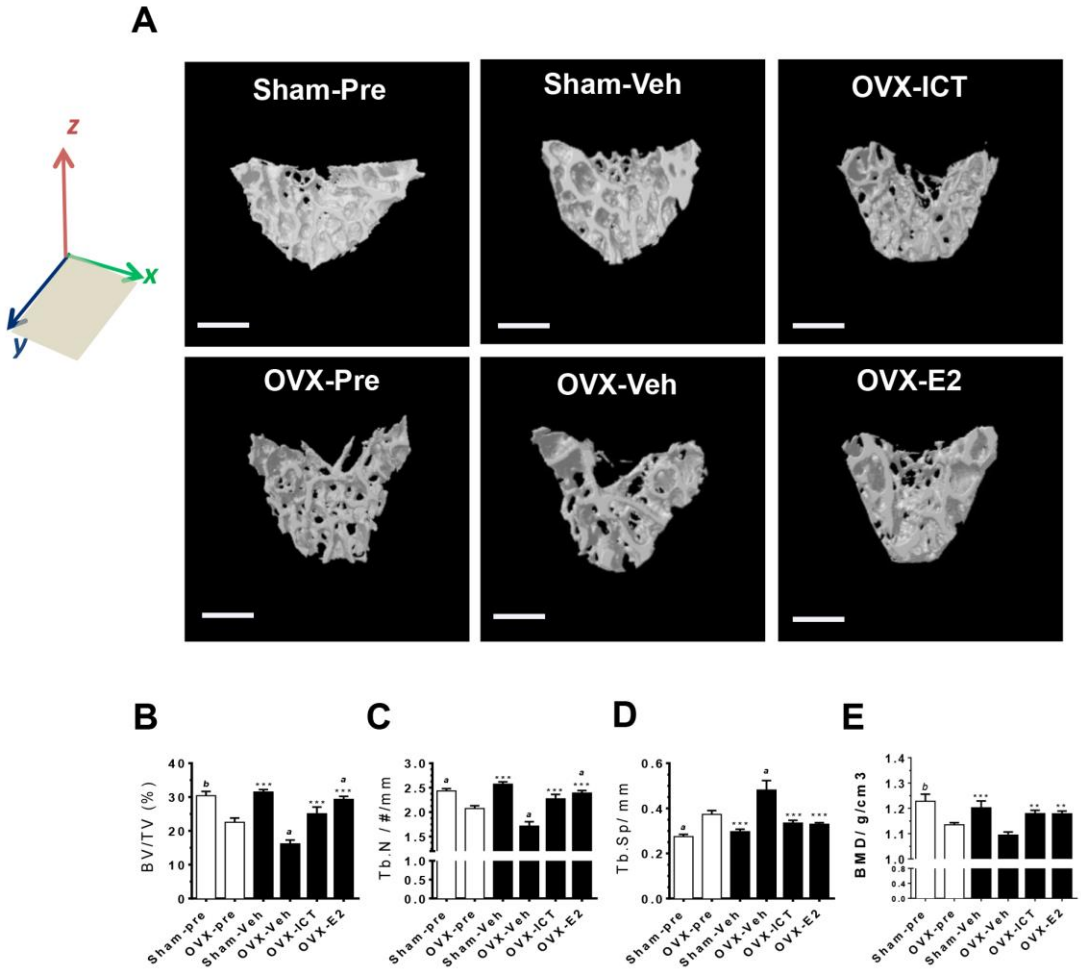

Figure 4.16 Effects of ICT on trabeculae of the 5th lumbar vertebrae (*A*) Representative microCT reconstructions of trabecular bone in L5, scale bar = 1 mm. (*B*) Bone volume/ total volume (BV/TV), (*C*) trabecular number (Tb.N) and (*D*) trabecular space (Tb.Sp), and (*E*) Bone mineral density (BMD) of L5 were analyzed with the CTan software. Data in graphs represented as mean ± SEM (n=8). *a* P< 0.05, *b* P< 0.01, *c* P< 0.001 vs OVX-pre; * P< 0.05, ** P< 0.01, *** P < 0.001 vs OVX-Veh.

4.3.3 Icaritin treatment prevented OVX-induced decline in bone strength

Osteoporosis is characterized by a decline in bone strength that results from the deterioration in bone architecture and decreased bone mineral density (Ammann & Rizzoli, 2003). To assess the effects of ICT on OVX-induced changes in bone strength, the mechanical properties of the femur neck (Fig 4.17*A*), femur shaft (Fig 4.17*B*) and L5 vertebral body (Fig 4.17*C*) were evaluated by loading these bones to failure using a materials testing machine. Mechanical properties evaluated include ultimate strength, the maximum force per unit area the bones can withstand before fracturing; stiffness, which reflects the rigidity of the bones as it measures the extent to which the bones resist deformation in response to an applied force; and energy to failure, a measure of the amount of energy the bone absorbs before fracturing. Analyses of baseline controls revealed that ovariectomy led to deterioration in mechanical properties of the femur neck, femur shaft and L5 vertebrae (Fig 4.17*A-C*, Sham-pre vs OVX-pre). Further deterioration in these mechanical properties was detected in the vehicle-treated OVX rats (Fig 4.17*A-C*, OVX-pre vs OVX-Veh), and this deterioration was prevented by ICT treatment, such that ultimate strength, stiffness and energy to failure of these bones were non-significantly different from that in OVX-pre rats. Estradiol treatment also prevented deterioration in mechanical properties of the femur neck, femur shaft and L5. In this study, energy to failure of bones was used as an indicator of the fracture toughness or resistance of the bone to fracture in terms of work done. It is noteworthy that the trends observed in the energy to failure of

these bones are consistent with the quality of bones (bone architecture and density) measured by microCT analyses (Fig. 4.15, 4.16).

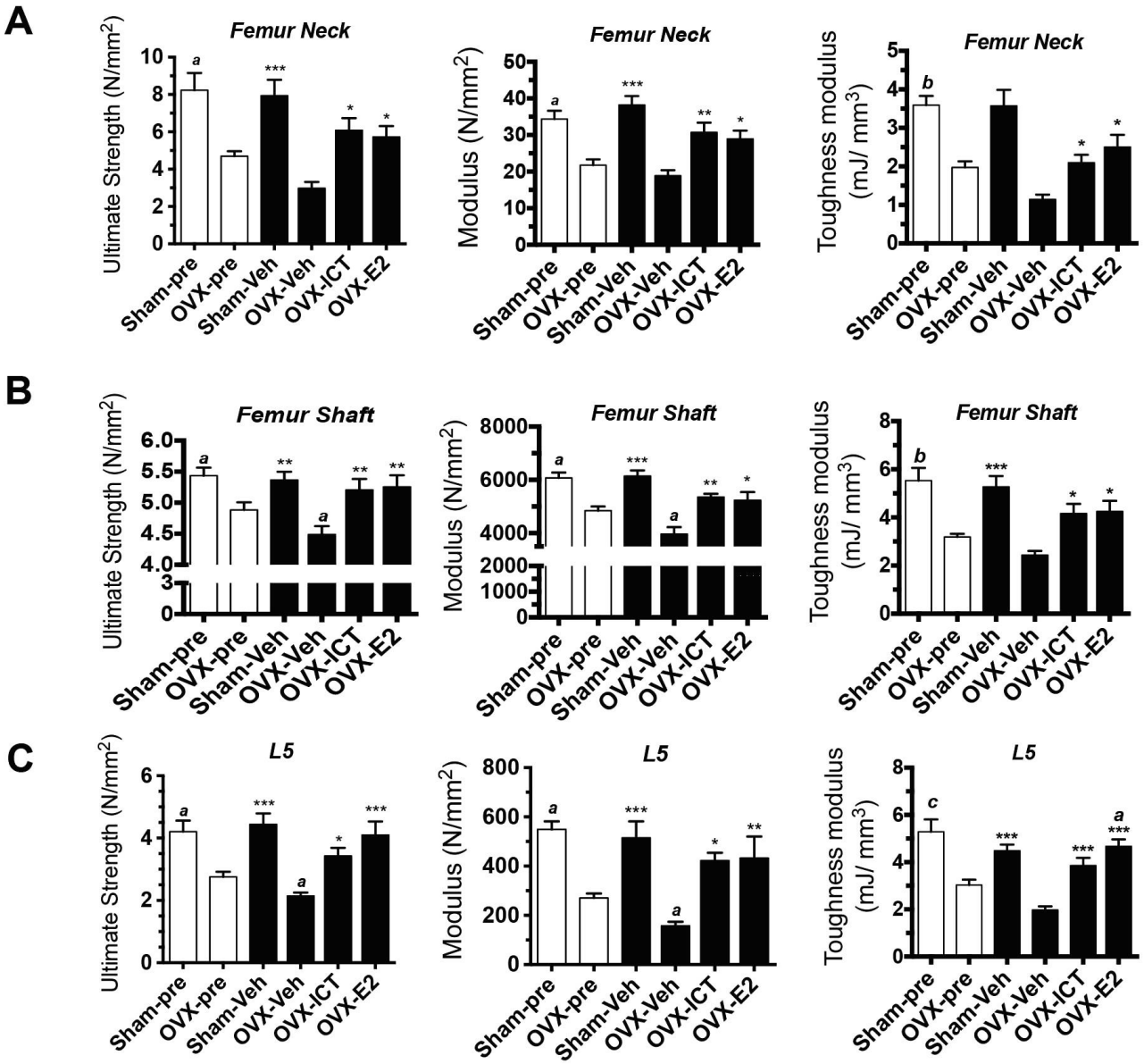

Figure 4.17 Effects of ICT on mechanical properties of bone. Ultimate strength, modulus and energy to failure of (*A*) femur neck, (*B*) femur shaft and (*C*) L5 vertebrae were evaluated using a materials testing machine. Data in graphs represented as mean ± SEM (n=8). *a* P< 0.05 vs OVX-pre; * P< 0.05, ** P< 0.01, *** P < 0.001 vs OVX-Veh.

4.3.4 Icaritin treatment suppressed osteoclast formation and resorption *in vivo*

It is well established that increased osteoclast formation and activity is pivotal to the pathogenesis of estrogen deficiency-mediated osteoporosis (Khosla et al., 2012). To investigate the effect of ICT on osteoclastogenesis *in vivo*, histologic sections of the distal femur were stained for the osteoclast marker, TRAP. The distal femur is a region rich in trabecular bone, the site of active bone remodeling. Analysis of baseline controls showed that there was a significant increase in the area covered by osteoclasts (identified by purple TRAP stain) in OVX-pre rats compared with Sham-pre. Indeed, there was a further increase in area covered by osteoclasts in vehicle-treated OVX rats compared with OVX-pre (Fig 4.15*A*). Correspondingly, surface measurements from the TRAP-stained sections revealed that ICT treatment decreased osteoclast-covered surface (Oc.S/BS) by 58.4%, reduced eroded surface (ES/BS) by 62.7% and reduced osteoclast numbers (N.OC/B.PM) by 44.9% compared to OVX-Veh (Fig. 4.15*B*). This reduction in osteoclast-covered surface, eroded surface and osteoclast numbers to levels similar to that of OVX-pre suggests that ICT abrogated OVX-induced osteoclast formation and activity.

C-terminal telopeptide 1 (CTX-I) is a degraded fragment of collagen type-1 that is generated during bone resorption (Henriksen et al., 2007). Thus, we assessed osteoclast activity by measuring serum levels of this bone resorption marker, CTX-I. Ovariectomy resulted in a ~2 fold increase in serum levels of CTX-I compared with sham-operated controls (Fig. 4.17C, Sham-Veh vs OVX-

Veh). There was a 36% decrease in serum levels of CTX-I in ICT-treated rats compared with OVX-Veh ($P< 0.01$), further supporting ICT inhibition of OVX-induced osteoclast activity *in vivo* (Fig. 4.15*C*).

Osteocalcin is a noncollagenous protein produced specifically by osteoblastic cells for deposition in the bone matrix (Patti, Gennari, Merlotti, Dotta, & Nuti, 2013) and is therefore used as a biochemical marker of bone formation. Ovariectomy resulted in a significant decrease in serum levels of osteocalcin at baseline (Fig 4.17*D,* Sham-pre vs OVX-pre). Interestingly, a small but non-significant increase in serum levels of osteocalcin was detected in OVX-Veh rats compared with OVX-pre, which could be attributed to an increase in bone remodeling. Compared with OVX-pre, treatment with ICT led to a ~70% increase ($P< 0.01$) in serum levels of osteocalcin.

Estradiol, as the positive control, exhibited a similar inhibitory effect on osteoclast formation and activity *in vivo*, and decreased Oc.S/BS by 47%, reduced ES/BS by 64.8% and reduced osteoclast numbers (N.OC/B.PM) by 44.2% compared to OVX-Veh (Fig. 4.15*B*). There was a 57.7% decrease in serum levels of CTX-I in OVX-E2 rats compared to OVX-Veh rats. It is noteworthy that although ICT and E2 led to similar inhibitory effects on osteoclastogenesis and activity in the OVX rats, the effects of ICT are not mediated via ER-signaling as described in section 4.2.1.

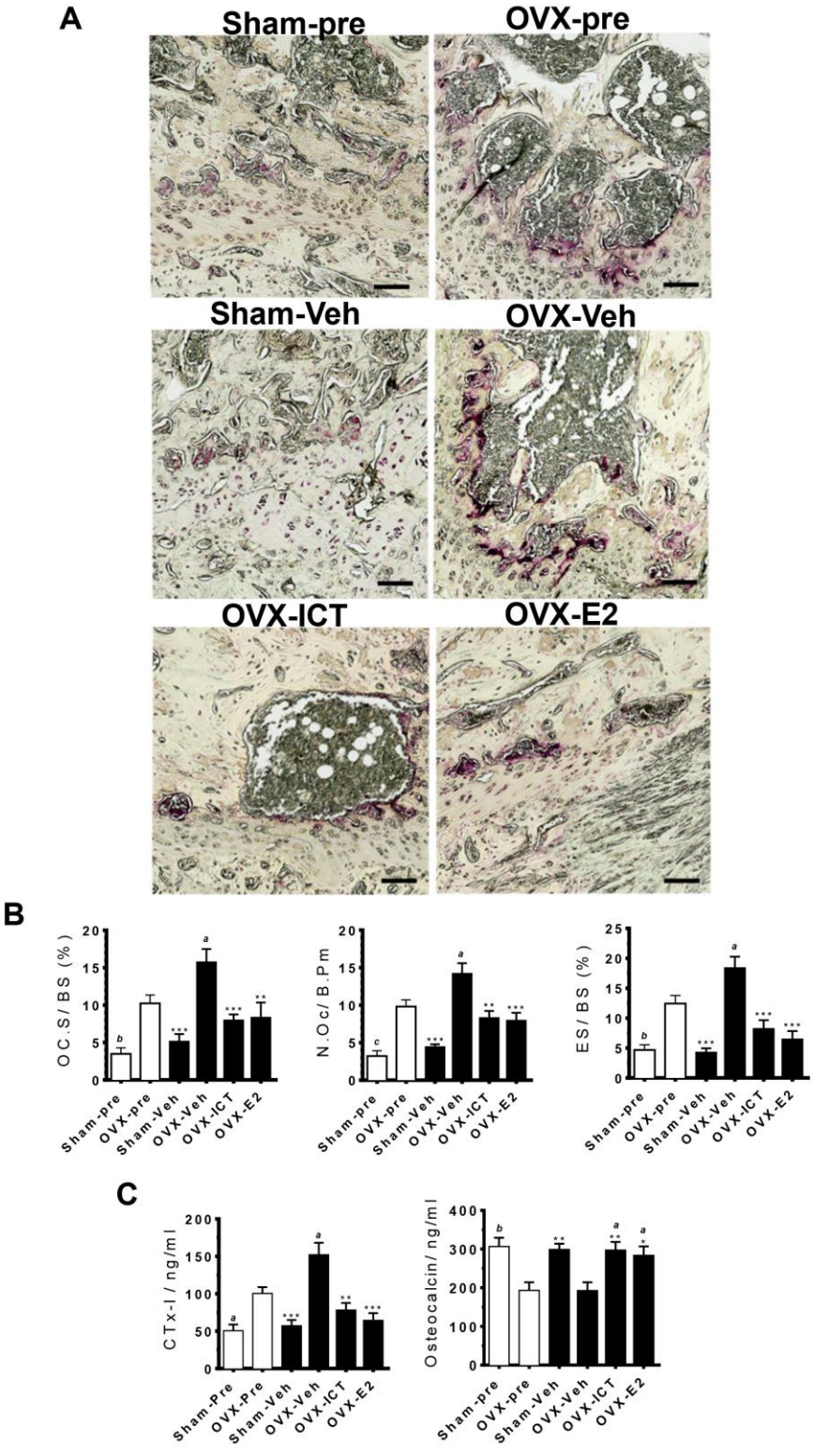

Figure 4.17 Effects of ICT on osteoclast formation and activity *in vivo* (*A*) Representative TRAP-stained histologic sections of distal femora showing effects on osteoclast (purple-stained area) numbers, scale bar = 200 μm. (*B*) Fold change in osteoclast surface/ bone surface (Oc.S/ BS), number of osteoclasts/ bone perimeter (N.Oc/ B.Pm), and eroded surface/ bone surface (ES/BS) based on analysis of TRAP-stained histologic sections. (*C*) Serum concentrations of CTx-I and osteocalcin quantified by ELISA. Data in graphs represented as mean ± SEM (n=8). *a* P< 0.05, *b* P< 0.01, *c* P< 0.001 vs OVX-pre* P < 0.05, ** P < 0.01, *** P < 0.001 vs OVX-Veh.

4.3.5 Icaritin treatment suppressed TRAF6 protein expression

Since we have demonstrated in our cellular studies that ICT suppressed osteoclastogenesis by regulating proteasomal degradation of the critical adaptor protein TRAF6 (section 4.2.8), we sought to study TRAF6 protein expression in the OVX rat model by examining TRAF6 protein expression in the circulating osteoclast precursors.

Identifying osteoclast precursor population in peripheral blood mononuclear cells & bone marrow

To ascertain the osteoclastogeneic potential of cell populations present in the peripheral blood and bone marrow, PBMC and bone marrow cells were separately harvested from 3 rats, pooled, and stained for the cell surface markers CD11b and granulocyte receptor-1 (Gr-1). Using fluorescence-assisted cell sorting, cell populations were collected separately then cultured in the presence of RANKL and M-CSF. We demonstrated that in both the blood and bone marrow, $Cd11b^{+}/Gr\text{-}1^{-/low}$ cells differentiated into multinucleated TRAP-positive cells (Fig 4.16, R2). The $Cd11b^{+}/Gr\text{-}1^{hi}$ cells (Fig. 4.16, R3) isolated from the bone marrow but not the blood were able to differentiate into multinucleated cells, while $Cd11b^{-}/Gr\text{-}1^{-/low}$ cells (Fig. 4.16, R4) from both the blood and bone marrow showed no osteoclastogenic potential. These findings are consistent with previous reports demonstrating that Cd11b and Gr-1 are cell surface markers expressed on circulating osteoclast precursors (Z. Yao et al., 2006). We therefore identified $Cd11b^{+}/Gr\text{-}1^{-/low}$ cells as osteoclast precursors in our subsequent experiments and analyses.

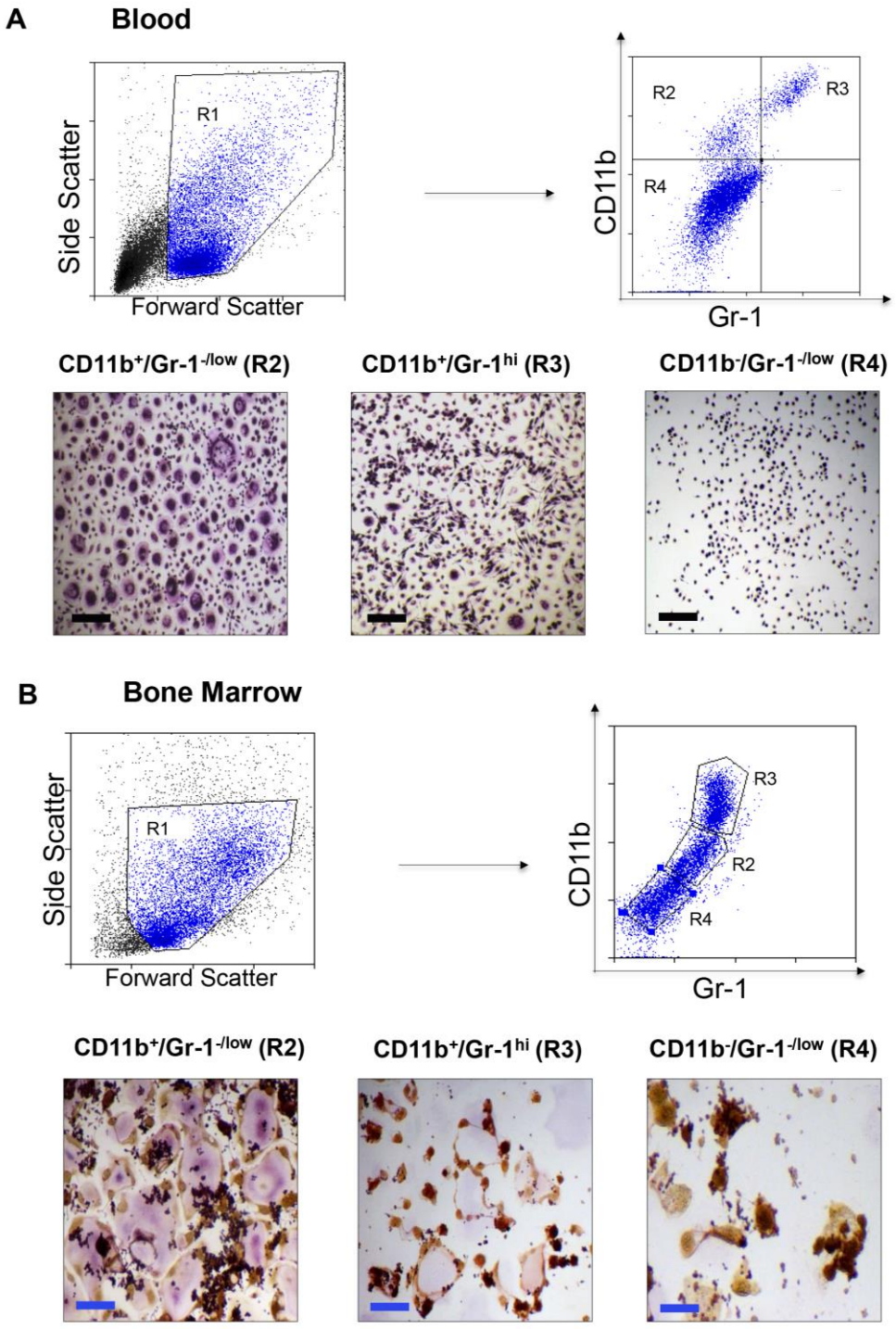

Figure 4.18 Identification of cell populations with osteoclastogenic potential from peripheral blood and bone marrow cells. (*A*) PBMC or (*B*) bone marrow cells pooled from 3 rats were stained with anti-CD11b and anti-Gr-1 antibodies and subjected to FACS analysis. Live cells were gated using forward and side scatter *(R1)*. $CD11b^{+}/Gr\text{-}1^{-/low}$ (*R2*), $CD11b^{+}/Gr\text{-}1^{hi}$ (*R3*), and $CD11b^{-}/Gr\text{-}1^{-}$ (*R4*) populations were collected separately and cultured with M-CSF and RANKL to generate osteoclasts. Representative light microscope images of TRAP-positive osteoclasts formed from the respective populations of the PBMC and bone marrow in *upper* and *lower* panels, respectively. Scale bar = 100 μm.

Icaritin treatment suppressed TRAF6 protein expression in circulating osteoclast precursors

To study the effect of ICT treatment on osteoclast precursors, blood and bone marrow cells from rats were stained for Cd11b and Gr-1 surface markers and analyzed by flow-cytometry, where $Cd11b^{+}/Gr\text{-}1^{-/low}$ cells were gated and expression of TRAF6 quantified. Interestingly, analysis of circulating osteoclast precursors showed that ovariectomy led to 90% increase in TRAF6 expression in $Cd11b^{+}/Gr\text{-}1^{-/low}$ PBMCs ($P< 0.001$) and 50% in TRAF6 expression in $Cd11b^{+}/Gr\text{-}1^{-/low}$ bone marrow cells ($P< 0.01$) (Fig 4.19*A,B*). Compared with OVX-Veh rats, treatment with ICT (Fig. 4.19*A,B*, open bars) led to a 25.8% and 16.6% reduction in TRAF6 protein levels in the osteoclast precursors present in PBMC ($P< 0.001$) and bone marrow cells ($P< 0.05$), respectively. Estradiol treatment also led to a 20.5% and 18.8% suppression in TRAF6 expression in the osteoclast precursors present in PBMC ($P< 0.01$) and bone marrow cells ($P< 0.05$), respectively. These results showed that ICT treatment suppressed OVX-induced TRAF6 protein expression in the circulating osteoclast precursors.

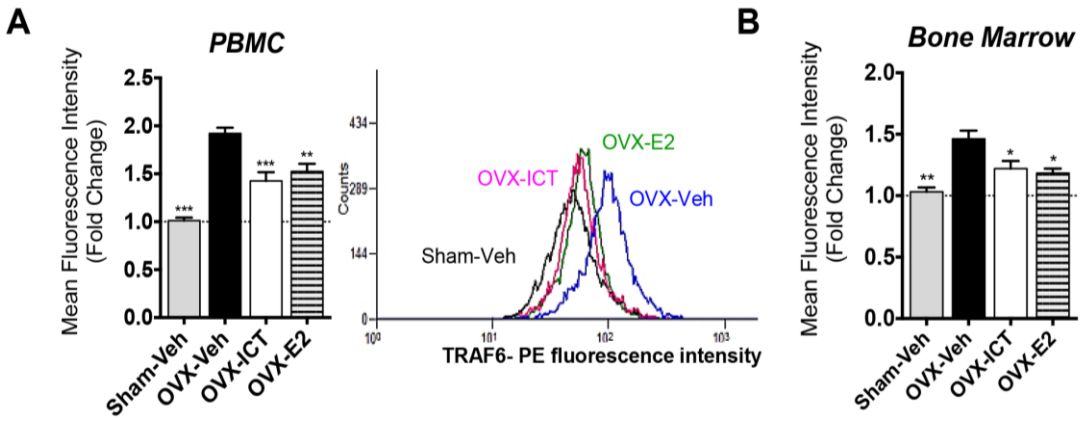

Figure 4.19 Effect of ICT on TRAF6 protein expression in osteoclast precursors. Rat (*A*) PBMC and (*B*) bone marrow cells were labeled with Cd11b and Gr-1 antibodies and osteoclast precursors ($CD11b^{+}/Gr\text{-}1^{-/low}$) were gated and analyzed by flow cytometry. Mean fluorescence intensity of TRAF6 in 10, 000 $CD11b^{+}/Gr\text{-}1^{-/low}$ cells in (*A*) PBMC and (*B*) bone marrow were analyzed. Results expressed as fold change with respect to sham-operated controls (Sham-Veh). Data expressed as mean ± SEM of 8 rats per group. (*A*) Histogram shows representative distribution of PE-labeled TRAF6 protein in 10,000 osteoclast precursors (from PBMC) of an animal in each treatment arm. * P< 0.05, ** P< 0.01, *** P < 0.001 vs OVX-Veh.

Icaritin treatment suppressed TRAF6 protein expression in bone

To assess the effect of ICT on TRAF6 protein expression in the bone, tibial bone lysates were subjected to immunoblot analysis (Fig. 4.18*A,B*). Ovariectomy led to a drastic increase in TRAF6 protein expression (~ 9.5 folds, P< 0.01) in the bone compared with sham-operated controls. Compared to OVX-Veh controls, ICT treatment reduced TRAF6 protein expression by 80% (P< 0.01). Estradiol reduced TRAF6 protein levels in the bone by 76.1% compared with OVX-Veh rats (P< 0.05). These results corroborate our findings that ICT treatment reduced TRAF6 protein expression in OVX rats.

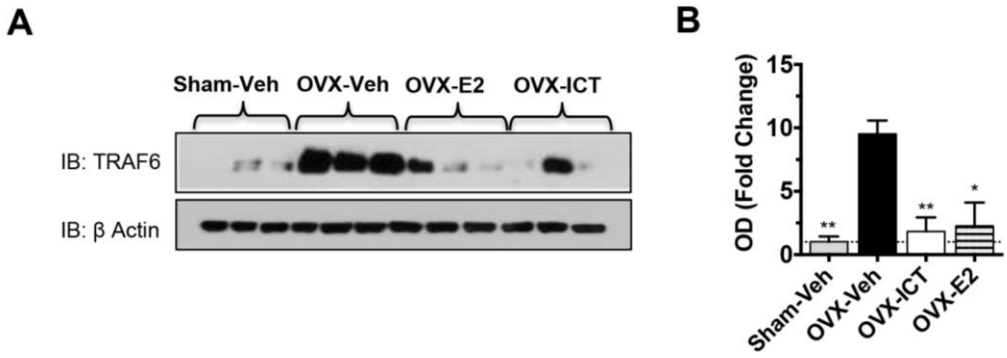

Figure 4.20 Effect of ICT on TRAF6 protein levels in the bone. (*A*) Immunoblot analysis of TRAF6 protein expression in tibial bone tissue from 3 representative rats per group and (*B*) corresponding densitometry analysis. Data are expressed as mean ± SEM, * P < 0.05, ** P < 0.01, *** P < 0.001 vs OVX-Veh.

4.3.6 Icaritin treatment suppressed NFATc1 protein expression

Given our *in vitro* findings that ICT treatment suppressed osteoclast formation and resorption, and downregulated the expression and activity of NFATc1, the master transcription factor regulating osteoclastogenesis, we sought to determine whether ICT resulted in similar effects on NFATc1 in the OVX rats.

Icaritin treatment suppressed NFATc1 protein expression in circulating osteoclast precursors

To study the effect of ICT treatment on osteoclast precursors, blood and bone marrow cells from rats were stained for Cd11b and Gr-1 surface markers and analyzed by flow-cytometry, where $Cd11b^{+}/Gr\text{-}1^{-/low}$ cells were gated and expression of NFATc1 quantified. Analysis of circulating osteoclast precursors showed that ovariectomy led to 37.7% increase in TRAF6 expression in $Cd11b^{+}/Gr\text{-}1^{-/low}$ PBMCs ($P< 0.05$) and 22% in TRAF6 expression in $Cd11b^{+}/Gr\text{-}1^{-/low}$ bone marrow cells ($P< 0.05$) (Fig 4.21*A,B*). Compared with OVX-Veh rats, treatment with ICT (Fig. 4.21*A,B*, open bars) led to a 34.2% and 23.5% reduction in TRAF6 protein levels in the osteoclast precursors present in PBMC ($P< 0.05$) and bone marrow cells ($P< 0.01$), respectively. Estradiol treatment also led to a 25.2% and 15% suppression in TRAF6 expression in the osteoclast precursors present in PBMC ($P< 0.05$) and bone marrow cells ($P< 0.05$), respectively. These results showed that ICT treatment suppressed OVX-induced NFATc1 protein expression in the circulating osteoclast precursors.

Icaritin treatment suppressed NFATc1 protein expression in bone

To assess the effect of ICT on NFATc1 protein expression in the bone, tibial bone lysates were subjected to immunoblot analysis (Fig. 4.21*C,D*). Ovariectomy led to a significant increase (~14 folds, P< 0.05) in NFATc1 protein expression in the bone compared with sham-operated controls. Both ICT (P< 0.01) and estradiol (P< 0.05) treatments reduced NFATc1 protein expression to levels similar to that of sham-operated controls. These results show that ICT treatment suppressed NFATc1 protein expression *in vivo*.

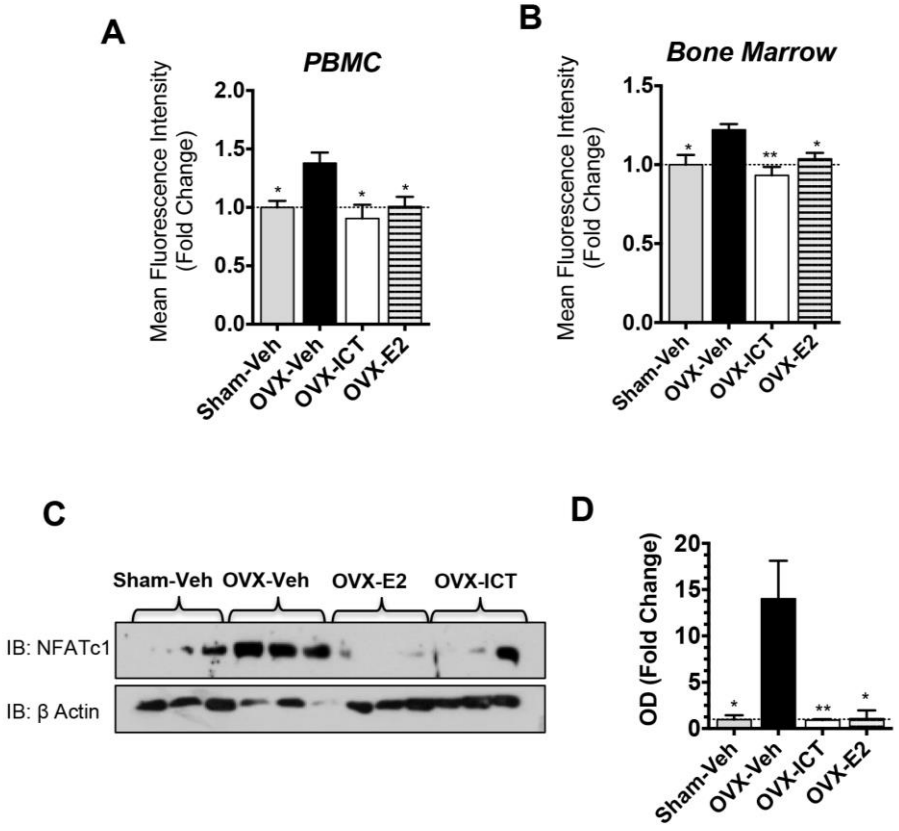

Figure 4.21 Effect of ICT on NFATc1 protein expression in OVX rats. Rat (*A*) PBMC and (*B*) bone marrow cells were labeled with Cd11b and Gr-1 antibodies and osteoclast precursors ($CD11b^{+}/Gr\text{-}1^{-/low}$) were gated and analyzed by flow cytometry. Mean fluorescence intensity of NFATc1 in 10, 000 $CD11b^{+}/Gr\text{-}1^{-/low}$ cells from (*A*) PBMC and (*B*) bone marrow were analyzed. Results expressed as fold change with respect to sham-operated controls (Sham-Veh). (*C*) Immunoblot analysis of NFATc1 protein expression in tibial bone tissue from 3 representative rats per group and (*D*) corresponding densitometry analysis. Data expressed as mean ± SEM, * P< 0.05, ** P< 0.01, *** P < 0.001 vs OVX-Veh.

4.3.7 Icaritin treatment did not lead to changes in RANKL levels

To investigate whether ICT treatment downregulated RANKL levels leading to its consequential suppression of osteoclast numbers and activity, we analyzed serum RANKL concentrations in our animal model in response to ICT. Consistent with previous reports (Ominsky et al., 2008), ovariectomy led to a 2 fold increase (P< 0.01) in serum levels of RANKL compared to sham-operated rats (Fig. 4.22, baseline: Sham-Veh vs OVX rats). After 8 weeks' treatment, ICT did not lead to significant changes in RANKL levels compared to vehicle-treated OVX controls (Fig 4.22, OVX-Veh vs OVX-ICT). In contrast, estradiol treatment led to a 10% decrease (P< 0.01) in serum levels of RANKL (Fig 4.22, OVX-Veh vs OVX-E2). These results show that ICT suppression of OVX-induced osteoclastogenesis and osteoclast resorption was independent of its effects on RANKL.

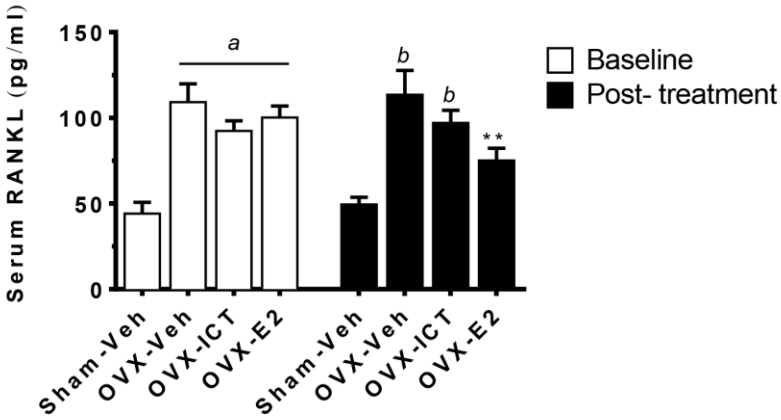

Figure 4.22 Serum estradiol levels of rats measured at baseline: 4 weeks after sham surgery or bilatery OVX, or post-treatment: after 8 weeks treatment. Serum RANKL levels measured by ELISA. Data represented as mean ± SEM, n=8 rats per group. *a* p< 0.01 vs baseline Sham-Veh; *b* p< 0.01 vs post-treatment Sham-Veh; ** p< 0.01 vs post-treatment OVX-Veh.

4.3.8 Icaritin treatment has favourable short-term safety profile in OVX rats

Icaritin treatment did not lead to significant changes in body weight of rats

The body weight of rats can be used as a clinical sign of morbidity if the decrease in body weight is > 20% from baseline or rapid weight loss (>10% body weight) occurs within a week (Foltz & Ullman-Cullere, 1999). Body weight of the rats was thus measured weekly as the animals received treatment. While ovariectomy led to a signficant increase in bodyweight of rats compared to sham-operated controls (Fig 4.23*A*, Week 4: Sham-Veh vs OVX rats). There was no significant change in the bodyweight of ICT-treated rats over the 8 weeks of treatment (Fig 4.23*A*, Weeks 4-12).

Icaritin treatment did not lead to uterine hypertrophy of rats

ICT has been shown to exhibit estrogenic activity *in vitro* leading to the proliferation of the MCF-7 breast cancer cells (Tiong et al., 2012), and it is well-established that estrogen leads to uterine hypertrophy substantially increasing the risks of endometrial cancer (Knowler, 1983; Million Women Study), we therefore examined the effects ICT of uterine weight in the OVX rat model (Fig. 4.23*B,C*). Indeed, ovariectomy led to a drastic decrease in uterine weight compared with sham-operated controls (Sham-Veh vs OVX-Veh). Compared to OVX-Veh rats, ICT treatment did not lead to significant changes in uterine weight while estradiol treatment resulted in ~ 4 folds increase in uterine weight of the OVX-rats (Fig 4.23*B*, OVX-Veh vs OVX-E2), which was significantly higher than that of sham controls ($P < 0.01$). ICT treatment also did not lead to significant changes in serum concentrations of estradiol

compared with vehicle-treated OVX rats (Fig 4.23*D*). Put together, these results support our *in vitro* findings that ICT did not inhibit osteoclastogenesis via the ER-signaling. Additionally, unlike estradiol, ICT did not lead to uterine hypertrophy suggesting that ICT treatment may not result in the same increase in risks of endometrial cancer.

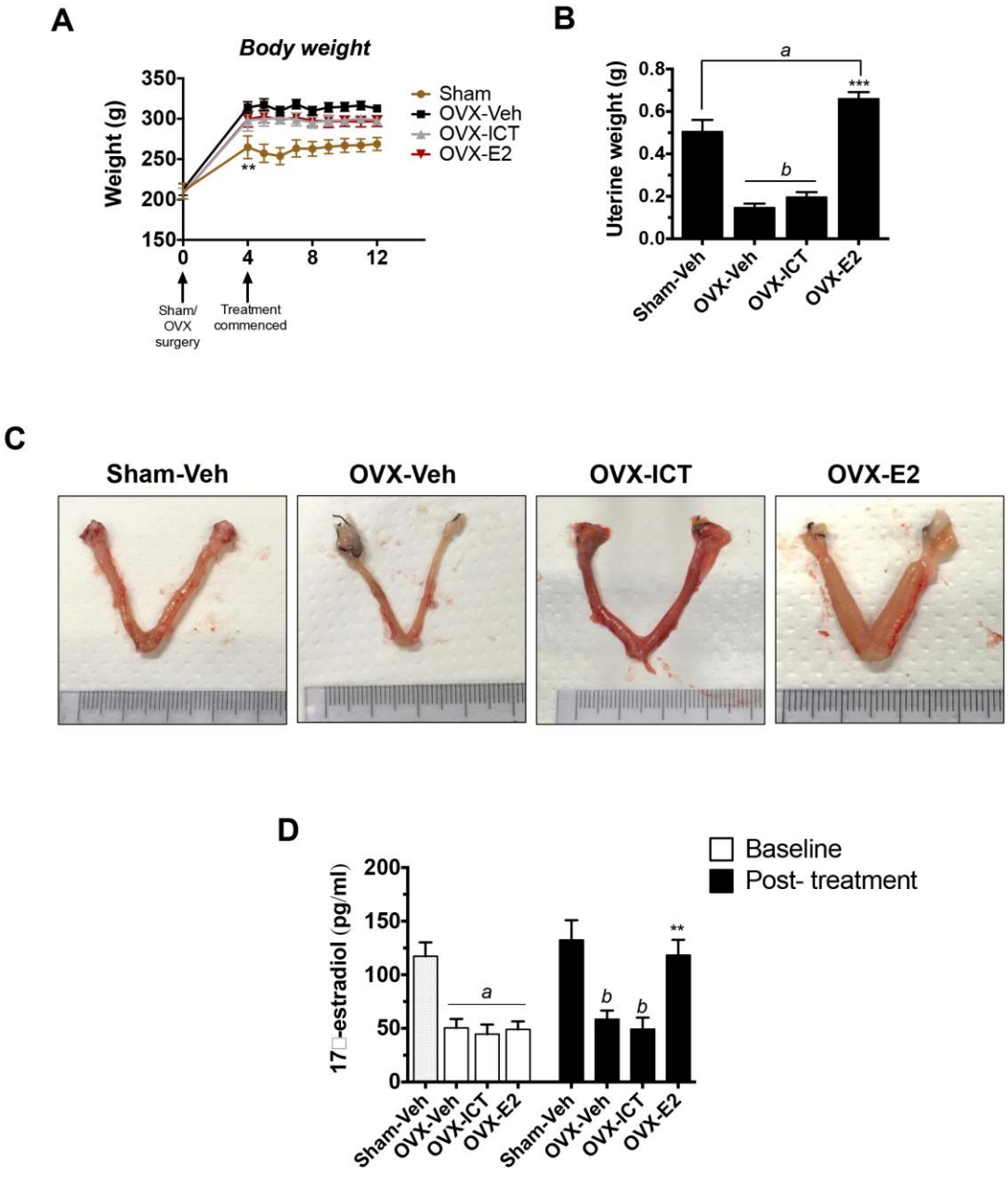

Figure 4.23 Effect of ICT on body weight and uterine weight of OVX rats. (*A*) Body weight of rats measured weekly. Data represented as mean ± SEM, n=8 rats per group, * P < 0.01 vs time-matched OVX-Veh. (*B,C*) Uteri of rats were harvested at termination, surrounding fat tissue removed and weighed. Data represented as mean ± SEM, n=8 rats per group. *a* P < 0.05, *b* P < 0.01 vs Sham-Veh; *** p< 0.001 vs OVX-Veh. (*D*) Serum estradiol levels measured by ELISA. Data represented as mean ± SEM, n=8. *a* P < 0.01 vs baseline Sham-Veh; *b* *P*< 0.001 vs post-treatment Sham-Veh; ** P < 0.01 vs post-treatment OVX-Veh.

CHAPTER 5. DISCUSSION

In this thesis, we present the novel finding that proteasome-mediated degradation of the adaptor protein TRAF6 mediates the anti-osteoporotic effects of icaritin. We show that icaritin suppresses osteoclastogenesis and osteoclast function both *in vitro and in vivo*, thereby preventing estrogen deficiency-mediated osteoporosis. The mechanism(s) by which icaritin inhibits osteoclast differentiation was investigated *in vitro* and in an OVX rat model. ICT reduced TRAF6 protein expression, thereby inhibiting RANKL/RANK activation of downstream NFκB, MAPK/AP-1 and ROS signaling pathways in the RAW 264.7 osteoclast precursor cell model. Ultimately, suppression of TRAF6-mediated pathways reduced the expression and activity of the key osteoclastogenic transcription factor NFATc1 (Fig 5.1). Similarly in estrogen-deficient rats, maintenance of bone mass, strength and suppression of bone resorption by ICT was associated with reduction in TRAF6 and NFATc1 protein expression in osteoclast precursor macrophages. Taken together, the findings of this thesis uncover the clinical potential of icaritin as an anti-osteoporotic agent, and points to TRAF6 adaptor protein as a promising target for the design of novel anti-osteoporotic drugs.

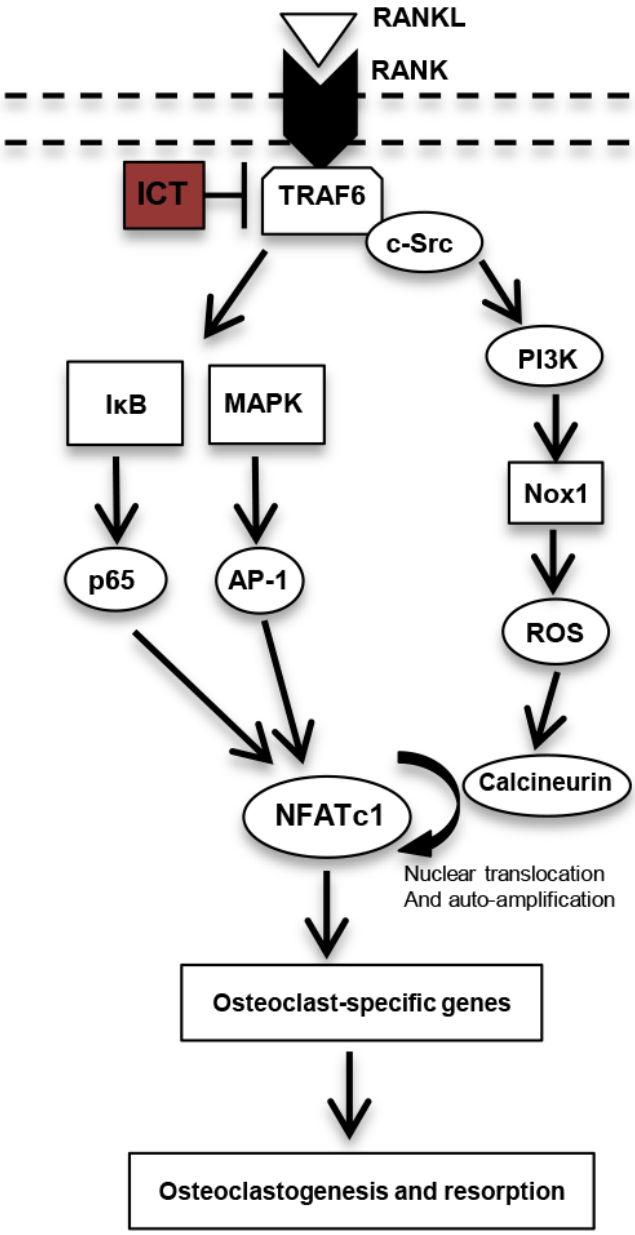

Figure 5.1 Schematic model: ICT induced TRAF6 degradation results in inhibition of NFATc1 expression and activity. Hypothesized mechanism by which ICT inhibits osteoclastogenesis. Activation of RANK by its ligand induces NFATc1 gene expression and activity through NFkB/p65 and MAPK/AP-1 signaling pathways and calcineurin activation, thereby upregulating osteoclast-specific genes. ICT mediates proteasomal degradation of TRAF6, thus blocking RANKL-induced activation of the downstream signaling pathways, suppressing expression of osteoclast-specific genes and inhibit osteoclast differentiation.

5.1 Effects of icaritin on osteoclastogenesis

5.1.1 Icaritin inhibits osteoclast differentiation

As previously outlined, osteoclastogenesis can be broadly divided into three stages: the commitment of monocyte/ macrophages into osteoclast precursors and their proliferation, fusion of the osteoclast precursors to form mature multinucleated osteoclasts, followed by activation of these osteoclasts to resorb bone (Soysa et al., 2012; Takayanagi, 2007). Given that ICT suppressed osteoclast formation and inhibited the expression of osteoclast-specific genes, we sought to determine if this was due to ICT effects on the osteoclast precursors. The viability of monocytes and osteoclast precursors (in the presence of RANKL) was not inhibited at doses of ICT that suppressed osteoclastogenesis, indicating that the reduction in osteoclast numbers was not due to non-specific cytotoxicity. Additionally, ICT did not affect sealing zone formation or resorptive capacity of mature osteoclasts, suggesting that ICT could act to inhibit the commitment and differentiation of osteoclast precursors into mature multinucleated osteoclasts. These findings set the anti-osteoclast effects of ICT apart from that of bisphosphonates, whose effects are exerted on mature osteoclasts leading to osteoclast inactivation and apoptosis (Hughes et al., 1995; Matsumoto et al., 2000; Reszka & Rodan, 2003). Given that ICT did not reduce viability of the osteoclast precursors nor exert effects on mature osteoclasts, coupled with the reduction in expression of NFATc1, the master transcriptional regulator of osteoclast differentiation, suggest that ICT inhibits osteoclast differentiation.

5.2 Mechanism by which icaritin inhibits osteoclast differentiation

5.2.1 Icaritin inhibited NFATc1 expression via NFκB and MAPK/AP-1 pathways

The importance of the NFκB family of dimeric transcription factors to osteoclastogenesis was revealed when deletion of the NFκB1/p50 and NFκB2/p52 subunits led to severe osteopetrosis in mice as a result of osteoclast deficiency (Iotsova et al., 1997; Monje et al., 2005). It has since been well established that RANKL, after binding to its cognate receptor, triggers the canonical NFκB pathway by activating the IKK complex, resulting in the phosphorylation and degradation of IκB to release the p50-p65 dimer for nuclear translocation (Soysa & Alles, 2009). While RANKL has also been shown to activate the alternative NFκB pathway by triggering the NFκB-inducing kinase leading to the eventual generation of the p52-RelB dimer (Novack et al., 2003), it remains unclear which of the two NFκB pathways are dominant in osteoclast differentiation. Nonetheless, Asagiri et al. (2005) have shown that the p50-p65 subunits are recruited to the NFATc1 promoter following RANKL stimulation, indicating that these NFκB components are crucial in regulating the expression of NFATc1. In this thesis, we present substantial evidence to show that icaritin downregulates NFATc1 expression by inhibition of the RANKL-induced canonical NFκB pathway that resulted in decreased p65 nuclear translocation and suppressed NFκB transcriptional activity.

In addition to the NFκB pathway, c-Fos, a member of the AP-1 family of transcription factors, has also been shown to be indispensable for osteoclast differentiation given the osteopetrotic phenotype of c-Fos knockout mice (Wang et al., 1992). It was further delineated that c-Fos is crucial to the induction of NFATc1 since recruitment of c-Fos to the NFATc1 promoter has also been demonstrated. Additionally, induction of NFATc1 mRNA by RANKL is abrogated in c-Fos deficient cells (Asagiri et al., 2005; Iotsova et al., 1997). Given that c-Fos can only heterodimerize with members of the Jun family to form the AP-1 heterodimer, Soysa and Alles (2009) demonstration that expression of NFATc1 is Fos/Jun dependent is in keeping with the presence of AP-1 response elements in the NFATc1 promoter (Asagiri et al., 2005). As explained in the introduction, the expression and activity of the AP-1 transcription factor is regulated by the mitogen-activated protein kinases JNK, ERK and p38 (Monje et al., 2005; Novack et al., 2003). Indeed, we have shown in this thesis that RANKL induces activation of the JNK, ERP and p38 MAPKs that was inhibited by icaritin treatment and correspondingly, icaritin downregulated AP-1 transcriptional activity. Put together, our results therefore suggest that icaritin's inhibition of NFATc1 expression is dependent on its suppression of both NFκB and MAPK/AP-1 pathways.

5.2.2 Icaritin inhibits NFATc1 nuclear translocation and transcriptional activity by suppressing the TRAF6/cSrc/Nox1 pathway

There has been a recent accumulation of evidence supporting the importance of intracellular reactive oxygen species (ROS) as a secondary messenger in RANKL-mediated osteoclastogenesis (Kim et al., 2010; Lee et al., 2005; Lee & Jang, 2015; Moon et al., 2011). While there has been consensus in the signaling cascade set off by RANKL that leads to activation of the Nox1 enzyme responsible for the intracellular ROS production, Lee et al. (2005) demonstrated that this increase in intracellular ROS occurs in the acute time frame following RANKL stimulation and lies upstream of MAPK activation. On the contrary, the results of our study are aligned with that of M. S. Kim et al. (2010), which showed that the chronic ROS production mediates calcineurin activation via calcium oscillations. While ICT suppressed NFATc1 mRNA and protein expressions, we show that ICT, by suppressing the superoxide-generating enzyme Nox1, inhibited ROS production and subsequent calcineurin phosphatase activity to prevent NFATc1 nuclear translocation. Indeed, both the reduction in NFATc1 protein levels and inhibition in nuclear translocation contributed to a decreased NFATc1 transcriptional activity.

Interestingly, resveratrol, the red wine polyphenol, has also been shown to inhibit osteoclastogenesis by attenuating chronic ROS production (He et al., 2010). However, the mechanism underlying resveratrol's effects has yet to be elucidated. Given the similarities observed, our findings suggest a common pathway through which compounds like Resveratrol and ICT inhibits ROS production to reduce NFATc1 function and osteoclastogenesis.

5.2.3 Proteasomal degradation of the critical adaptor protein, TRAF6, mediates icaritin's suppression of osteoclastogenesis

The activation of the membrane receptor RANK by its ligand is a sufficient and necessary condition for transformation of monocytes/macrophages to functioning bone-resorptive osteoclasts. However, the RANK receptor protein lacks intrinsic kinase activity and depends on the recruitment of intermediate adapter proteins to activate downstream signaling pathways. Although RANK associates with several TRAFs, emerging evidence points to a critical regulatory function for the adapter protein TRAF6 in RANKL/RANK mediated signaling (Walsh & Choi, 2014). The importance of TRAF6 in bone metabolism was demonstrated with TRAF6-deficient mice exhibiting defective osteoclastogenesis and severe osteopetrosis (Lomaga et al., 1999; Naito et al., 1999). Upon stimulation with RANKL, TRAF6 forms an intermediate complex to regulate downstream NFκB, MAPK/AP-1 and ROS signaling (Boudot et al., 2010; Mizukami et al., 2002; Park et al., 2004). We therefore hypothesized that RANKL/RANK/TRAF6 system, the critical apex regulator of osteoclastogenesis, might be the mechanism through which ICT exerts its pleiotropic effects. Since no changes were observed in serum RANKL levels in the ovariectomized rats or RANK expression, we deduced that TRAF6 might be the direct target for ICT. Indeed, our cellular and animal studies indicate that ICT regulates proteasomal degradation of TRAF6, leading to a reduction in TRAF6 protein expression in circulating osteoclast precursors and bone. The degradative action of ICT on TRAF6 protein is reminiscent of the manner in which T cells negatively regulate bone resorption by secretion of IFNγ

(Takayanagi et al., 2000). Indeed, the inhibitory effects of ICT on osteoclastogenesis were reversed in the presence of the proteasomal inhibitor MG 132. We have previously shown that ICT leads to destabilization of ERα protein via aryl hydrocarbon receptor (AhR) signaling pathways (Tiong et al., 2012). Additionally, it has been shown that AhR mediates the expression of the transcription factor suppressors of cytokine signaling 2, leading to TRAF6 lysine48-linked polyubiquitination and proteasome-mediated degradation (McBerry et al., 2012). Furthermore, our immunoprecipitation studies revealed increased ubiquitination, specifically lysine 48-linked polyubiquitination, of TRAF6 in the presence of ICT. On the other hand, AhR has also been shown to be a positive regulator of osteoclastogenesis *in vitro* (Yu et al., 2015) and AhR knockout mice exhibit increased bone mass with decreased bone resorption (Iqbal et al., 2013; Izawa et al., 2016). As such, a challenge for the future remains to investigate if ICT could mediate proteasomal degradation of TRAF6 as a result of being an AhR agonist. Overall, our data indicate that ICT leads to proteasomal-mediated degradation of TRAF6 to suppress osteoclastogenesis.

Interestingly, the degradative effect of ICT on TRAF6 differs from that of estrogen, which sequesters the critical adaptor protein in an ERα-BCAR1 complex, thereby inhibiting RANKL-induced osteoclast differentiation (Robinson et al., 2009). Concurring with previous reports (Galal et al., 2007), we show that estradiol led to a reduction in RANK expression in osteoclast precursors. This suppressive effect of estradiol on RANK expression could account for the potency of estradiol in inhibiting osteoclast differentiation.

Using immunoprecipitation studies, Li et al. (2015) showed that Xanthohumol, a prenylflavonoid abundant in hops plants, disrupts the association of RANK and TRAF6. Given that Xanthohumol led to a dose-dependent decrease in the amount of TRAF6 bound to RANK and not vice versa, our findings suggest a possible mechanism by which Xanthohumol could lead to proteasomal degradation of TRAF6, thereby disrupting the association of RANK and TRAF6.

5.2.4 Comparison with other flavonoids that inhibit RANKL signaling

Flavonoids, as natural bioactive molecules, have garnered much interest in recent years as alternatives for the treatment of postmenopausal osteoporosis (Chiba et al., 2003; Horcajada-Molteni et al., 2000; Morabito et al., 2002). Indeed, it has been demonstrated that the soybean isoflavones, genistein and dadzein, inhibits NFκB and MAPK activation (Karieb & Fox, 2011; Lee et al., 2014). Although the suppressive effect of ICT on NFκB- and MAPK/AP-1-mediated osteoclastogenesis is similar to that of genistein and dadzein, our results suggest a divergence in the underlying mechanism. The inhibitory effects of these soybean isoflavones on c-Fos and NFATc1 expressions have been shown to be estrogen receptor (ER)- dependent (Karieb & Fox, 2011); in contrast, the effects of ICT on osteoclastogenesis cannot be reversed with the ER antagonist ICI 182,780, suggesting that effects of ICT are ER-independent. Indeed, genistein as a result of its estrogenic activity, has been demonstrated to lead to uterine hypertrophy in OVX mice (Ishimi et al., 2000), while we showed in our animal study that ICT treatment did not lead to changes in uterine weight, circumventing the increased risk of endometrial cancer that accompanies estrogenic compounds.

Quercetin, found in many fruits and vegetables, and Ikarisoside A, a flavonoid present in the *Epimedium* genus of herbs, also inhibits osteoclastogenesis in RAW 264.7 cells by suppressing both NFκB and AP-1 transcriptional activity (Choi et al., 2010; Wattel et al., 2004). Xanthohumol, a prenylflavonoid abundant in hops has also been shown to inhibit NFκB and Ca^{2+}/NFATc1 signaling pathways to inhibit osteoclastogenesis. As discussed in the previous section, Xanthohumol has also been shown to disrupt the association between RANK and TRAF6 (Li et al., 2015). Indeed, our experimental data indicate that a singular target, TRAF6, may be the key to understanding the plurality of actions that lead to suppression of osteoclastogenesis by these flavonoids. Our results further suggest a possible mechanism that by mediating proteasomal degradation of TRAF6, the decreased TRAF6 protein expression could disrupt the association between RANK and TRAF6, thereby inhibiting osteoclastogenesis.

Table 5.1 Comparison of effects of ICT and flavonoids on RANKL signaling pathway

	RANKL signaling pathway				
	NFκB	**MAPK/ AP-1**	**Ca^{2+}/NFATc1**	**ER-dependent**	**TRAF6**
Genistein	↓	↓	↓ NFATc1 expression	Yes	↓ expression
Dadzein	↓	↓	↓ NFATc1 expression	Yes	unknown
Quercetin	↓	↓	unknown	No	↓ expression in LPS-induced RAW 264.7 cells
Ikarisoside A	↓	↓	↓ NFATc1 expression and activity	unknown	unknown
Xanthohumol	↓	↔	↓ Ca^{2+} signaling, ↓ NFATc1 expression and activity	unknown	↓ TRAF6 association with RANK
Icaritin	↓	↓	↓ NFATc1 expression and activity	No	↓ expression via proteasomal degradation

↓ Inhibition; ↔ no effect

(Choi et al., 2010; Karieb & Fox, 2011; Lee et al., 2014; Li et al., 2015; Tsuji et al., 2009; Wattel et al., 2004)

5.3 Beneficial effects of icaritin in the OVX rat model

5.3.1 The OVX rat model and timing of administration of icaritin

Given that our *in vitro* data shows that ICT inhibits osteoclastogenesis, we sought to evaluate the anti-osteoclastogenic effects of ICT in the ovariectomized rat as a model for estrogen deficiency-mediated osteoporosis.

Although the ovariectomized rat is a well-employed model for studying estrogen deficiency-mediated osteoporosis, there has been no consensus on timing of administration of treatments (Hsiao et al., 2013; Li et al., 2015; Peng et al., 2013; Wu et al., 2012). Our baseline data indicate the establishment of the ovariectomy-induced osteoporotic rat model, as we recapitulated the endocrine disruptions (estrous acyclicity, weight gain, drastic decrease in serum estrogen levels and uterine atrophy) and osteoporotic phenotype of the ovariectomized rats. We opted to begin ICT treatment at 4 weeks' post-ovariectomy in order that we can ascertain the estrogen-deficient and mild osteoporotic status of rats. Furthermore, our experimental model was designed to obtain preclinical data to guide clinical studies that assess the effect of ICT on postmenopausal women. It is noteworthy that there was a further deterioration in the bone architecture and strength of the vehicle-treated OVX rats from baseline till 8 weeks' post OVX, which was accompanied by an increase in osteoclast numbers and activity as indicated by serum markers of bone resorption. These data suggest that the worsening of osteoporotic phenotype from baseline till 8 weeks' post OVX could be

attributed to the increased osteoclastic activity, supporting the validity of our model to assess the anti-osteoclastogenic efficacy of ICT.

5.3.2 Preventing OVX-induced deterioration in bone architecture & strength

With our initial findings that ICT inhibits osteoclast differentiation and activity *in vitro*, we postulated that ICT treatment in OVX rats would inhibit estrogen deficiency-induced osteoclastogenesis thereby preventing osteoporosis. Indeed, treatment of OVX rats with ICT inhibited the deterioration in bone architecture, density and strength in both the femur and lumbar vertebrae. In concordance with our *in vitro* studies, ICT treatment significantly inhibited the OVX-induced increase in osteoclast numbers and bone resorption. Subcutaneous estradiol valerate treatment, as the positive control (da Paz et al., 2001; Takano-Yamamoto & Rodan, 1990), also inhibited osteoclast formation and activity in the OVX rats. In contrast, ICT treatment at this dose did not lead to an increase in estrogenic activity of the serum nor did it lead to uterine hypertrophy. These findings support ICT as an alternative for the treatment of estrogen deficiency-mediated osteoporosis.

5.3.3 Ameliorating OVX-induced increase in TRAF6 and NFATc1 expression

The prevention of estrogen deficiency-mediated osteoporosis by ICT treatment was associated with reduced TRAF6 protein expression in $Cd11b^{+}/Gr\text{-}1^{-/low}$ osteoclast precursors isolated from OVX rats. Interestingly, our data indicate that osteoporosis, induced by estrogen-deficiency, is also

accompanied by increased TRAF6 protein expressions in the osteoclast precursors and tibial bone tissue. While this increase in TRAF6 protein expression in the vehicle-treated OVX rats could be accounted for by increased serum RANKL levels, the suppressive effect of ICT on TRAF6 expression is independent of its effects on RANKL levels. Estradiol treatment, on the contrary, led to reductions in serum RANKL levels, further pointing to differences in the mechanism of action between ICT and estradiol.

We present novel findings that estrogen deficiency-mediated osteoporosis is associated with increased NFATc1 protein expression in osteoclast precursors and tibial lysates. Similarly, while the increased NFATc1 expression in the vehicle-treated OVX rats could be attributed to the increased serum RANKL levels, the suppressive effect of ICT is independent of its effects on RANKL. In keeping with our *in vitro* studies, the decrease in NFATc1 protein expression in the $Cd11b^{+}/Gr\text{-}1^{-/low}$ osteoclast precursors and tibial lysates suggest that ICT treatment inhibited osteoclast differentiation in the OVX rats.

5.3.4 Anabolic effect of ICT in osteoporotic bone

As previously outlined in the introduction, ICT has been shown to enhance rat osteoblast proliferation and differentiation, leading to increased calcium deposition and enhanced mRNA expression of osteoblast genes (Huang et al., 2007). ICT has also been shown to enhance osteogenic differentiation of human MSCs to osteoblasts under osteogenic induction conditions while inhibiting adipogenic differentiation (Yao et al., 2012). Furthermore, *ex-vivo* culture of bone marrow stromal cells (BMSCs) from ICT-treated OVX rats also

showed increased osteogenic differentiation along with suppressed adipogenesis (Peng et al., 2013). Nonetheless, using a similar OVX-rat model, treatment dose and duration, we show that ICT inhibited estrogen deficiency-induced osteoclast differentiation and activity by downregulating TRAF6 expression in the OVX rats.

Although the anabolic effects of ICT was not within the focus of the current study, we showed that ICT treatment resulted in an increase in the bone formation marker, osteocalcin, suggesting that the bone protective effect of ICT was in part mediated by its enhancing bone formation.

5.4 Potential clinical applications

5.4.1 Inflammatory diseases

TRAF6, as a crucial signaling molecule, also mediates signaling downstream of the Interleukin-1/Toll-like receptor superfamily (Martin & Wesche, 2002; O'Neill, 2002). Thus, our findings that ICT downregulates TRAF6 protein expression may have implications for the treatment of inflammatory diseases. Indeed, TRAF6 inhibitors have been shown to reduce inflammation in models of peritonitis and sepsis (Zarzycka et al., 2015). Additionally, the anti-inflammatory properties of ICT have been demonstrated in models of peritonitis as well as in myocardial ischaemia and reperfusion injuries (Lai et al., 2013; Zhang et al., 2015). Coupled with our findings that this prenylflavonoid promotes proteasomal degradation of TRAF6, suggest that ICT may be a promising therapeutic option for dysregulated inflammatory responses.

Besides its detection in Lewy Bodies, TRAF6 has also been demonstrated to play a role in the development of familial Parkinson's disease (PD). Zucchelli et al. (2010) showed that TRAF6, by mediating atypical ubiquitination of DJ-1, facilitates its accumulation into insoluble aggregates, one of the hallmarks of PD. Chronic inflammation associated with increased TRAF6 expression and enhanced activation of NFκB signaling has also been demonstrated in a mouse model of PD (Chung et al., 2013). Furthermore, ICT, by promoting proteasomal degradation of TRAF6, mimics the physiological role of Parkin in suppressing

inflammation and cytokine-induced cell death, thus ICT's potential in modulating Parkin-deficiency-induced PD should be explored.

5.4.2 Treatment of postmenopausal osteoporosis and future work

The clinical trials reported in the literature that studied the effects of Epimedium-derived flavonoids on postmenopausal women used either a mixture of flavonoids (Zhang et al., 2007) or a decoction that included other types of herbs (Zhu et al., 2012). The novel findings presented in this thesis opens new possibilities into the study of ICT and its value for treating postmenopausal osteoporosis. There is immense clinical potential for our findings and we believe that future work should include bringing this research into the clinical phase of development. Given that the clinical safety of Epimedium-derived flavonoids has been demonstrated in randomized controlled trials (Zhang et al., 2007), the efficacy of ICT in improving the bone health of postmenopausal women should be investigated.

Based on our *in vivo* studies, the efficacious dose of ICT that significantly ameliorated estrogen-deficiency mediated osteoporosis in the ovariectomized rats was 40 mg/kg/day. Using the guidelines published by the US Food and Drug Administration for conversion of animal doses to human equivalent doses based on body surface area, we converted this efficacious dose to its human equivalent dose (U.S. Food and Drug administration, 2005), which works out to be approximately 400 mg of ICT daily, for a 60 kg human. This is well within the 600 mg twice-daily dose found to be safe and tolerable in a

Phase I clinical study of ICT in advanced breast cancer patients (U.S. National Institutes of Health, 2015, NCT01972672).

Subject to funding approval, the following trial is currently in the pipeline and has been designed as follows: To prevent investigator bias, the study will be conducted as a randomized, double-blinded, placebo-controlled outcome study. The primary outcome of the study focuses on determining if ICT reduces serum markers of bone resorption (CTx and TRAP5b), and to determine if any changes occur in serum markers of bone formation (P1NP and osteocalcin). BMD measurements of the femoral neck and lumbar vertebrae will also be assessed at baseline and at a minimum of 6 months after treatment commences. BMD measurements will be combined with the aforementioned serum markers to determine the effect of ICT treatment on bone turnover. Although recognized to be safe, laboratory biochemical examinations (liver function, renal function and full blood count) will be conducted to monitor for adverse events. To prevent findings from being confounded by other drugs, subjects who are currently or have been taking medications or dietary supplements that affect bone turnover (eg. bisphosphonates, hormone replacement therapy) within 3 months of the study will be excluded. All participants will receive daily elemental calcium in calcium carbonate (500 mg) and vitamin D3 (200 IU) supplementation and agree to limit their calcium-containing and soy-containing food intake to a standardized amount.

5.5 Concluding remarks

In summary, the findings of this thesis uncover new possibilities into the study of prenylflavonoids like ICT and provide the grounds for further exploration of ICT in treating postmenopausal osteoporosis. Our *in vitro* mechanistic study revealed that ICT inhibited RANKL-induced activation in both the NFκB and MAPK/AP-1 pathways to downregulate NFATc1 expression and suppressed its transcriptional activity by inhibiting the TRAF6/cSrc/PI3K pathway. ICT treatment prevented ovariectomy-induced osteoclast formation and activity to suppress estrogen deficiency-induced bone loss and deterioration in bone strength. Crucially, the effects of ICT were associated with decreased TRAF6 protein expression, which was consistently observed both *in vitro* and *in vivo.* We further delineated that ICT mediates proteasomal degradation of TRAF6 by increasing lysine 48-specific polyubiquitination of this critical adaptor protein. Not only have Epimedium-derived flavonoids long been used in eastern ethnopharmacology for the treatment of menstrual irregularities and to improve bone health, ICT has also been shown to exert anabolic effects on bone. Furthermore, given our findings that ICT inhibits osteoclastogenesis and osteoclast resorption strongly support the potential of ICT for the treatment of postmenopausal osteoporosis. The findings of this thesis suggest that mechanistically, the pleiotropic effects of prenylflavonoids on inhibiting osteoclast differentiation could be coordinated through the degradation of the adaptor protein TRAF6, and as such TRAF6 is a promising target for the design of novel anti-osteoporotic drugs.

REFERENCES

Abu-Amer, Y., Ross, F. P., Edwards, J., & Teitelbaum, S. L. (1997). Lipopolysaccharide-stimulated osteoclastogenesis is mediated by tumor necrosis factor via its P55 receptor. *J Clin Invest, 100*(6), 1557-1565. doi: 10.1172/jci119679

Adomaityte, J., Farooq, M., & Qayyum, R. (2008). Effect of raloxifene therapy on venous thromboembolism in postmenopausal women. A meta-analysis. *Thromb Haemost, 99*(2), 338-342. doi: 10.1160/th07-07-0468

Almeida, M., Han, L., Martin-Millan, M., Plotkin, L. I., Stewart, S. A., Roberson, P. K., . . . Manolagas, S. C. (2007). Skeletal involution by age-associated oxidative stress and its acceleration by loss of sex steroids. *J Biol Chem, 282*(37), 27285-27297. doi: 10.1074/jbc.M702810200

Almeida, M., Martin-Millan, M., Ambrogini, E., Bradsher, R., 3rd, Han, L., Chen, X. D., . . . Manolagas, S. C. (2010). Estrogens attenuate oxidative stress and the differentiation and apoptosis of osteoblasts by DNA-binding-independent actions of the ERalpha. *J Bone Miner Res, 25*(4), 769-781. doi: 10.1359/jbmr.091017

Ammann, P., & Rizzoli, R. (2003). Bone strength and its determinants. *Osteoporos Int, 14 Suppl 3*, S13-18. doi: 10.1007/s00198-002-1345-4

Asagiri, M., Sato, K., Usami, T., Ochi, S., Nishina, H., Yoshida, H., . . . Takayanagi, H. (2005). Autoamplification of NFATc1 expression determines its essential role in bone homeostasis. *J Exp Med, 202*(9), 1261-1269. doi: 10.1084/jem.20051150

Aslan, D., Andersen, M. D., Gede, L. B., de Franca, T. K., Jorgensen, S. R., Schwarz, P., & Jorgensen, N. R. (2012). Mechanisms for the bone anabolic effect of parathyroid hormone treatment in humans. *Scand J Clin Lab Invest, 72*(1), 14-22. doi: 10.3109/00365513.2011.624631

Audran, M., Jakob, F. J., Palacios, S., Brandi, M. L., Broll, H., Hamdy, N. A., & McCloskey, E. V. (2013). A large prospective European cohort study of patients treated with strontium ranelate and followed up over 3 years. *Rheumatol Int, 33*(9), 2231-2239. doi: 10.1007/s00296-012-2594-y

Augat, Peter, & Schorlemmer, Sandra. (2006). The role of cortical bone and its microstructure in bone strength. *Age and Ageing, 35*(suppl 2), ii27-ii31. doi: 10.1093/ageing/afl081

Bakker, A. D., & Klein-Nulend, J. (2012). Osteoblast isolation from murine calvaria and long bones. *Methods Mol Biol, 816*, 19-29. doi: 10.1007/978-1-61779-415-5_2

Barger-Lux, M. J., & Heaney, R. P. (1995). Caffeine and the calcium economy revisited. *Osteoporosis International, 5*(2), 97-102. doi: 10.1007/bf01623310

Barrett-Connor, E., Chang, J. C., & Edelstein, S. L. (1994). Coffee-associated osteoporosis offset by daily milk consumption. The Rancho Bernardo Study. *JAMA, 271*(4), 280-283. doi: 10.1001/jama.1994.03510280042030

Barrett-Connor, E., Mosca, L., Collins, P., Geiger, M. J., Grady, D., Kornitzer, M., . . . Wenger, N. K. (2006). Effects of raloxifene on cardiovascular events and breast cancer in postmenopausal women. *N Engl J Med, 355*(2), 125-137. doi: 10.1056/NEJMoa062462

Beals, C. R., Clipstone, N. A., Ho, S. N., & Crabtree, G. R. (1997). Nuclear localization of NF-ATc by a calcineurin-dependent, cyclosporin-sensitive

intramolecular interaction. *Genes Dev, 11*(7), 824-834. doi: 10.1101/gad.11.7.824

Bennett, S., & Breit, S. N. (1994). Variables in the isolation and culture of human monocytes that are of particular relevance to studies of HIV. *J Leukoc Biol, 56*(3), 236-240. doi: 10.1002/0471142735.im1204s42

Bennett, S., Por, S. B., Stanley, E. R., & Breit, S. N. (1992). Monocyte proliferation in a cytokine-free, serum-free system. *J Immunol Methods, 153*(1-2), 201-212. doi: 10.1016/0022-1759(92)90323-l

Bernabei, Roberto, Martone, Anna Maria, Ortolani, Elena, Landi, Francesco, & Marzetti, Emanuele. (2014). Screening, diagnosis and treatment of osteoporosis: a brief review. *Clinical Cases in Mineral and Bone Metabolism, 11*(3), 201-207. doi: 10.11138/ccmbm/2014.11.3.201

Bernstein, Leslie, Deapen, Dennis, Cerhan, James R., Schwartz, Stephen M., Liff, Jonathan, McGann-Maloney, Erin, . . . Ford, Leslie. (1999). Tamoxifen Therapy for Breast Cancer and Endometrial Cancer Risk. *Journal of the National Cancer Institute, 91*(19), 1654-1662. doi: 10.1093/jnci/91.19.1654

Bischoff-Ferrari, H. A., Dawson-Hughes, B., Willett, W. C., Staehelin, H. B., Bazemore, M. G., Zee, R. Y., & Wong, J. B. (2004). Effect of Vitamin D on falls: a meta-analysis. *JAMA, 291*(16), 1999-2006. doi: 10.1001/jama.291.16.1999

Black, D. M., Delmas, P. D., Eastell, R., Reid, I. R., Boonen, S., Cauley, J. A., . . . Cummings, S. R. (2007). Once-yearly zoledronic acid for treatment of postmenopausal osteoporosis. *N Engl J Med, 356*(18), 1809-1822. doi: 10.1056/NEJMoa067312

Bonaiuti, D., Shea, B., Iovine, R., Negrini, S., Robinson, V., Kemper, H. C., . . . Cranney, A. (2002). Exercise for preventing and treating osteoporosis in postmenopausal women. *Cochrane Database Syst Rev*(3), CD000333. doi: 10.1002/14651858.cd000333

Bone, H. G., Chapurlat, R., Brandi, M. L., Brown, J. P., Czerwinski, E., Krieg, M. A., . . . Papapoulos, S. (2013). The effect of three or six years of denosumab exposure in women with postmenopausal osteoporosis: results from the FREEDOM extension. *J Clin Endocrinol Metab, 98*(11), 4483-4492. doi: 10.1210/jc.2013-1597

Bonewald, L. F. (2006). Mechanosensation and Transduction in Osteocytes. *Bonekey Osteovision, 3*(10), 7-15. doi: 10.1138/20060233

Boonen, S., Body, J. J., Boutsen, Y., Devogelaer, J. P., Goemaere, S., Kaufman, J. M., . . . Reginster, J. Y. (2005). Evidence-based guidelines for the treatment of postmenopausal osteoporosis: a consensus document of the Belgian Bone Club. *Osteoporos Int, 16*(3), 239-254. doi: 10.1007/s00198-004-1812-1

Borgstrom, F., Sobocki, P., Strom, O., & Jonsson, B. (2007). The societal burden of osteoporosis in Sweden. *Bone, 40*(6), 1602-1609. doi: 10.1016/j.bone.2007.02.027

Boudot, C., Saidak, Z., Boulanouar, A. K., Petit, L., Gouilleux, F., Massy, Z., . . . Kamel, S. (2010). Implication of the calcium sensing receptor and the Phosphoinositide 3-kinase/Akt pathway in the extracellular calcium-mediated migration of RAW 264.7 osteoclast precursor cells. *Bone, 46*(5), 1416-1423. doi: 10.1016/j.bone.2010.01.383

Boyce, B. F., Xing, L., & Jilka, R. L. (2002). Apoptosis in bone cells. In J. P. Bilezikian, L. G. Raisz & G. A. Rodan (Eds.), *Principles of bone biology* (2nd ed., pp. 151-168). San Diego, CA.: Academic Press. doi: 10.1016/b978-0-12-373884-4.x0001-8

Boyle, William J., Simonet, W. Scott, & Lacey, David L. (2003). Osteoclast differentiation and activation. *Nature, 423*(6937), 337-342. doi: 10.1038/nature01658

Burge, R., Dawson-Hughes, B., Solomon, D. H., Wong, J. B., King, A., & Tosteson, A. (2007). Incidence and economic burden of osteoporosis-related fractures in the United States, 2005-2025. *J Bone Miner Res, 22*(3), 465-475. doi: 10.1359/jbmr.061113

Cagnetta, V., & Patella, V. (2012). The role of the immune system in the pathophysiology of osteoporosis. *Clin Cases in Mineral and Bone Metabolism, 9*(2), 4. doi: 10.1007/s11914-005-0016-8

Caudrillier, A., Hurtel-Lemaire, A. S., Wattel, A., Cournarie, F., Godin, C., Petit, L., . . . Brazier, M. (2010). Strontium ranelate decreases receptor activator of nuclear factor-KappaB ligand-induced osteoclastic differentiation in vitro: involvement of the calcium-sensing receptor. *Mol Pharmacol, 78*(4), 569-576. doi: 10.1124/mol.109.063347

Cauley, J. A., Robbins, J., Chen, Z., Cummings, S. R., Jackson, R. D., LaCroix, A. Z., . . . Watts, N. B. (2003). Effects of estrogen plus progestin on risk of fracture and bone mineral density: the Women's Health Initiative randomized trial. *JAMA, 290*(13), 1729-1738. doi: 10.1001/jama.290.13.1729

Cenci, S., Weitzmann, M. N., Roggia, C., Namba, N., Novack, D., Woodring, J., & Pacifici, R. (2000). Estrogen deficiency induces bone loss by enhancing T-cell production of TNF-alpha. *J Clin Invest, 106*(10), 1229-1237. doi: 10.1172/jci11066

Chen, S. H., Lei, M., Xie, X. H., Zheng, L. Z., Yao, D., Wang, X. L., . . . Qin, L. (2013). PLGA/TCP composite scaffold incorporating bioactive phytomolecule icaritin for enhancement of bone defect repair in rabbits. *Acta Biomater, 9*(5), 6711-6722. doi: 10.1016/j.actbio.2013.01.024

Chiba, H., Uehara, M., Wu, J., Wang, X., Masuyama, R., Suzuki, K., . . . Ishimi, Y. (2003). Hesperidin, a citrus flavonoid, inhibits bone loss and decreases serum and hepatic lipids in ovariectomized mice. *J Nutr, 133*(6), 1892-1897. doi: 10.1002/ptr.5001

Choi, H. J., Park, Y. R., Nepal, M., Choi, B. Y., Cho, N. P., Choi, S. H., . . . Soh, Y. (2010). Inhibition of osteoclastogenic differentiation by Ikarisoside A in RAW 264.7 cells via JNK and NF-kappaB signaling pathways. *Eur J Pharmacol, 636*(1-3), 28-35. doi: 10.1016/j.ejphar.2010.03.023

Chung, J. Y., Park, H. R., Lee, S. J., Lee, S. H., Kim, J. S., Jung, Y. S., . . . Park, B. J. (2013). Elevated TRAF2/6 expression in Parkinson's disease is caused by the loss of Parkin E3 ligase activity. *Lab Invest, 93*(6), 663-676. doi: 10.1038/labinvest.2013.60

Collin-Osdoby, P., & Osdoby, P. (2012). RANKL-mediated osteoclast formation from murine RAW 264.7 cells. *Methods Mol Biol, 816*, 187-202. doi: 10.1007/978-1-61779-415-5_13

Collins, Peter, Mosca, Lori, Geiger, Mary Jane, Grady, Deborah, Kornitzer, Marcel, Amewou-Atisso, Messan G., . . . Wenger, Nanette K. (2009). Effects of the Selective Estrogen Receptor Modulator Raloxifene on Coronary Outcomes in The Raloxifene Use for the Heart Trial. *Results of Subgroup Analyses by Age and Other Factors, 119*(7), 922-930. doi: 10.1161/circulationaha.108.817577

Cooper, C., Campion, G., & Melton, L. J., 3rd. (1992). Hip fractures in the elderly: a world-wide projection. *Osteoporos Int, 2*(6), 285-289. doi: 10.1007/bf01623184

Cooper, C., Cole, Z. A., Holroyd, C. R., Earl, S. C., Harvey, N. C., Dennison, E. M., . . . Kanis, J. A. (2011). Secular trends in the incidence of hip and other

osteoporotic fractures. *Osteoporos Int, 22*(5), 1277-1288. doi: 10.1007/s00198-011-1601-6

Cosman, F., de Beur, S. J., LeBoff, M. S., Lewiecki, E. M., Tanner, B., Randall, S., & Lindsay, R. (2014). Clinician's Guide to Prevention and Treatment of Osteoporosis. *Osteoporos Int, 25*(10), 2359-2381. doi: 10.1007/s00198-014-2794-2

Coxon, F. P., & Taylor, A. (2008). Vesicular trafficking in osteoclasts. *Semin Cell Dev Biol, 19*(5), 424-433. doi: 10.1016/j.semcdb.2008.08.004

Cuetara, Bethany L. V., Crotti, Tania N., O'Donoghue, Anthony J., & McHugh, Kevin P. (2006). CLONING AND CHARACTERIZATION OF OSTEOCLAST PRECURSORS FROM THE RAW264.7 CELL LINE. *In vitro cellular & developmental biology. Animal, 42*(7), 182-188. doi: 10.1290/0510075.1

Cummings, S. R., San Martin, J., McClung, M. R., Siris, E. S., Eastell, R., Reid, I. R., . . . Christiansen, C. (2009). Denosumab for prevention of fractures in postmenopausal women with osteoporosis. *N Engl J Med, 361*(8), 756-765. doi: 10.1056/NEJMoa0809493

D'Amelio, P., Grimaldi, A., Di Bella, S., Brianza, S. Z., Cristofaro, M. A., Tamone, C., . . . Isaia, G. (2008). Estrogen deficiency increases osteoclastogenesis up-regulating T cells activity: a key mechanism in osteoporosis. *Bone, 43*(1), 92-100. doi: 10.1016/j.bone.2008.02.017

da Paz, L. H., de Falco, V., Teng, N. C., dos Reis, L. M., Pereira, R. M., & Jorgetti, V. (2001). Effect of 17beta-estradiol or alendronate on the bone densitometry, bone histomorphometry and bone metabolism of ovariectomized rats. *Braz J Med Biol Res, 34*(8), 1015-1022. doi: 10.1590/s0100-879x2001000800007

Darnay, B. G., Haridas, V., Ni, J., Moore, P. A., & Aggarwal, B. B. (1998). Characterization of the intracellular domain of receptor activator of NF-kappaB (RANK). Interaction with tumor necrosis factor receptor-associated factors and activation of NF-kappab and c-Jun N-terminal kinase. *J Biol Chem, 273*(32), 20551-20555. doi: 10.1074/jbc.273.32.20551

de Almeida, M. C., Silva, A. C., Barral, A., & Barral Netto, M. (2000). A simple method for human peripheral blood monocyte isolation. *Mem Inst Oswaldo Cruz, 95*(2), 221-223. doi: 10.1590/s0074-02762000000200014

Delmas, P. D. (2002). Treatment of postmenopausal osteoporosis. *Lancet, 359*(9322), 2018-2026. doi: 10.1016/s0140-6736(02)08827-x

Delmas , Pierre D., Bjarnason , Nina H., Mitlak , Bruce H., Ravoux , Anne-Catherine, Shah , Aarti S., Huster , William J., . . . Christiansen , Claus. (1997). Effects of Raloxifene on Bone Mineral Density, Serum Cholesterol Concentrations, and Uterine Endometrium in Postmenopausal Women. *New England Journal of Medicine, 337*(23), 1641-1647. doi: doi:10.1056/NEJM199712043372301

Deng, L., Wang, C., Spencer, E., Yang, L., Braun, A., You, J., . . . Chen, Z. J. (2000). Activation of the IkappaB kinase complex by TRAF6 requires a dimeric ubiquitin-conjugating enzyme complex and a unique polyubiquitin chain. *Cell, 103*(2), 351-361. doi: 10.1016/s0092-8674(00)00126-4

Drake, Matthew T., Clarke, Bart L., & Khosla, Sundeep. (2008). Bisphosphonates: Mechanism of Action and Role in Clinical Practice. *Mayo Clinic proceedings. Mayo Clinic, 83*(9), 1032-1045. doi: 0.4065/83.9.1032

Early breast cancer trialists' collaborative group, investigators. (2005). Effects of chemotherapy and hormonal therapy for early breast cancer on recurrence and 15-year survival: an overview of the randomised trials. *Lancet, 365*(9472), 1687-1717. doi: 10.1016/s0140-6736(05)66544-0

Eghbali-Fatourechi, Guitty, Khosla, Sundeep, Sanyal, Arunik, Boyle, William J., Lacey, David L., & Riggs, B. Lawrence. Role of RANK ligand in mediating

increased bone resorption in early postmenopausal women. *J Clin Invest, 111*(8), 1221-1230. doi: 10.1172/JCI17215

Engelke, K., & Gluer, C. C. (2006). Quality and performance measures in bone densitometry: part 1: errors and diagnosis. *Osteoporos Int, 17*(9), 1283-1292. doi: 10.1007/s00198-005-0039-0

Erben, R. G. (1996). Trabecular and endocortical bone surfaces in the rat: modeling or remodeling? *Anat Rec, 246*(1), 39-46. doi: 10.1002/(sici)1097-0185(199609)246:1<39::aid-ar5>3.0.co;2-a

Ettinger, B., Black, D. M., Mitlak, B. H., Knickerbocker, R. K., Nickelsen, T., Genant, H. K., . . . Cummings, S. R. (1999). Reduction of vertebral fracture risk in postmenopausal women with osteoporosis treated with raloxifene: results from a 3-year randomized clinical trial. Multiple Outcomes of Raloxifene Evaluation (MORE) Investigators. *JAMA, 282*(7), 637-645. doi: 10.1001/jama.282.7.637

Ettinger, B., Black, D. M., Nevitt, M. C., Rundle, A. C., Cauley, J. A., Cummings, S. R., & Genant, H. K. (1992). Contribution of vertebral deformities to chronic back pain and disability. The Study of Osteoporotic Fractures Research Group. *J Bone Miner Res, 7*(4), 449-456. doi: 10.1002/jbmr.5650070413

Falahati-Nini, A., Riggs, B. L., Atkinson, E. J., O'Fallon, W. M., Eastell, R., & Khosla, S. (2000). Relative contributions of testosterone and estrogen in regulating bone resorption and formation in normal elderly men. *J Clin Invest, 106*(12), 1553-1560. doi: 10.1172/jci10942

Fechtenbaum, J., Cropet, C., Kolta, S., Horlait, S., Orcel, P., & Roux, C. (2005). The severity of vertebral fractures and health-related quality of life in osteoporotic postmenopausal women. *Osteoporosis International, 16*(12), 2175-2179. doi: 10.1007/s00198-005-2023-0

Feng, X., & McDonald, J. M. (2011). Disorders of bone remodeling. *Annu Rev Pathol, 6*, 121-145. doi: 10.1146/annurev-pathol-011110-130203

Fernandez, J. M., Molinuevo, M. S., McCarthy, A. D., & Cortizo, A. M. (2014). Strontium ranelate stimulates the activity of bone-specific alkaline phosphatase: interaction with Zn(2+) and Mg (2+). *Biometals, 27*(3), 601-607. doi: 10.1007/s10534-014-9733-8

Foltz, C.J., & Ullman-Cullere, M. (1999). Guidelines for assessing the health and condition of mice. *Lab animal, 28*(4), 5.

Fournier, P., Boissier, S., Filleur, S., Guglielmi, J., Cabon, F., Colombel, M., & Clezardin, P. (2002). Bisphosphonates inhibit angiogenesis in vitro and testosterone-stimulated vascular regrowth in the ventral prostate in castrated rats. *Cancer Res, 62*(22), 6538-6544. doi: 10.1016/s1569-9056(02)80196-8

Fujikawa, Y, Quinn, J M, Sabokbar, A, McGee, J O, & Athanasou, N A. (1996). The human osteoclast precursor circulates in the monocyte fraction. *Endocrinology, 137*(9), 4058-4060. doi: doi:10.1210/endo.137.9.8756585

Gabriel, S. E., Tosteson, A. N., Leibson, C. L., Crowson, C. S., Pond, G. R., Hammond, C. S., & Melton, L. J., 3rd. (2002). Direct medical costs attributable to osteoporotic fractures. *Osteoporos Int, 13*(4), 323-330. doi: 10.1007/s001980200033

Galal, N., El-Beialy, W. R., Deyama, Y., Yoshimura, Y., Suzuki, K., & Totsuka, Y. (2007). Novel effect of estrogen on RANK and c-fms expression in RAW 264.7 cells. *Int J Mol Med, 20*(1), 97-101. doi: 10.3892/ijmm.20.1.97

Galibert, L., Tometsko, M. E., Anderson, D. M., Cosman, D., & Dougall, W. C. (1998). The involvement of multiple tumor necrosis factor receptor (TNFR)-associated factors in the signaling mechanisms of receptor activator of NF-kappaB, a member of the TNFR superfamily. *J Biol Chem, 273*(51), 34120-34127. doi: 10.1074/jbc.273.51.34120

Galsworthy, T. D., & Wilson, P. L. (1996). Osteoporosis. It steals more than bone. *Am J Nurs, 96*(6), 26-33; quiz 34. doi: 10.2307/3464884

Garnero, P., Sornay-Rendu, E., Duboeuf, F., & Delmas, P. D. (1999). Markers of bone turnover predict postmenopausal forearm bone loss over 4 years: the OFELY study. *J Bone Miner Res, 14*(9), 1614-1621. doi: 10.1359/jbmr.1999.14.9.1614

Gennari, C. (2001). Calcium and vitamin D nutrition and bone disease of the elderly. *Public Health Nutr, 4*(2B), 547-559. doi: 10.1079/phn2001140

Glickman, M. H., & Ciechanover, A. (2002). The ubiquitin-proteasome proteolytic pathway: destruction for the sake of construction. *Physiol Rev, 82*(2), 373-428. doi: 10.1152/physrev.00027.2001

Gold, D.T., Stegmaier, K., Bales, C.N., Lyles, K.W., Westlund, R.E., & Drezner, M.K. (2009). Psychosocial functioning and osteoporosis in late life: results of a multidisciplinary intervention. *J Women's Health, 2*(2), 7. doi: 10.1089/jwh.1993.2.149

Grigoriadis, A. E., Wang, Z. Q., Cecchini, M. G., Hofstetter, W., Felix, R., Fleisch, H. A., & Wagner, E. F. (1994). c-Fos: a key regulator of osteoclast-macrophage lineage determination and bone remodeling. *Science, 266*(5184), 443-448. doi: 10.1126/science.7939685

Hadjidakis, D.J., Androulakis, I. I. (2006). Bone remodeling. *Ann N Y Acad Sci 1092, 385 – 396.* doi: 10.1196/annals.1365.035

Hardcastle, A. C., Aucott, L., Reid, D. M., & Macdonald, H. M. (2011). Associations between dietary flavonoid intakes and bone health in a Scottish population. *J Bone Miner Res, 26*(5), 941-947. doi: 10.1002/jbmr.285

He, X., Andersson, G., Lindgren, U., & Li, Y. (2010). Resveratrol prevents RANKL-induced osteoclast differentiation of murine osteoclast progenitor RAW 264.7 cells through inhibition of ROS production. *Biochem Biophys Res Commun, 401*(3), 356-362. doi: 10.1016/j.bbrc.2010.09.053

Henriksen, K., Tanko, L. B., Qvist, P., Delmas, P. D., Christiansen, C., & Karsdal, M. A. (2007). Assessment of osteoclast number and function: application in the development of new and improved treatment modalities for bone diseases. *Osteoporosis International, 18*(5), 681-685. doi: 10.1007/s00198-006-0286-8

Hilberg, F., Aguzzi, A., Howells, N., & Wagner, E. F. (1993). c-jun is essential for normal mouse development and hepatogenesis. *Nature, 365*(6442), 179-181. doi: 10.1038/365179a0

Hodge, J. M., Kirkland, M. A., & Nicholson, G. C. (2007). Multiple roles of M-CSF in human osteoclastogenesis. *J Cell Biochem, 102*(3), 759-768. doi: 10.1002/jcb.21331

Hoerger, T.J., Downs, K.E., Lakshmanan, M.C., Lindrooth, R.C., Plouffe, L.J., Wendling, B., . . . Ohsfeldt, R.L. (2009). Healthcare use among U.S. women aged 45 and older: Total costs and costs for selected postmenopausal health risks. *J Women's Health & Gender-based Medicine, 8*(8), 13. doi: 10.1089/jwh.1.1999.8.1077

Hogan, P. G., Chen, L., Nardone, J., & Rao, A. (2003). Transcriptional regulation by calcium, calcineurin, and NFAT. *Genes Dev, 17*(18), 2205-2232. doi: 10.1101/gad.1102703

Holt, I., & Marshall, M. J. (1998). Integrin subunit beta3 plays a crucial role in the movement of osteoclasts from the periosteum to the bone surface. *J Cell Physiol, 175*(1), 1-9. doi: 10.1002/(sici)1097-4652(199804)175:1<1::aid-jcp1>3.0.co;2-s

Horcajada-Molteni, M. N., Crespy, V., Coxam, V., Davicco, M. J., Remesy, C., & Barlet, J. P. (2000). Rutin inhibits ovariectomy-induced osteopenia in rats. *J Bone Miner Res, 15*(11), 2251-2258. doi: 10.1359/jbmr.2000.15.11.2251

Horowitz, M. C. (1993). Cytokines and estrogen in bone: anti-osteoporotic effects. *Science, 260*(5108), 626-627. doi: 10.1126/science.8480174

Hsiao, H. B., Lin, H., Wu, J. B., & Lin, W. C. (2013). Kinsenoside prevents ovariectomy-induced bone loss and suppresses osteoclastogenesis by regulating classical NF-κB pathways. *Osteoporosis International, 24*(5), 1663-1676. doi: 10.1007/s00198-012-2199-z

Hsu, H., Lacey, D. L., Dunstan, C. R., Solovyev, I., Colombero, A., Timms, E., . . . Boyle, W. J. (1999). Tumor necrosis factor receptor family member RANK mediates osteoclast differentiation and activation induced by osteoprotegerin ligand. *Proc Natl Acad Sci U S A, 96*(7), 3540-3545. doi: 0.1073/pnas.96.7.3540

Huang, J., Yuan, L., Wang, X., Zhang, T. L., & Wang, K. (2007). Icaritin and its glycosides enhance osteoblastic, but suppress osteoclastic, differentiation and activity in vitro. *Life Sci, 81*(10), 832-840. doi: 10.1016/j.lfs.2007.07.015

Hughes, David E, Wright, Kenneth R, Uy, Harry L, Sasaki, Akira, Yoneda, Toshiyuki, Roodman, David G, . . . Boyce, Brendan F. (1995). Bisphosphonates promote apoptosis in murine osteoclasts in vitro and in vivo. *Journal of Bone and Mineral Research, 10*(10), 1478-1487. doi: 10.1002/jbmr.5650101008

Indran, I. R., Liang, R. L., Min, T. E., & Yong, E. L. (2016). Preclinical studies and clinical evaluation of compounds from the genus Epimedium for osteoporosis and bone health. *Pharmacol Ther*. doi: 10.1016/j.pharmthera.2016.01.015

Inoue, M., Ross, F. P., Erdmann, J. M., Abu-Amer, Y., Wei, S., & Teitelbaum, S. L. (2000). Tumor necrosis factor alpha regulates alpha(v)beta5 integrin expression by osteoclast precursors in vitro and in vivo. *Endocrinology, 141*(1), 284-290. doi: 10.1210/endo.141.1.7285

Iotsova, V., Caamano, J., Loy, J., Yang, Y., Lewin, A., & Bravo, R. (1997). Osteopetrosis in mice lacking NF-kappaB1 and NF-kappaB2. *Nat Med, 3*(11), 1285-1289. doi: 10.1038/nm1197-1285

Iqbal, J., Sun, L., Cao, J., Yuen, T., Lu, P., Bab, I., . . . Avadhani, N. G. (2013). Smoke carcinogens cause bone loss through the aryl hydrocarbon receptor and induction of Cyp1 enzymes. *Proc Natl Acad Sci U S A, 110*(27), 11115-11120. doi: 10.1073/pnas.1220919110

Ishimi, Yoshiko, Arai, Naoko, Wang, Xinxiang, Wu, Jian, Umegaki, Keizo, Miyaura, Chisato, . . . Ikegami, Sachie. (2000). Difference in Effective Dosage of Genistein on Bone and Uterus in Ovariectomized Mice. *Biochem Biophys Res Commun, 274*(3), 697-701. doi: 10.1006/bbrc.2000.3175

Itzstein, C., & van 't Hof, R. J. (2012). Osteoclast formation in mouse co-cultures. *Methods Mol Biol, 816*, 177-186. doi: 10.1007/978-1-61779-415-5_12

Izawa, T., Arakaki, R., Mori, H., Tsunematsu, T., Kudo, Y., Tanaka, E., & Ishimaru, N. (2016). The Nuclear Receptor AhR Controls Bone Homeostasis by Regulating Osteoclast Differentiation via the RANK/c-Fos Signaling Axis. *J Immunol, 197*(12), 4639-4650. doi: 10.4049/jimmunol.1600822

Janssen, Hennie CJP, Samson, Monique M, & Verhaar, Harald JJ. (2002). Vitamin D deficiency, muscle function, and falls in elderly people. *The American Journal of Clinical Nutrition, 75*(4), 611-615. doi: 10.1016/s0261-5614(14)50367-6

Jaworski, Z.F.G. (1992). Haversian systems and haversian bone. In B. K. Hall (Ed.), *Bone: Bone Metabolism and Mineralization* (Vol. 4, pp. 21 - 34). Boca Raton, FL: CRC Press. doi: 10.1016/b9-78-012088-5/62650-0133

Jee, W. S., & Yao, W. (2001). Overview: animal models of osteopenia and osteoporosis. *J Musculoskelet Neuronal Interact, 1*(3), 193-207. doi: 10.1016/8756-3282(95)00283-j

Jilka, R. L. (2003). Biology of the basic multicellular unit and the pathophysiology of osteoporosis. *Med Pediatr Oncol, 41*(3), 182-185. doi: 10.1002/mpo.10334

Johnell, O., Gullberg, B., Kanis, J. A., Allander, E., Elffors, L., Dequeker, J., . . . et al. (1995). Risk factors for hip fracture in European women: the MEDOS Study. Mediterranean Osteoporosis Study. *J Bone Miner Res, 10*(11), 1802-1815. doi: 10.1002/jbmr.5650101125

Johnell, O., & Kanis, J. A. (2006). An estimate of the worldwide prevalence and disability associated with osteoporotic fractures. *Osteoporos Int, 17*(12), 1726-1733. doi: 10.1007/s00198-006-0172-4

Johnell, O., Kanis, J. A., Odén, A., Sernbo, I., Redlund-Johnell, I., Petterson, C., . . . Jönsson, B. (2004). Mortality after osteoporotic fractures. *Osteoporosis International, 15*(1), 38-42. doi: 10.1007/s00198-003-1490-4

Jonville-Bera, A. P., & Autret-Leca, E. (2011). [Adverse drug reactions of strontium ranelate(Protelos((R)) in France]. *Presse Med, 40*(10), e453-462. doi: 10.1016/j.lpm.2011.07.010

Kanayama, A., Seth, R. B., Sun, L., Ea, C. K., Hong, M., Shaito, A., . . . Chen, Z. J. (2004). TAB2 and TAB3 activate the NF-kappaB pathway through binding to polyubiquitin chains. *Mol Cell, 15*(4), 535-548. doi: 10.1016/j.molcel.2004.08.008

Kaneps, A. J., Stover, S. M., & Lane, N. E. (1997). Changes in canine cortical and cancellous bone mechanical properties following immobilization and remobilization with exercise. *Bone, 21*(5), 419-423. doi: 10.1016/s8756-3282(97)00167-1

Kanis, J. A., Burlet, N., Cooper, C., Delmas, P. D., Reginster, J.-Y., Borgstrom, F., & Rizzoli, R. (2008). European guidance for the diagnosis and management of osteoporosis in postmenopausal women. *Osteoporosis International, 19*(4), 399-428. doi: 10.1007/s00198-008-0560-z

Kanis, J. A., & Gluer, C. C. (2000). An update on the diagnosis and assessment of osteoporosis with densitometry. Committee of Scientific Advisors, International Osteoporosis Foundation. *Osteoporos Int, 11*(3), 192-202. doi: 10.1007/s001980050281

Kanis, J.A., Johansson, H., Odén, A, Johnell, O., De LAet, C., Eisman, J.A., . . . Tenenhouse, A. (2004) A familiy history of fracture and fracture risk: a meta-analysis. *Bone, 35,1029-37.* doi: 10.1016/j.bone.2004.06.017

Kanis, J. A., Johnell, O., Oden, A., Sembo, I., Redlund-Johnell, I., Dawson, A., . . . Jonsson, B. (2000). Long-term risk of osteoporotic fracture in Malmo. *Osteoporos Int, 11*(8), 669-674. doi: 10.1007/s001980070064

Karieb, S., & Fox, S. W. (2011). Phytoestrogens directly inhibit TNF-alpha-induced bone resorption in RAW264.7 cells by suppressing c-fos-induced NFATc1 expression. *J Cell Biochem, 112*(2), 476-487. doi: 10.1002/jcb.22935

Kashiwada, M., Shirakata, Y., Inoue, J. I., Nakano, H., Okazaki, K., Okumura, K., . . . Takemori, T. (1998). Tumor necrosis factor receptor-associated factor 6 (TRAF6) stimulates extracellular signal-regulated kinase (ERK) activity in CD40 signaling along a ras-independent pathway. *J Exp Med, 187*(2), 237-244. doi: 10.1084/jem.187.2.237

Kavanagh, K. L., Guo, K., Dunford, J. E., Wu, X., Knapp, S., Ebetino, F. H., . . . Oppermann, U. (2006). The molecular mechanism of nitrogen-containing bisphosphonates as antiosteoporosis drugs. *Proc Natl Acad Sci U S A, 103*(20), 7829-7834. doi: 10.1073/pnas.0601643103

Ke, H. Z., Jee, W. S., Zeng, Q. Q., Li, M., & Lin, B. Y. (1993). Prostaglandin E2 increased rat cortical bone mass when administered immediately following ovariectomy. *Bone Miner, 21*(3), 189-201. doi: 10.1016/s0169-6009(08)80230-9

Kharkwal, G., Chandra, V., Fatima, I., & Dwivedi, A. (2012). Ormeloxifene inhibits osteoclast differentiation in parallel to downregulating RANKL-induced ROS generation and suppressing the activation of ERK and JNK in murine RAW264.7 cells. *J Mol Endocrinol, 48*(3), 261-270. doi: 10.1530/JME-11-0061

Khosla, S., Burr, D., Cauley, J., Dempster, D. W., Ebeling, P. R., Felsenberg, D., . . . Shane, E. (2007). Bisphosphonate-associated osteonecrosis of the jaw: report of a task force of the American Society for Bone and Mineral Research. *J Bone Miner Res, 22*(10), 1479-1491. doi: 10.1359/jbmr.0707onj

Khosla, S., Oursler, M. J., & Monroe, D. G. (2012). Estrogen and the skeleton. *Trends Endocrinol Metab, 23*(11), 576-581. doi: 10.1016/j.tem.2012.03.008

Kiel, D. P., Felson, D. T., Hannan, M. T., Anderson, J. J., & Wilson, P. W. (1990). Caffeine and the risk of hip fracture: the Framingham Study. *Am J Epidemiol, 132*(4), 675-684. doi: 10.1093/oxfordjournals.aje.a115709

Kim, J. H., Jin, H. M., Kim, K., Song, I., Youn, B. U., Matsuo, K., & Kim, N. (2009). The mechanism of osteoclast differentiation induced by IL-1. *J Immunol, 183*(3), 1862-1870. doi: 10.4049/jimmunol.0803007

Kim, J. H., Kim, N. (2016). Signaling pathways in osteoclast differentiation. *Chonnam Med J, 52(1), 12 – 17.* doi: 10.4068/cmj.2016.52.1.12

Kim, M. S., Yang, Y. M., Son, A., Tian, Y. S., Lee, S. I., Kang, S. W., . . . Shin, D. M. (2010). RANKL-mediated reactive oxygen species pathway that induces long lasting Ca2+ oscillations essential for osteoclastogenesis. *J Biol Chem, 285*(10), 6913-6921. doi: 10.1074/jbc.M109.051557

Kimmel, D.B. (1996). Animal models for in vivo experimentation in osteoporosis research. In R. Marcus, D. Feldman & J. Kelsey (Eds.), *Osteoporosis* (pp. 671- 690). San Diego: Academic Press. doi: 10.1016/b978-012470862-4/50038-6

Knowler, John T. (1983). Estrogen-Induced Uterine Hypertrophy. In K. W. McKerns (Ed.), *Regulation of Gene Expression by Hormones* (pp. 129-150). Boston, MA: Springer US. doi: 10.1007/978-1-4684-4418-6_7

Koh, L. K., Saw, S. M., Lee, J. J., Leong, K. H., & Lee, J. (2001). Hip fracture incidence rates in Singapore 1991-1998. *Osteoporos Int, 12*(4), 311-318. doi: 10.1007/s001980170121

Koh, L. K., Sedrine, W. B., Torralba, T. P., Kung, A., Fujiwara, S., Chan, S. P., . . . Reginster, J. Y. (2001). A simple tool to identify asian women at increased risk of osteoporosis. *Osteoporos Int, 12*(8), 699-705. doi: 10.1007/s001980170070

Krall, E. A., & Dawson-Hughes, B. (1993). Heritable and life-style determinants of bone mineral density. *J Bone Miner Res, 8*(1), 1-9. doi: 10.1002/jbmr.5650080102

Kuiper, G. G., Lemmen, J. G., Carlsson, B., Corton, J. C., Safe, S. H., van der Saag, P. T., . . . Gustafsson, J. A. (1998). Interaction of estrogenic chemicals and phytoestrogens with estrogen receptor beta. *Endocrinology, 139*(10), 4252-4263. doi: 10.1210/endo.139.10.6216

Kyung, Tae-Wook, Lee, Ji-Eun, Shin, Hyun-Hee, & Choi, Hye-Seon. (2008). Rutin inhibits osteoclast formation by decreasing reactive oxygen species and TNF-[alpha] by inhibiting activation of NF-[kappa]B. *Exp Mol Med, 40*, 52-58. doi: 10.3858/emm.2008.40.1.52

Lai, X., Ye, Y., Sun, C., Huang, X., Tang, X., Zeng, X., . . . Zeng, Y. (2013). Icaritin exhibits anti-inflammatory effects in the mouse peritoneal macrophages and peritonitis model. *Int Immunopharmacol, 16*(1), 41-49. doi: 10.1016/j.intimp.2013.03.025

Lee, N. K., Choi, Y. G., Baik, J. Y., Han, S. Y., Jeong, D. W., Bae, Y. S., . . . Lee, S. Y. (2005). A crucial role for reactive oxygen species in RANKL-induced osteoclast differentiation. *Blood, 106*(3), 852-859. doi: 10.1182/blood-2004-09-3662

Lee, S. H., & Jang, H. D. (2015). Scoparone attenuates RANKL-induced osteoclastic differentiation through controlling reactive oxygen species production and scavenging. *Exp Cell Res, 331*(2), 267-277. doi: 10.1016/j.yexcr.2014.12.018

Lee, S. H., Kim, J. K., & Jang, H. D. (2014). Genistein inhibits osteoclastic differentiation of RAW 264.7 cells via regulation of ROS production and scavenging. *Int J Mol Sci, 15*(6), 10605-10621. doi: 10.3390/ijms150610605

Lerner, U. H. (2006). Bone remodeling in post-menopausal osteoporosis. *J Dent Res, 85, 584 – 595.* doi: 10.1177/154405910608500703

Li, J., Zeng, L., Xie, J., Yue, Z., Deng, H., Ma, X., . . . Liu, M. (2015). Inhibition of Osteoclastogenesis and Bone Resorption in vitro and in vivo by a prenylflavonoid xanthohumol from hops. *Sci Rep, 5*, 17605. doi: 10.1038/srep17605

Li, M., Shen, Y., Qi, H., & Wronski, T. J. (1996). Comparative study of skeletal response to estrogen depletion at red and yellow marrow sites in rats. *Anat Rec, 245*(3), 472-480. doi: 10.1002/(sici)1097-0185(199607)245:3<472::aid-ar3>3.0.co;2-u

Lim, K. L., & Lim, G. G. (2011). K63-linked ubiquitination and neurodegeneration. *Neurobiol Dis, 43*(1), 9-16. doi: 10.1016/j.nbd.2010.08.001

Lindsay, R., Gallagher, J. C., Kleerekoper, M., & Pickar, J. H. (2002). Effect of lower doses of conjugated equine estrogens with and without medroxyprogesterone acetate on bone in early postmenopausal women. *JAMA, 287*(20), 2668-2676. doi: 10.1001/jama.287.20.2668

Lomaga, M. A., Yeh, W. C., Sarosi, I., Duncan, G. S., Furlonger, C., Ho, A., . . . Mak, T. W. (1999). TRAF6 deficiency results in osteopetrosis and defective interleukin-1, CD40, and LPS signaling. *Genes Dev, 13*(8), 1015-1024. doi: 10.1101/gad.13.8.1015

Long, Fanxin. (2012). Building strong bones: molecular regulation of the osteoblast lineage. *Nat Rev Mol Cell Biol, 13*(1), 27-38. doi: 10.1038/nrm3254

Ma, H., He, X., Yang, Y., Li, M., Hao, D., & Jia, Z. (2011). The genus Epimedium: an ethnopharmacological and phytochemical review. *J Ethnopharmacol, 134*(3), 519-541. doi: 10.1016/j.jep.2011.01.001

Ma, Y. F., Ke, H. Z., & Jee, W. S. (1994). Prostaglandin E2 adds bone to a cancellous bone site with a closed growth plate and low bone turnover in ovariectomized rats. *Bone, 15*(2), 137-146. doi: 10.1016/8756-3282(94)90700-5

Magaziner, J., Simonsick, E. M., Kashner, T. M., Hebel, J. R., & Kenzora, J. E. (1990). Predictors of functional recovery one year following hospital discharge for hip fracture: a prospective study. *J Gerontol, 45*(3), M101-107. doi: 10.1093/geronj/45.3.m101

Mallette, Frederick A., & Richard, Stephane. (2012). K48-linked ubiquitination and protein degradation regulate 53BP1 recruitment at DNA damage sites. *Cell Res, 22*(8), 1221-1223. doi: 10.1038/cr.2012.58

Manolagas, S. C., & Jilka, R. L. (1995). Bone marrow, cytokines, and bone remodeling. Emerging insights into the pathophysiology of osteoporosis. *N Engl J Med, 332*(5), 305-311. doi: 10.1056/nejm199502023320506

Marino, S., Logan, J. G., Mellis, D., & Capulli, M. (2014). Generation and culture of osteoclasts. *Bonekey Rep, 3*, 570. doi: 10.1038/bonekey.2014.65

Marshall, D., Johnell, O., & Wedel, H. (1996). Meta-analysis of how well measures of bone mineral density predict occurrence of osteoporotic fractures. *BMJ, 312*(7041), 1254-1259. doi: 10.1136/bmj.312.7041.1254

Martin, M. U., & Wesche, H. (2002). Summary and comparison of the signaling mechanisms of the Toll/interleukin-1 receptor family. *Biochim Biophys Acta, 1592*(3), 265-280. doi: 10.1016/s0167-4889(02)00320-8

Massey, L. K., & Whiting, S. J. (1996). Dietary salt, urinary calcium, and bone loss. *J Bone Miner Res, 11*(6), 731-736. doi: 10.1002/jbmr.5650110603

Matsumoto, M., Sudo, T., Saito, T., Osada, H., & Tsujimoto, M. (2000). Involvement of p38 mitogen-activated protein kinase signaling pathway in osteoclastogenesis mediated by receptor activator of NF-kappa B ligand (RANKL). *J Biol Chem, 275*(40), 31155-31161. doi: 10.1074/jbc.M001229200

Matsumoto, Masahito, Sudo, Tatsuhiko, Saito, Tamio, Osada, Hiroyuki, & Tsujimoto, Masafumi. (2000). Involvement of p38 Mitogen-activated Protein Kinase Signaling Pathway in Osteoclastogenesis Mediated by Receptor Activator of NF-κB Ligand (RANKL). *Journal of Biological Chemistry, 275*(40), 31155-31161. doi: 10.1074/jbc.M001229200

McBerry, C., Gonzalez, R. M., Shryock, N., Dias, A., & Aliberti, J. (2012). SOCS2-induced proteasome-dependent TRAF6 degradation: a common anti-inflammatory pathway for control of innate immune responses. *PLoS One, 7*(6), e38384. doi: 10.1371/journal.pone.0038384

McClung, M. R., Lewiecki, E. M., Cohen, S. B., Bolognese, M. A., Woodson, G. C., Moffett, A. H., . . . Bekker, P. J. (2006). Denosumab in postmenopausal women with low bone mineral density. *N Engl J Med, 354*(8), 821-831. doi: 10.1056/NEJMoa044459

Melton, L. J., 3rd. (1995). How many women have osteoporosis now? *J Bone Miner Res, 10*(2), 175-177. doi: 10.1002/jbmr.5650100202

Meng, F. H., Li, Y. B., Xiong, Z. L., Jiang, Z. M., & Li, F. M. (2005). Osteoblastic proliferative activity of Epimedium brevicornum Maxim. *Phytomedicine, 12*(3), 189-193. doi: 10.1016/j.phymed.2004.03.007

Meunier, P. (1996). Prevention of hip fractures by correcting calcium and vitamin D insufficiencies in elderly people. *Scand J Rheumatol Suppl, 103*, 75-78; discussion 79-80. doi: 10.3109/03009749609103753

Meunier, P. J., Roux, C., Seeman, E., Ortolani, S., Badurski, J. E., Spector, T. D., . . . Reginster, J. Y. (2004). The effects of strontium ranelate on the risk of vertebral fracture in women with postmenopausal osteoporosis. *N Engl J Med, 350*(5), 459-468. doi: 10.1056/NEJMoa022436

Million Women Study, Collaborators. Endometrial cancer and hormone-replacement therapy in the Million Women Study. *The Lancet, 365*(9470), 1543-1551. doi: 10.1016/S0140-6736(05)66455-0

Minaire, P. (1989). Immobilization osteoporosis: a review. *Clinical Rheumatology, 8*(2), 95-103. doi: 10.1007/bf02207242

Mithal, A., & Kaur, P. (2012). Osteoporosis in Asia: a call to action. *Curr Osteoporos Rep, 10*(4), 245-247. doi: 10.1007/s11914-012-0114-3

Mizukami, J., Takaesu, G., Akatsuka, H., Sakurai, H., Ninomiya-Tsuji, J., Matsumoto, K., & Sakurai, N. (2002). Receptor activator of NF-kappaB ligand (RANKL) activates TAK1 mitogen-activated protein kinase kinase kinase through a

signaling complex containing RANK, TAB2, and TRAF6. *Mol Cell Biol, 22*(4), 992-1000. doi: 10.1128/mcb.22.4.992-1000.2002

Monje, P., Hernandez-Losa, J., Lyons, R. J., Castellone, M. D., & Gutkind, J. S. (2005). Regulation of the transcriptional activity of c-Fos by ERK. A novel role for the prolyl isomerase PIN1. *J Biol Chem, 280*(42), 35081-35084. doi: 10.1074/jbc.C500353200

Moon, Ho-Jin, Kim, Sung Eun, Yun, Young Pil, Hwang, Yu-Shik, Bang, Jae Beum, Park, Jae-Hong, & Kwon, Il Keun. (2011). Simvastatin inhibits osteoclast differentiation by scavenging reactive oxygen species. *Exp Mol Med, 43*, 605-612. doi: 10.3858/emm.2011.43.11.067

Morabito, N., Crisafulli, A., Vergara, C., Gaudio, A., Lasco, A., Frisina, N., . . . Squadrito, F. (2002). Effects of genistein and hormone-replacement therapy on bone loss in early postmenopausal women: a randomized double-blind placebo-controlled study. *J Bone Miner Res, 17*(10), 1904-1912. doi: 10.1359/jbmr.2002.17.10.1904

Mundy, Gregory R. (2007). Osteoporosis and Inflammation. *Nutrition Reviews, 65*(suppl 3), S147-S151. doi: 10.1111/j.1753-4887.2007.tb00353.x

Naito, A., Azuma, S., Tanaka, S., Miyazaki, T., Takaki, S., Takatsu, K., . . . Inoue, J. (1999). Severe osteopetrosis, defective interleukin-1 signalling and lymph node organogenesis in TRAF6-deficient mice. *Genes Cells, 4*(6), 353-362. doi: 10.1046/j.1365-2443.1999.00265.x

Nakamura, T., Imai, Y., Matsumoto, T., Sato, S., Takeuchi, K., Igarashi, K., . . . Kato, S. (2007). Estrogen prevents bone loss via estrogen receptor alpha and induction of Fas ligand in osteoclasts. *Cell, 130*(5), 811-823. doi: 10.1016/j.cell.2007.07.025

Neer, R. M., Arnaud, C. D., Zanchetta, J. R., Prince, R., Gaich, G. A., Reginster, J. Y., . . . Mitlak, B. H. (2001). Effect of parathyroid hormone (1-34) on fractures and bone mineral density in postmenopausal women with osteoporosis. *N Engl J Med, 344*(19), 1434-1441. doi: 10.1056/nejm200105103441904

Nicholson, Geoffrey C., MALAKELLIS, Mary, COLLIER, Fiona M., CAMERON, Paul U., HOLLOWAY, Wayne R., GOUGH, Tamara J., . . . MYERS, Damian E. (2000). Induction of osteoclasts from CD14-positive human peripheral blood mononuclear cells by receptor activator of nuclear factor κB ligand (RANKL). *Clinical Science, 99*(2), 133-140. doi: 10.1042/cs0990133

Nijveldt, R. J., van Nood, E., van Hoorn, D. E., Boelens, P. G., van Norren, K., & van Leeuwen, P. A. (2001). Flavonoids: a review of probable mechanisms of action and potential applications. *Am J Clin Nutr, 74*(4), 418-425.

Novack, D. V., Yin, L., Hagen-Stapleton, A., Schreiber, R. D., Goeddel, D. V., Ross, F. P., & Teitelbaum, S. L. (2003). The IkappaB function of NF-kappaB2 p100 controls stimulated osteoclastogenesis. *J Exp Med, 198*(5), 771-781. doi: 10.1084/jem.20030116

O'Neill, L. A. (2002). Signal transduction pathways activated by the IL-1 receptor/toll-like receptor superfamily. *Curr Top Microbiol Immunol, 270*, 47-61. doi: 10.1007/978-3-642-59430-4_3

Odvina, C. V., Zerwekh, J. E., Rao, D. S., Maalouf, N., Gottschalk, F. A., & Pak, C. Y. (2005). Severely suppressed bone turnover: a potential complication of alendronate therapy. *J Clin Endocrinol Metab, 90*(3), 1294-1301. doi: 10.1210/jc.2004-0952

Okamura, H., Aramburu, J., Garcia-Rodriguez, C., Viola, J. P., Raghavan, A., Tahiliani, M., . . . Rao, A. (2000). Concerted dephosphorylation of the transcription factor NFAT1 induces a conformational switch that regulates transcriptional activity. *Mol Cell, 6*(3), 539-550. doi: 10.1016/s1097-2765(00)00053-8

Ominsky, M. S., Li, X., Asuncion, F. J., Barrero, M., Warmington, K. S., Dwyer, D., . . . Kostenuik, P. J. (2008). RANKL inhibition with osteoprotegerin increases bone strength by improving cortical and trabecular bone architecture in ovariectomized rats. *J Bone Miner Res, 23*(5), 672-682. doi: 10.1359/jbmr.080109

Pacifici, R., Brown, C., Puscheck, E., Friedrich, E., Slatopolsky, E., Maggio, D., . . . Avioli, L. V. (1991). Effect of surgical menopause and estrogen replacement on cytokine release from human blood mononuclear cells. *Proc Natl Acad Sci U S A, 88*(12), 5134-5138.

Parfitt, A. M. (2002). Targeted and nontargeted bone remodeling: relationship to basic multicellular unit origination and progression. *Bone, 30*(1), 5-7.

Parfitt, A.M. (1990). Bone-forming cells in clinical conditions. In B. K. Hall (Ed.), *The osteoblast and osteocyte* (Vol. 1, pp. 351 - 429). Boca Raton, FL.: Telford Press and CRC Press. doi: 10.1016/b978-012319060-4/50026-9

Park, H. S., Lee, S. H., Park, D., Lee, J. S., Ryu, S. H., Lee, W. J., . . . Bae, Y. S. (2004). Sequential activation of phosphatidylinositol 3-kinase, beta Pix, Rac1, and Nox1 in growth factor-induced production of H2O2. *Mol Cell Biol, 24*(10), 4384-4394. doi: 10.1128/mcb.24.10.4384-4394.2004

Patti, Aurora, Gennari, Luigi, Merlotti, Daniela, Dotta, Francesco, & Nuti, Ranuccio. (2013). Endocrine Actions of Osteocalcin. *International Journal of Endocrinology, 2013*, 10. doi: 10.1155/2013/846480

Peng, S., Zhang, G., Zhang, B. T., Guo, B., He, Y., Bakker, A. J., . . . Leung, W. N. (2013). The beneficial effect of icaritin on osteoporotic bone is dependent on the treatment initiation timing in adult ovariectomized rats. *Bone, 55*(1), 230-240. doi: 10.1016/j.bone.2013.02.012

Prince, R. L., Smith, M., Dick, I. M., Price, R. I., Webb, P. G., Henderson, N. K., & Harris, M. M. (1991). Prevention of postmenopausal osteoporosis. A comparative study of exercise, calcium supplementation, and hormone-replacement therapy. *N Engl J Med, 325*(17), 1189-1195. doi: 10.1056/nejm199110243251701

Prince, R., Sipos, A., Hossain, A., Syversen, U., Ish-Shalom, S., Marcinowska, E., . . . Mitlak, B. H. (2005). Sustained nonvertebral fragility fracture risk reduction after discontinuation of teriparatide treatment. *J Bone Miner Res, 20*(9), 1507-1513. doi: 10.1359/jbmr.050501

Proff, P., Römer, P. (2009). The molecular mechanism behind bone remodelling: a review. *Clin Oral Invest, 13(4), 355 – 362.* doi: 10.1007/s00784-009-0268-2

Pullen, S. S., Dang, T. T., Crute, J. J., & Kehry, M. R. (1999). CD40 signaling through tumor necrosis factor receptor-associated factors (TRAFs). Binding site specificity and activation of downstream pathways by distinct TRAFs. *J Biol Chem, 274*(20), 14246-14254. doi: 10.1074/jbc.274.20.14246

Qin, L., Yao, D., Zheng, L., Liu, W. C., Liu, Z., Lei, M., . . . Cheng, C. Y. (2015). Phytomolecule icaritin incorporated PLGA/TCP scaffold for steroid-associated osteonecrosis: Proof-of-concept for prevention of hip joint collapse in bipedal emus and mechanistic study in quadrupedal rabbits. *Biomaterials, 59*, 125-143. doi: 10.1016/j.biomaterials.2015.04.038

Quinn, J. M., Elliott, J., Gillespie, M. T., & Martin, T. J. (1998). A combination of osteoclast differentiation factor and macrophage-colony stimulating factor is sufficient for both human and mouse osteoclast formation in vitro. *Endocrinology, 139*(10), 4424-4427. doi: 10.1210/endo.139.10.6331

Reginster, Jean-Yves, & Burlet, Nansa. (2006). Osteoporosis: A still increasing prevalence. *Bone, 38*(2), 4-9. doi: 10.1016/j.bone.2005.11.024

Reszka, A. A., & Rodan, G. A. (2003). Bisphosphonate mechanism of action. *Curr Rheumatol Rep, 5*(1), 65-74. doi: 10.1007/s11926-003-0085-6

Rizzoli, René, Schürch, Marc-André, Chevalley, Thierry, Ammann, Patrick, & Bonjour, Jean-Philippe. (1998). Protein Intake and Osteoporosis. In P. Burckhardt, B. Dawson-Hughes & R. P. Heaney (Eds.), *Nutritional Aspects of Osteoporosis: A Serono Symposia S.A. Publication* (pp. 141-154). New York, NY: Springer New York. doi: 10.1007/978-1-4612-2228-6_15

Robinson, Lisa J., Yaroslavskiy, Beatrice B., Griswold, Reed D., Zadorozny, Eva V., Guo, Lida, Tourkova, Irina L., & Blair, Harry C. (2009). Estrogen Inhibits RANKL-stimulated Osteoclastic Differentiation of Human Monocytes through Estrogen and RANKL-regulated Interaction of Estrogen Receptor-α with BCAR1 and Traf6. *Exp Cell Res, 315*(7), 1287-1301. doi: 10.1016/j.yexcr.2009.01.014

Rodan, G. A., & Fleisch, H. A. (1996). Bisphosphonates: mechanisms of action. *J Clin Invest, 97*(12), 2692-2696. doi: 10.1172/jci118722

Roggia, C., Gao, Y., Cenci, S., Weitzmann, M. N., Toraldo, G., Isaia, G., & Pacifici, R. (2001). Up-regulation of TNF-producing T cells in the bone marrow: a key mechanism by which estrogen deficiency induces bone loss in vivo. *Proc Natl Acad Sci U S A, 98*(24), 13960-13965. doi: 10.1073/pnas.251534698

Ross, F. P. (2006). M-CSF, c-Fms, and signaling in osteoclasts and their precursors. *Ann N Y Acad Sci, 1068*, 110-116. doi: 10.1196/annals.1346.014

Ross, P. D., Norimatsu, H., Davis, J. W., Yano, K., Wasnich, R. D., Fujiwara, S., . . . Melton, L. J., 3rd. (1991). A comparison of hip fracture incidence among native Japanese, Japanese Americans, and American Caucasians. *Am J Epidemiol, 133*(8), 801-809. doi: 10.1093/oxfordjournals.aje.a115959

Rousselle, A. V., & Heymann, D. (2002). Osteoclastic acidification pathways during bone resorption. *Bone, 30*(4), 533-540.

Russell, R. G. (2006). Bisphosphonates: from bench to bedside. *Ann N Y Acad Sci, 1068*, 367-401. doi: 10.1196/annals.1346.041

Samelson, Elizabeth J., Hannan, Marian T., Zhang, Yuqing, Genant, Harry K., Felson, David T., & Kiel, Douglas P. (2006). Incidence and Risk Factors for Vertebral Fracture in Women and Men: 25-Year Follow-Up Results From the Population-Based Framingham Study. *Journal of Bone and Mineral Research, 21*(8), 1207-1214. doi: 10.1359/jbmr.060513

Sasaki, H., Yamamoto, H., Tominaga, K., Masuda, K., Kawai, T., Teshima-Kondo, S., & Rokutan, K. (2009). NADPH oxidase-derived reactive oxygen species are essential for differentiation of a mouse macrophage cell line (RAW264.7) into osteoclasts. *J Med Invest, 56*(1-2), 33-41. doi: 10.2152/jmi.56.33

Schilcher, Jörg, Michaëlsson, Karl, & Aspenberg, Per. (2011). Bisphosphonate Use and Atypical Fractures of the Femoral Shaft. *New England Journal of Medicine, 364*(18), 1728-1737. doi: doi:10.1056/NEJMoa1010650

Schnell, Scott, Friedman, Susan M., Mendelson, Daniel A., Bingham, Karilee W., & Kates, Stephen L. (2010). The 1-Year Mortality of Patients Treated in a Hip Fracture Program for Elders. *Geriatric Orthopaedic Surgery & Rehabilitation, 1*(1), 6-14. doi: 10.1177/2151458510378105

Shane, E., Burr, D., Ebeling, P. R., Abrahamsen, B., Adler, R. A., Brown, T. D., . . . Whyte, M. (2010). Atypical subtrochanteric and diaphyseal femoral fractures: report of a task force of the American Society for Bone and Mineral Research. *J Bone Miner Res, 25*(11), 2267-2294. doi: 10.1002/jbmr.253

Shao, B., Liao, L., Yu, Y., Shuai, Y., Su, X., Jing, H., . . . Jin, Y. (2015). Estrogen preserves Fas ligand levels by inhibiting microRNA-181a in bone marrow-derived mesenchymal stem cells to maintain bone remodeling balance. *FASEB J, 29*(9), 3935-3944. doi: 10.1096/fj.15-272823

Shedd-Wise, K. M., Alekel, D. L., Hofmann, H., Hanson, K. B., Schiferl, D. J., Hanson, L. N., & Van Loan, M. D. (2011). The soy isoflavones for reducing bone loss study: 3-yr effects on pQCT bone mineral density and strength measures in postmenopausal women. *J Clin Densitom, 14*(1), 47-57. doi: 10.1016/j.jocd.2010.11.003

Shen, P., Guo, B. L., Gong, Y., Hong, D. Y., Hong, Y., & Yong, E. L. (2007). Taxonomic, genetic, chemical and estrogenic characteristics of Epimedium species. *Phytochemistry, 68*(10), 1448-1458. doi: 10.1016/j.phytochem.2007.03.001

Shevde, Nirupama K., Bendixen, Amy C., Dienger, Krista M., & Pike, J. Wesley. (2000). Estrogens suppress RANK ligand-induced osteoclast differentiation via a stromal cell independent mechanism involving c-Jun repression. *Proceedings of the National Academy of Sciences, 97*(14), 7829-7834. doi: 10.1073/pnas.130200197

Silverman, Stuart L., & Calderon, Andrew D. (2010). The Utility and Limitations of FRAX: A US Perspective. *Curr Osteoporos Rep, 8*(4), 192-197. doi: 10.1007/s11914-010-0032-1

Soysa, N. S., & Alles, N. (2009). NF-kappaB functions in osteoclasts. *Biochem Biophys Res Commun, 378*(1), 1-5. doi: 10.1016/j.bbrc.2008.10.146

Soysa, N. S., Alles, N., Aoki, K., & Ohya, K. (2012). Osteoclast formation and differentiation: an overview. *J Med Dent Sci, 59*(3), 65-74. doi: 10.1016/j.bbrc.2016.05.019

Srivastava, S., Toraldo, G., Weitzmann, M. N., Cenci, S., Ross, F. P., & Pacifici, R. (2001). Estrogen decreases osteoclast formation by down-regulating receptor activator of NF-kappa B ligand (RANKL)-induced JNK activation. *J Biol Chem, 276*(12), 8836-8840. doi: 10.1074/jbc.M010764200

Stearn W.T , Shaw J. (2002). *The Genus Epimedium and Other Herbaceous Berberidaceae.*: Timber Press, 2002. doi: 10.5860/choice.40-4610

Stepan, J. J. (2013). Strontium ranelate: in search for the mechanism of action. *J Bone Miner Metab, 31*(6), 606-612. doi: 10.1007/s00774-013-0494-1

Sun, F., Indran, I. R., Zhang, Z. W., Tan, M.H., Li, Y., Lim, Z. L. R, . . . Yong, E.L. (2015). A novel prostate cancer therapeutic strategy using icaritin-activated arylhydrocarbon-receptor to co-target androgen receptor and its splice variants. *Carcinogenesis, 36*(7), 757-768. doi: 10.1093/carcin/bgv040

Takahashi, N., Ejiri, S., Yanagisawa, S., & Ozawa, H. (2007). Regulation of osteoclast polarization. *Odontology, 95*(1), 1-9. doi: 10.1007/s10266-007-0071-y

Takano-Yamamoto, T., & Rodan, G. A. (1990). Direct effects of 17 beta-estradiol on trabecular bone in ovariectomized rats. *Proc Natl Acad Sci U S A, 87*(6), 2172-2176. doi: 10.1073/pnas.87.6.2172

Takata, S., & Yasui, N. (2001). Disuse osteoporosis. *J Med Invest, 48*(3-4), 147-156.

Takayanagi, H. (2007). Osteoimmunology: shared mechanisms and crosstalk between the immune and bone systems. *Nat Rev Immunol, 7*(4), 292-304. doi: 10.1038/nri2062

Takayanagi, H., Kim, S., Koga, T., Nishina, H., Isshiki, M., Yoshida, H., . . . Taniguchi, T. (2002). Induction and activation of the transcription factor NFATc1 (NFAT2) integrate RANKL signaling in terminal differentiation of osteoclasts. *Dev Cell, 3*(6), 889-901. doi: 10.1016/s1534-5807(02)00369-6

Takayanagi, H., Ogasawara, K., Hida, S., Chiba, T., Murata, S., Sato, K., . . . Taniguchi, T. (2000). T-cell-mediated regulation of osteoclastogenesis by signalling cross-talk between RANKL and IFN-gamma. *Nature, 408*(6812), 600-605. doi: 10.1038/35046102

Takayanagi, Hiroshi. (2007). The Role of NFAT in Osteoclast Formation. *Ann N Y Acad Sci, 1116*(1), 227-237. doi: 10.1196/annals.1402.071

Taku, K., Melby, M. K., Nishi, N., Omori, T., & Kurzer, M. S. (2011). Soy isoflavones for osteoporosis: an evidence-based approach. *Maturitas, 70*(4), 333-338. doi: 10.1016/j.maturitas.2011.09.001

Tang, B. M., Eslick, G. D., Nowson, C., Smith, C., & Bensoussan, A. (2007). Use of calcium or calcium in combination with vitamin D supplementation to prevent fractures and bone loss in people aged 50 years and older: a meta-analysis. *Lancet, 370*(9588), 657-666. doi: 10.1016/s0140-6736(07)61342-7

Teitelbaum, S.L. (2000). Bone resorption by osteoclasts. *Science, 289, 1504 – 1508.* doi: 10.1126/science.289.5484.1504

Teng, Gim Gee, Curtis, effrey R., & Saag, Kenneth G. (2008). Mortality and osteoporotic fractures: is the link causal, and is it modifiable? *Clinical and Experimental Rheumatology, 26*(5 0 51), S125-S137. doi: 10.1097/bor.0000000000000300

Teucher, B., Dainty, J. R., Spinks, C. A., Majsak-Newman, G., Berry, D. J., Hoogewerff, J. A., . . . Fairweather-Tait, S. J. (2008). Sodium and bone health: impact of moderately high and low salt intakes on calcium metabolism in postmenopausal women. *J Bone Miner Res, 23*(9), 1477-1485. doi: 10.1359/jbmr.080408

Thompson, D. D., Simmons, H. A., Pirie, C. M., & Ke, H. Z. (1995). FDA Guidelines and animal models for osteoporosis. *Bone, 17*(4 Suppl), 125S-133S. doi: 10.1016/8756-3282(95)00285-l

Thompson, J.C. (2016) *Netter's Concise Orthopaedic Anatomy*. New York, NY: Elsevier.

Thrower, J. S., Hoffman, L., Rechsteiner, M., & Pickart, C. M. (2000). Recognition of the polyubiquitin proteolytic signal. *EMBO J, 19*(1), 94-102. doi: 10.1093/emboj/19.1.94

Tiong, C. T., Chen, C., Zhang, S. J., Li, J., Soshilov, A., Denison, M. S., . . . Yong, E. L. (2012). A novel prenylflavone restricts breast cancer cell growth through AhR-mediated destabilization of ERalpha protein. *Carcinogenesis, 33*(5), 1089-1097. doi: 10.1093/carcin/bgs110

Tosteson, A. A. N., Gabriel, E. S., Grove, R. M., Moncur, M. M., Kneeland, S. T., & Melton III, J. L. (2001). Impact of Hip and Vertebral Fractures on Quality-Adjusted Life Years. *Osteoporosis International, 12*(12), 1042-1049. doi: 10.1007/s001980170015

Tsuji, M., Yamamoto, H., Sato, T., Mizuha, Y., Kawai, Y., Taketani, Y., . . . Takeda, E. (2009). Dietary quercetin inhibits bone loss without effect on the uterus in ovariectomized mice. *J Bone Miner Metab, 27*(6), 673-681. doi: 10.1007/s00774-009-0088-0

Udagawa, Nobuyuki. (2012). Osteoclastic bone resorption directly activates osteoblast function. *Arthritis Research & Therapy, 14*(1), O26. doi: 10.1186/ar3581

Verborgt, O., Gibson, G. J., & Schaffler, M. B. (2000). Loss of osteocyte integrity in association with microdamage and bone remodeling after fatigue in vivo. *J Bone Miner Res, 15*(1), 60-67. doi: 10.1359/jbmr.2000.15.1.60

Vincent, C., Kogawa, M., Findlay, D. M., & Atkins, G. J. (2009). The generation of osteoclasts from RAW 264.7 precursors in defined, serum-free conditions. *J Bone Miner Metab, 27*(1), 114-119. doi: 10.1007/s00774-008-0018-6

Walsh, M. C., & Choi, Y. (2014). Biology of the RANKL-RANK-OPG System in Immunity, Bone, and Beyond. *Front Immunol, 5*, 511. doi: 10.3389/fimmu.2014.00511

Wang, C., Deng, L., Hong, M., Akkaraju, G. R., Inoue, J., & Chen, Z. J. (2001). TAK1 is a ubiquitin-dependent kinase of MKK and IKK. *Nature, 412*(6844), 346-351. doi: 10.1038/35085597

Wang, X. L., Xie, X. H., Zhang, G., Chen, S. H., Yao, D., He, K., . . . Qin, L. (2013). Exogenous phytoestrogenic molecule icaritin incorporated into a porous scaffold for enhancing bone defect repair. *J Orthop Res, 31*(1), 164-172. doi: 10.1002/jor.22188

Wang, Z. Q., Ovitt, C., Grigoriadis, A. E., Mohle-Steinlein, U., Ruther, U., & Wagner, E. F. (1992). Bone and haematopoietic defects in mice lacking c-fos. *Nature, 360*(6406), 741-745. doi: 10.1038/360741a0

Wattel, A., Kamel, S., Prouillet, C., Petit, J. P., Lorget, F., Offord, E., & Brazier, M. (2004). Flavonoid quercetin decreases osteoclastic differentiation induced by RANKL via a mechanism involving NF kappa B and AP-1. *J Cell Biochem, 92*(2), 285-295. doi: 10.1002/jcb.20071

Watts, N. B., Ettinger, B., & LeBoff, M. S. (2009). FRAX facts. *J Bone Miner Res, 24*(6), 975-979. doi: 10.1359/jbmr.090402

Weaver, C. M., Alekel, D. L., Ward, W. E., & Ronis, M. J. (2012). Flavonoid intake and bone health. *J Nutr Gerontol Geriatr, 31*(3), 239-253. doi: 10.1080/21551197.2012.698220

Weitzmann, M. N., Cenci, S., Rifas, L., Brown, C., & Pacifici, R. (2000). Interleukin-7 stimulates osteoclast formation by up-regulating the T-cell production of soluble osteoclastogenic cytokines. *Blood, 96*(5), 1873-1878. doi: 10.1002/art.24877

Welch, A., MacGregor, A., Jennings, A., Fairweather-Tait, S., Spector, T., & Cassidy, A. (2012). Habitual flavonoid intakes are positively associated with bone mineral density in women. *J Bone Miner Res, 27*(9), 1872-1878. doi: 10.1002/jbmr.1649

Wong, S. P., Shen, P., Lee, L., Li, J., & Yong, E. L. (2009). Pharmacokinetics of prenylflavonoids and correlations with the dynamics of estrogen action in sera following ingestion of a standardized Epimedium extract. *J Pharm Biomed Anal, 50*(2), 216-223. doi: 10.1016/j.jpba.2009.04.022

Wood, J., Bonjean, K., Ruetz, S., Bellahcene, A., Devy, L., Foidart, J.M., . . . Green, JR. (2002). Novel antiangiogenic effects of the bisphosphonate compound zolendronic acid. *J Pharmacol Exp Ther, 302*(3), 7. doi: 10.1124/jpet.102.035295

Writing Group for the PEPI, investigators. (1996). Effects of hormone therapy on bone mineral density: results from the postmenopausal estrogen/progestin interventions (PEPI) trial. *JAMA, 276*(17), 1389-1396. doi: 10.1001/jama.1996.03540170033029

Writing Group for the Women's Health Initiative, Investigators. (2002). Risks and benefits of estrogen plus progestin in healthy postmenopausal women: Principal results from the women's health initiative randomized controlled trial. *JAMA, 288*(3), 321-333. doi: 10.1001/jama.288.3.321

Wu, H., & Arron, J. R. (2003). TRAF6, a molecular bridge spanning adaptive immunity, innate immunity and osteoimmunology. *Bioessays, 25*(11), 1096-1105. doi: 10.1002/bies.10352

Wu, X., Li, Z., Yang, Z., Zheng, C., Jing, J., Chen, Y., . . . Luo, J. (2012). Caffeic acid 3,4-dihydroxy-phenethyl ester suppresses receptor activator of NF-kappaB ligand-induced osteoclastogenesis and prevents ovariectomy-induced bone loss through inhibition of mitogen-activated protein kinase/activator protein 1 and Ca2+-nuclear factor of activated T-cells cytoplasmic 1 signaling pathways. *J Bone Miner Res, 27*(6), 1298-1308. doi: 10.1002/jbmr.1576

Yang, Y. H., Chen, K., Li, B., Chen, J. W., Zheng, X. F., Wang, Y. R., . . . Jiang, L. S. (2013). Estradiol inhibits osteoblast apoptosis via promotion of autophagy through the ER-ERK-mTOR pathway. *Apoptosis, 18*(11), 1363-1375. doi: 10.1007/s10495-013-0867-x

Yao, D., Xie, X. H., Wang, X. L., Wan, C., Lee, Y. W., Chen, S. H., . . . Qin, L. (2012). Icaritin, an exogenous phytomolecule, enhances osteogenesis but not angiogenesis--an in vitro efficacy study. *PLoS One, 7*(8), e41264. doi: 10.1371/journal.pone.0041264

Yao, Z., Li, P., Zhang, Q., Schwarz, E. M., Keng, P., Arbini, A., . . . Xing, L. (2006). Tumor necrosis factor-alpha increases circulating osteoclast precursor numbers by promoting their proliferation and differentiation in the bone marrow through up-regulation of c-Fms expression. *J Biol Chem, 281*(17), 11846-11855. doi: 10.1074/jbc.M512624200

Yasuda, H., Shima, N., Nakagawa, N., Yamaguchi, K., Kinosaki, M., Mochizuki, S., . . . Suda, T. (1998). Osteoclast differentiation factor is a ligand for osteoprotegerin/osteoclastogenesis-inhibitory factor and is identical to TRANCE/RANKL. *Proc Natl Acad Sci U S A, 95*(7), 3597-3602. doi: 10.1073/pnas.95.7.3597

Ye, H. Y., & Lou, Y. J. (2005). Estrogenic effects of two derivatives of icariin on human breast cancer MCF-7 cells. *Phytomedicine, 12*(10), 735-741. doi: 10.1016/j.phymed.2004.10.002

Ye, Y. B., Tang, X. Y., Verbruggen, M. A., & Su, Y. X. (2006). Soy isoflavones attenuate bone loss in early postmenopausal Chinese women : a single-blind randomized, placebo-controlled trial. *Eur J Nutr, 45*(6), 327-334. doi: 10.1007/s00394-006-0602-2

Yu, T. Y., Pang, W. J., & Yang, G. S. (2015). Aryl hydrocarbon receptors in osteoclast lineage cells are a negative regulator of bone mass. *PLoS One, 10*(1), e0117112. doi: 10.1371/journal.pone.0117112

Zarzycka, B., Seijkens, T., Nabuurs, S. B., Ritschel, T., Grommes, J., Soehnlein, O., . . . Nicolaes, G. A. (2015). Discovery of small molecule CD40-TRAF6 inhibitors. *J Chem Inf Model, 55*(2), 294-307. doi: 10.1021/ci500631e

Zhang, G., Qin, L., Hung, W. Y., Shi, Y. Y., Leung, P. C., Yeung, H. Y., & Leung, K. S. (2006). Flavonoids derived from herbal Epimedium Brevicornum Maxim prevent OVX-induced osteoporosis in rats independent of its enhancement in intestinal calcium absorption. *Bone, 38*(6), 818-825. doi: 10.1016/j.bone.2005.11.019

Zhang, G., Qin, L., & Shi, Y. (2007). Epimedium-derived phytoestrogen flavonoids exert beneficial effect on preventing bone loss in late postmenopausal women: a 24-month randomized, double-blind and placebo-controlled trial. *J Bone Miner Res, 22*(7), 1072-1079. doi: 10.1359/jbmr.070405

Zhang, S. Q. (2014). Biodistribution evaluation of icaritin in rats by ultra-performance liquid chromatography-tandem mass spectrometry. *J Ethnopharmacol, 155*(2), 1382-1387. doi: 10.1016/j.jep.2014.07.045

Zhang, W., Xing, B., Yang, L., Shi, J., & Zhou, X. (2015). Icaritin Attenuates Myocardial Ischemia and Reperfusion Injury Via Anti-Inflammatory and Anti-Oxidative Stress Effects in Rats. *Am J Chin Med, 43*(6), 1083-1097. doi: 10.1142/s0192415x15500627

Zhang, X., Shu, X. O., Li, H., Yang, G., Li, Q., Gao, Y. T., & Zheng, W. (2005). Prospective cohort study of soy food consumption and risk of bone fracture among postmenopausal women. *Arch Intern Med, 165*(16), 1890-1895. doi: 10.1001/archinte.165.16.1890

Zhang, Yan-Hong, Heulsmann, Antoinette, Tondravi, M. Mehrdad, Mukherjee, Aditi, & Abu-Amer, Yousef. (2001). Tumor Necrosis Factor-α (TNF) Stimulates RANKL-induced Osteoclastogenesis via Coupling of TNF Type 1

Receptor and RANK Signaling Pathways. *Journal of Biological Chemistry, 276*(1), 563-568. doi: 10.1074/jbc.M008198200

Zhen, M., Tan, W., Bee, C. S. , & Chandran, M. . (2012). A Review of the 2008 Singapore Ministry of Health Clinical Practice Guidelines on Osteoporosis and an Update. *J Asean Fed Endocrine Soc, 27*(2), 6. doi: 10.15605/jafes.027.02.05

Zhu, H. M., Qin, L., Garnero, P., Genant, H. K., Zhang, G., Dai, K., . . . Zhao, S. J. (2012). The first multicenter and randomized clinical trial of herbal Fufang for treatment of postmenopausal osteoporosis. *Osteoporos Int, 23*(4), 1317-1327. doi: 10.1007/s00198-011-1577-2

Zucchelli, S., Codrich, M., Marcuzzi, F., Pinto, M., Vilotti, S., Biagioli, M., . . . Gustincich, S. (2010). TRAF6 promotes atypical ubiquitination of mutant DJ-1 and alpha-synuclein and is localized to Lewy bodies in sporadic Parkinson's disease brains. *Hum Mol Genet, 19*(19), 3759-3770. doi: 10.1093/hmg/ddq290